# SARS-CoV-2 causes periodontal fibrosis by deregulating mitochondrial β-oxidation

Yan Gao[1], Wai Ling Kok[1], Vikram Sharma[2], Charlotte Sara Illsley[1], Sally Hanks[1], Christopher Tredwin[1], Bing Hu[1*]

1. Stem Cells & Regenerative Medicine Laboratory, Peninsula Dental School, Faculty of Health, University of Plymouth, 16 Research Way, Plymouth, PL6 8BU, UK

2. School of Biomedical Sciences, Faculty of Health, University of Plymouth, 16 Research Way, Plymouth, PL6 8BU, UK

* Corresponding author

Professor Bing Hu

Email: bing.hu@plymouth.ac.uk

**Running title:** SARS-CoV-2 infection causes periodontal fibrosis

**Key words:** COVID-19; SARS-CoV-2; Tooth; Periodontal ligament; Fibrosis; Mitochondria

**Word count:** 3021

**Reference count:** 30

**Figure/table counts:** 5

## Abstract

The global high prevalence of COVID-19 is a major challenge for health professionals and patients. SARS-CoV-2 virus mutate predominantly in the spike proteins, whilst the other key viral components remain stable. Previous studies have shown that the human oral cavity can potentially act as reservoir of the SARS-CoV-2 virus and COVID-19 is likely to be connected with poor periodontal health. However, the consequence of SARS-CoV-2 viral infection on human oral health has not been systematically examined. In this research, we aimed to study the pathogenicity of SARS-CoV-2 viral components on human periodontal health. We found that human periodontal tissues, particularly the fibroblasts highly expressed ACE2 and TMPRSS2. Exposure to SARS-CoV-2, especially by the viral envelope and membrane proteins induced fibrotic pathogenic phenotypes, including periodontal fibroblast hyperproliferation, concomitant with increased apoptosis and senescence. The fibrotic degeneration was mediated by a down-regulation of mitochondrial β-oxidation. Fatty acid β-oxidation inhibitor, etomoxir treatment could mirror the same pathological consequence on the fibroblasts, similar to SARS-CoV-2 infection. Our results therefore provide novel mechanistic insights into how SARS-CoV-2 infection can affect human periodontal health at the cell and molecular level.

## Introduction

Since its outbreak, the coronavirus disease 2019 (COVID-19) pandemic has infected over 63 million people globally (https://covid19.who.int) and has been a major challenge to human health. The severe acute respiratory syndrome coronavirus 2 (SARS-CoV-2 virus) has multiple transmission routes such as through respiratory fluids, therefore is highly infectious (Ferretti et al. 2020). It has been reported that there were ever increasing "long COVID" (Lopez-Leon et al. 2021) and repeated infection cases (Wang et al. 2021), with the UK alone already having more than 2 million long COVID cases (Wise 2022). Although COVID-19 has been initially connected with acute inflammatory disease, which causes progressive pulmonary fibrosis (Spagnolo et al. 2020), increasing evidence have suggested that COVID-19 does affect other organs such as heart, skin, kidneys and brain (Wang et al. 2020). The human oral cavity and saliva have also been demonstrated to be an important reservoir of the SARS-CoV-2 virus (Huang et al. 2021), and saliva have been used for effective diagnosis of COVID-19 (Baghizadeh Fini 2020). Periodontal tissues are highly vulnerable to different infectious diseases and COVID-19 has been reported to be potentially connected with poor periodontal health (Qi et al. 2022). However, the pathological consequence of SARS-CoV-2 infection on human oral health has not been systematically investigated.

The evolution of SARS-CoV-2 has generated different variants that are responsible for infection speeds and symptoms (https://www.who.int/activities/tracking-SARS-CoV-2-variants). SARS-CoV-2 has four different structural protein components: envelope, membrane, nucleocapsid and spike (Figure 1A) (Huang et al. 2020). The mutations of SARS-CoV-2 predominantly occur in the spike proteins, particularly the receptor-binding domain (RBD), whilst the other key viral components remain stable (Satarker and Nampoothiri 2020) (Harvey et al. 2021). A key step of SARS-CoV-2 infection is the

binding of spike RBD to angiotensin-converting enzyme 2 (ACE2) receptor on the target cells (Ni et al. 2020) and co-receptor transmembrane serine protease 2 (TMPRSS2) to trigger viral internalization together with the molecular downstream cascades (Hoffmann et al. 2020). Currently, most of the COVID-19 related research and vaccine development have focused on the spike protein, leaving the other structural proteins' pathological functions remain to be elucidated.

As part of a series of research on the biological connection of COVID-19 with oral health, this study intended to apply human periodontal tissue and cells as examples to dissect the direct pathological effects of SARS-CoV-2 viral structural components.

## Materials & methods

### Cell culture

Human periodontal ligament fibroblasts (HPLFs) were cultured in DMEM/F12 ((Gibco, 31331-028) containing 20% Fetal bovine serum (FBS) (Sigma, F7524), 1% penicillin-streptomycin (Hyclone, SV30079.01). Human gingival epithelial cells (HGEPp) were cultured in CnT-57 (CELLnTEC, CnT-57).

### Viral infection

Plasmids for SARS-CoV-2 structural proteins were purchased from Addgene (Appendix Table 2). Lentiviral supernatant was collected according to the manual using 293FT cells. HPLFs were infected with lentiviruses carrying target sequences above with 10 μg/ml polybrene (Merck, TR-1003). After 2 h, dishes were topped up with fresh culture medium. Samples were collected at 6 h or 48 h. For overexpressing ACE2 (Addgene, Appendix Table 2) in HPLFs, the cells were infected with lentiviruses carrying target sequences above with 10 μg/ml polybrene (Merck). After 2 h, dishes were topped up with fresh normal culture medium. Samples were collected according to different time points. Infected cells were selected with 1 μg/ml puromycin (Thermo Scientific, 10781691) for 7-10 days.

### Recombinant SARS-CoV-2 spike protein treatment

Recombinant SARS-CoV-2 spike protein with His-tag (Biotechne, 10549-CV) was diluted with culture medium to 500 ng/ml or 5 μg/ml and added into the cell culture medium. Samples were collected at 6 h or 48 h.

### Mitochondria β-oxidation inhibition assay.

Etomoxir (Sigma, E1905) was diluted with culture medium to aimed concentration then added into cell culture medium. Samples were collected at 6 h or 48 h.

**Human periodontal tissue 3D equivalents**

5*10^4 of HPLFs were mixed with 150 µl gel mixture of rat tail collagen (Fisher, 11519816), DMEM (Fisher, 21969-035) and FBS (Ratio of volume 9:1:1) homogenously on ice. 2.3 µl 1M Sodium hydroxide solution (NaOH, Sigma 71687) was added into the mixture for neutralization, 150 µl gel was pipetted into a 0.4 µm culture insert (Greiner, 662641) incubated at 37°C for 1 h then fresh culture medium was added into the insert. Culture medium was replaced by CnT-57 before seeding 5*10^5 of HGEPp on top of the gel. HGEPp was cultured for 72 h before airlifting. Culture medium inside the insert was removed every day and the medium outside was changed every 2 days. Samples were frozen directly in OCT (Agar Scientific, AGR1180) at day 14 and sectioned at 20 µm for further analysis.

**Hydrogel based 3D matrix production assay**

1*10^6 of HPLFs were mixed with 100 µl bioink (CELLINK, CELLINK SKIN+) slowly and gently. Gels were pipetted into 6 well plate then 1.5 ml crosslinking agent (CELLINK) was added to cover the gel at RT for 5 min. Crosslinking agent was removed and 1.5 ml fresh culture media was added which was replaced every 2 days. Samples were frozen directly in OCT at day 7 and sectioned at 30 µm for further analysis.

**Immunohistochemistry**

For the details of immunostaining, BrdU incorporation assay, Terminal deoxynucleotidyl transferase dUTP nick end labelling (TUNEL) assay and Senescence assay details please see **Appendix materials & methods.**

**Flow cytometry analysis**

HPLFs and ACE2 overexpressed HPLFs were harvested and fixed in 2% PFA solution in 10 mM PBS for 10 min then washed with FACS buffer (1% BSA in PBS). 1*10^6 cells were resuspended in 500 µl flow cytometry permeabilization buffer (0.1% Tween-20 in PBS) for 15 min then washed with FACS buffer again. Cells were resuspended in 100 µl FACS buffer and APC His-Tag conjugated antibody was added, incubated for 2 h at room temperature then kept in dark at 4 °C degree overnight. Samples were analyzed using the BD FACSAria™ II (BD Biosciences). Data was acquired using red laser (633-640nm) for APC signal. Results were analyzed using the FlowJo software (Tree Star Inc., Version 10.8.1). Gates and regions were placed around populations of cells with common characteristics based on SSC and APC.

**Western blotting**

A NuPage® Electrophoresis System (Thermo Fisher Scientific), 4-12% Bis-Tris gradient gel (Thermo Fisher Scientific, NP0335BOX), and MOPS buffer (Thermo Fisher Scientific, NP0001), 25-40 µg protein were used for protein separation. Transfer of protein samples onto a 0.45 µm PVDF membrane (Thermo Fisher Scientific, LC2005) was carried out using a NuPage® XCell II Blot Module, and transfer buffer (Thermo Fisher Scientific, NP0006) with 10% methanol (Sigma, 322415). The iBind™ Western System (Thermo Fisher Scientific) was used for blocking, primary and secondary antibody incubations which details could be found above. A C-Digit scanner (LI-COR) was used for band detection with Image studio software (LI-COR, Version 3.1).

**Proteomic analysis**

Sample preparation, in-gel digestion, sample cleanup and mass spectrometric analysis was carried out as described previously (Dunn, J et al, 2018). For details please see **Appendix material & methods**.

**Real-time PCR and data analysis**

Real-time RT-PCR analysis was performed on a LightCycler 480 Real-Time system (Roche) for 45 cycles, using a SYBR Green I MasterMix (Roche, 04887352001) and primers. 36b4 gene was used as housekeeping gene. Analyses were performed using three technical replicates using the 2-ΔΔCt method.

**Seahorse Mito Stress Test**

3*10^3 of HPLFs per well were seeded into Seahorse XFe96 well plate (Agilent Technologies, 200941) for overnight. After 6 h and 48 h of viral infection, the medium was removed but a nominal 20 µl per well was left. Each well was washed twice with pre-warmed assay medium (Agilent Technologies, 103680). 80µl assay medium were added into each well, and cells were then incubated for 1 h at 37°C. Meanwhile, effector working solutions were prepared and loaded into ports of the XFe96 cartridge which was already rehydrated in XF buffer at 37°C overnight. The cartridge and the utility plate were inserted into XFe96 instrument to calibrate probes. Once the calibration was finished, the utility plate was replaced by cell plate and continued with the assay as indicated. When the progress was completed, cell plate was removed from the instrument. Medium was aspirated slowly from wells and all wells were gently washed with warmed assay buffer, Plates were stored at -20°C or continued with DNA assay for further normalization. Data were analyzed by Seahorse Analytics website and Wave software (Agilent Technologies, Version 2.6.3).

**Statistics**

Statistical analyses were performed using Prism software (GraphPad software, Version 9.4.1). Unpaired t-test was applied to all measurements. Data from Seahorse mito stress assay was analyzed by Seahorse Analytics website and Wave software (Agilent Technologies, Version 2.6.3). All quantification and real time RT-PCR results were presented using style of Mean and Standard Deviation (error bars). Observed differences were calculated for p-values: * $p<0.05$; ** $p<0.01$; ***: $p<0.001$; ****: $p<0.0001$.

## Results

### Human periodontal tissues and fibroblasts express SARS-CoV-2 receptors

We first explored the presence of SARS-CoV-2 receptors: ACE2 and TMPRSS2 using immunofluorescence analysis. The results showed that both ACE2 and TMPRSS2 were highly expressed in the gingiva epithelium, as well as in the periodontal ligament (PDL) cells (Figure 1B). To exclude the noise of the other cell types in the periodontal tissues, we also established collagen gel based 3D human periodontal tissue equivalent using gingival epithelial cells and PDL fibroblasts (Appendix Figure 1A). By analyzing the established PDL 3D equivalent, we observed consistent clear expression of ACE2 and TMPRSS2 both in the epithelial cells and PDL fibroblasts (Figure 1C). Western blotting analysis further confirmed the expression of ACE2 and TMPRSS2 in the cultured PDL fibroblasts (Figure 1D).

### SARS-CoV-2 has high affinity to PDL fibroblasts

We next explored the potentiality of SARS-CoV-2 in infecting PDL fibroblasts. By treating the cells with His Tag conjugated spike protein, followed by immunofluorescent analysis of the spike protein location using an anti-His Tag APC conjugated antibody (Appendix Figure 1B), we could observe clear association of the spike protein with the cells either under natural growing condition (Figure 1E), or in lentitviral mediated ACE2 overexpression (Figure 1D and F). The affinity of spike protein to the cells could be further validated by fluorescence activated cell sorting (FACS) analysis (Figure 1G and H). Therefore, we confirmed that SARS-CoV-2 indeed could infect PDL fibroblasts directly.

### SARS-CoV-2 envelope and membrane proteins induce fibrotic pathogenic phenotypes in PDL fibroblasts

A key pathological hallmark of COVID-19 infection is fibrosis in the lung and potentially also in the other tissues (Spagnolo et al. 2020). To evaluate the consequence of COVID-19 infection on the PDL, we either adopted lentiviral mediated SARS-CoV-2 infection for envelope, membrane or nucleocapsid proteins (Gordon et al. 2020), or applied recombinant spike proteins at 500ng/ml or 5ug/ml, to cultured human PDL fibroblasts. We simulated acute and long infection by infecting or treating PDLs for 6 hours or 48 hours. Cell proliferation was evaluated using Bromodeoxyuridine (BrdU) incorporation followed by immunostaining for anti-BrdU antibodies. The results indicated that under our tested conditions, only membrane protein significantly increased cell proliferation at 6 hours, while at 48 hours, the envelope and membrane proteins could both elevate the BrdU incorporation index (Figure 2A and B; Appendix Figure 2A). Spike protein, on the contrary, could not modulate cell proliferation instead (Figure 2C and D; Appendix Figure 2B).

With Terminal deoxynucleotidyl transferase dUTP nick end labelling (TUNEL), we then evaluated apoptosis status in the cells. The results indicated that at 48 hours, again only the envelope and membrane proteins, but not the nucleocapsid nor spike proteins could increase apoptosis (Figure 2E-H; Appendix 3A and B). In the meanwhile, for cellular senescence status in the tested conditions, the results showed that at 6 and 48 hours, only the envelope and membrane protein groups resulted in a significant increase in senescent cells (Figure 2I-L; Appendix 4A and B).

We then investigated extracellular matrix production by focusing on Collagen I and MMP1, the two key components and enzymes responsible for PDL tissue integrity. Interestingly, western blotting analysis revealed that all the SARS-CoV-2 structure proteins could induce Collagen I production (Figure 3A-F), and reduce MMP1 production, spike protein elevated MMP1 expression under one of the two tested doses (Figure 3A-F). Real time RT-PCR analysis suggested the Collagen I expression induction and MMP1

downregulation were modulated at transcription levels (Figure 3G and H). By applying a hydrogel based 3D culture system, we evaluated Collagen I and MMP1 production and deposition at three dimensions. The results showed that Collagen I deposition were again highly elevated, especially in the envelope and membrane protein groups (Figure 3I and J). And membrane and nucleocapsid proteins could bring down the MMP1 expression (Figure 3K and L).

Together, with the evidence of elevated fibroblast proliferation, apoptosis and senescence concomitantly, alongside increased matrix deposition and reduced metalloprotease production, our results pointed out that the SARS-CoV-2's envelope and membrane were the most potent components to induce a fibrotic degeneration phenotype in PDL cells.

**SARS-CoV-2 envelope and membrane proteins down-regulate mitochondrial β-oxidation**

To understand the molecular regulation mechanisms behind the observed pathological consequence of SARS-CoV-2 infection, we performed proteomic analysis on the treated PDL fibroblasts, by focusing on the effects of the envelope, membrane and nucleocapsid proteins. We then identified a group of proteins that were both suppressed at 6 and 48 hours post infection (Figure 4A; Appendix Table 1). Among the significantly down-regulated proteins, the trifunctional enzyme subunit alpha, isoform 2 of very long-chain specific acyl-CoA dehydrogenase, cytochrome c oxidase subunit 2 and isoform cytoplasmic of fumarate hydratase are all essential enzymes in mitochondria functions and mitochondrial β-oxidation (Figure 4A). Particularly the trifunctional enzyme subunit alpha, isoform 2 of very long-chain specific acyl-CoA dehydrogenase were connected with mitochondrial fatty acid β-oxidation.

We therefore conducted Seahorse Mito stress test (Appendix Figure 5) for evaluating if and how the mitochondria fatty acid pathway's function could be affected by SARS-CoV-2 infection. The results showed that indeed, both SARS-CoV-2 envelope and membrane protein, could inhibit fatty acid β-oxidation at both 6 hours and 48 hours' time points (Figure 4B and C).

**Chemical inhibition of mitochondrial β-oxidation can mirror the fibrotic pathological consequence of SARS-CoV-2 infection**

To validate the effect of fatty acid β-oxidation pathway inhibition, we next treated the cells with etomoxir, a specific inhibitor of the pathway through inhibiting carnitine palmitoyltransferase I (CPT1), a key regulatory enzyme for fatty acid to be imported into mitochondria (Figure 5A). The results indicated that etomoxir treatment could indeed mirror the same pathological consequence on the fibroblasts, similar to SARS-CoV-2 infection. We again observed significantly increased cell proliferation (Figure 5B; Appendix figure 6), apoptosis (Figure 5C; Appendix figure 6), and senescence (Figure 5D and E), together with elevated Collagen I production (Figure 5F and G). Similarly, in the hydrogel based three dimension PDL fibroblasts culture, Collagen I deposition was highly increased in the etomoxir treated samples (Figure 5H and I).

## Discussion

COVID-19 infection can cause a series of symptoms. Among them, fibrosis particularly in lung tissues has evoked significant attention due to the severe consequence on patient life and health quality. Although the current dominant SARS-CoV-2 variants (such as the Omicron) induce milder symptoms in human bodies, the exact pathological consequence of COVID-19 to different human tissues and organs, particularly for oral cavity tissues are still missing. Current concepts of COVID-19 etiology suggest lung fibrosis caused by SARS-CoV-2 infection can be mainly due to damages on lung epithelial cells that trigger acute inflammation followed by fibroblast hyperproliferation (Merad and Martin 2020). However, as SARS-CoV-2 infection is rapid and it is difficult to distinguish if the deeper cells (such as fibroblasts) can also be infected directly. We therefore cannot neglect the potential direct infection of fibroblasts by SARS-CoV-2. In particular, PDL is one of the most vulnerable human tissues that extrinsic virus and bacteria can often enter PDL directly in pathological conditions (Kononen et al. 2019). As such, it is reasonable to postulate that SARS-CoV-2 can also directly infect PDL fibroblasts in the already damaged PDL and induce further pathological changes. Attentions should be made by dental clinicians to the patients who got COVID-19 and appeared to be diagnosed with periodontal disease at the same time, particularly for those long COVID and repeated infected cases.

Our results also suggested SARS-CoV-2 infection indeed can directly induce fibrotic disease phenotypes in fibroblasts through distinct pathways. Mitochondrial fatty acid β-oxidation is the major pathway responsible for fatty acids degradation, hence is essential for human body energy homeostasis. Impeding the pathway can cause different disorders (Merritt et al. 2018). Very recent studies have observed mitochondrial dysregulation in COVID-19 patient blood cells (Ajaz et al. 2021; Guntur et al. 2022). Interestingly, the dysfunction of the fatty acid oxidation has been previously connected with fibrosis

particularly in the lung and kidney (Geng et al. 2021; Jang et al. 2020){Merritt, 2018 #12}. For the first time, our findings further confirmed that in the fibroblasts, SARS-CoV-2 could induce fibrotic degeneration directly, through down-regulating fatty acid β-oxidation, particularly by the virus' envelope and membrane proteins.

Among the SARS-CoV-2's structural proteins: envelope, membrane, nucleocapsid and spike, the first three proteins are stable structure proteins for all the reported variants, while so far all of the identified mutations happen inside the spike proteins (Harvey et al. 2021). Although spike protein is still the target especially for COVID-19 vaccine development, increasing evidence suggest the other SARS-CoV-2 structural proteins might have unexpected important roles in inducing COVID-19 symptoms. Previous structural analysis of the envelope protein suggested it might be important for virus pathogenicity (Mandala et al. 2020). The envelope protein can also physically increase intra-Golgi pH and forms cation channel(Cabrera-Garcia et al. 2021), and biochemically modulate spike protein in the meantime (Boson et al. 2021). The most abundant protein: the membrane protein in the SARS-CoV-2 virus, is rationally important for virus assembly (Zhang et al. 2022). Our results further confirmed that the envelope and membrane proteins are actually responsible for the fibrosis phenotypes in the cells by down regulating the key fatty acid β-oxidation regulator such as the trifunctional enzyme subunit alpha. The molecular mechanism behind this regulation axis would require further biochemical analysis.

In this study, our results provide novel mechanistic insights into how SARS-CoV-2 infection can affect human health, particularly for inducing fibrosis, at the cell and molecular level. The findings could be possibly extended to the other body systems to explain and explore the fibrosis pathology and treatment.

**Acknowledgement**

We would like to thank the helps provided by Dr Jane Carré for assisting Seahorse analysis, Dr Paul Waines for FACS operation, and Prof. Simon Whawell for critical reading. This study was supported by a research grant from the European Orthodontic Society to Bing Hu. Yan Gao received a fellowship from the Peninsula Dental Social Enterprise.

Author contributions

Yan Gao: Contributed to conception and design, acquisition, analysis, and interpretation, critically revised the manuscript.

Wai Ling Kok: Contributed to acquisition and analysis and critically revised the manuscript.

Vikram Sharma: Contributed to acquisition and analysis and critically revised the manuscript.

Charlotte Sara Illsley: Contributed to conception and design, and critically revised the manuscript.

Sally Hanks: Contributed to conception and design, and critically revised the manuscript.

Christopher Tredwin: Contributed to conception and design, and critically revised the manuscript.

Bing Hu: Contributed to conception and design, interpretation, and drafted and critically revised the manuscript.

All authors gave their final approval and agree to be accountable for all aspects of the work. The authors declare that there is no conflict of interest regarding the publication of this article.

**Material and data availability statement**

The materials used and datasets generated during and/or analyzed during the current study are available from Professor Bing Hu on reasonable request.

## References

Ajaz S, McPhail MJ, Singh KK, Mujib S, Trovato FM, Napoli S, Agarwal K. 2021. Mitochondrial metabolic manipulation by sars-cov-2 in peripheral blood mononuclear cells of patients with covid-19. Am J Physiol Cell Physiol. 320(1):C57-C65.

Baghizadeh Fini M. 2020. Oral saliva and covid-19. Oral Oncol. 108:104821.

Boson B, Legros V, Zhou B, Siret E, Mathieu C, Cosset FL, Lavillette D, Denolly S. 2021. The sars-cov-2 envelope and membrane proteins modulate maturation and retention of the spike protein, allowing assembly of virus-like particles. J Biol Chem. 296:100111.

Cabrera-Garcia D, Bekdash R, Abbott GW, Yazawa M, Harrison NL. 2021. The envelope protein of sars-cov-2 increases intra-golgi ph and forms a cation channel that is regulated by ph. J Physiol. 599(11):2851-2868.

Ferretti L, Wymant C, Kendall M, Zhao L, Nurtay A, Abeler-Dorner L, Parker M, Bonsall D, Fraser C. 2020. Quantifying sars-cov-2 transmission suggests epidemic control with digital contact tracing. Science. 368(6491).

Geng J, Liu Y, Dai H, Wang C. 2021. Fatty acid metabolism and idiopathic pulmonary fibrosis. Front Physiol. 12:794629.

Gordon DE, Jang GM, Bouhaddou M, Xu J, Obernier K, O'Meara MJ, Guo JZ, Swaney DL, Tummino TA, Huttenhain R et al. 2020. A sars-cov-2-human protein-protein interaction map reveals drug targets and potential drug-repurposing. bioRxiv.

Guntur VP, Nemkov T, de Boer E, Mohning MP, Baraghoshi D, Cendali FI, San-Millan I, Petrache I, D'Alessandro A. 2022. Signatures of mitochondrial dysfunction and impaired fatty acid metabolism in plasma of patients with post-acute sequelae of covid-19 (pasc). Metabolites. 12(11).

Harvey WT, Carabelli AM, Jackson B, Gupta RK, Thomson EC, Harrison EM, Ludden C, Reeve R, Rambaut A, Consortium C-GU et al. 2021. Sars-cov-2 variants, spike mutations and immune escape. Nat Rev Microbiol. 19(7):409-424.

Hoffmann M, Kleine-Weber H, Schroeder S, Kruger N, Herrler T, Erichsen S, Schiergens TS, Herrler G, Wu NH, Nitsche A et al. 2020. Sars-cov-2 cell entry depends on ace2 and tmprss2 and is blocked by a clinically proven protease inhibitor. Cell. 181(2):271-280 e278.

Huang N, Perez P, Kato T, Mikami Y, Okuda K, Gilmore RC, Conde CD, Gasmi B, Stein S, Beach M et al. 2021. Sars-cov-2 infection of the oral cavity and saliva. Nat Med. 27(5):892-903.

Huang Y, Yang C, Xu XF, Xu W, Liu SW. 2020. Structural and functional properties of sars-cov-2 spike protein: Potential antivirus drug development for covid-19. Acta Pharmacol Sin. 41(9):1141-1149.

Jang HS, Noh MR, Kim J, Padanilam BJ. 2020. Defective mitochondrial fatty acid oxidation and lipotoxicity in kidney diseases. Front Med (Lausanne). 7:65.

Kononen E, Gursoy M, Gursoy UK. 2019. Periodontitis: A multifaceted disease of tooth-supporting tissues. J Clin Med. 8(8).

Lopez-Leon S, Wegman-Ostrosky T, Perelman C, Sepulveda R, Rebolledo PA, Cuapio A, Villapol S. 2021. More than 50 long-term effects of covid-19: A systematic review and meta-analysis. Sci Rep. 11(1):16144.

Mandala VS, McKay MJ, Shcherbakov AA, Dregni AJ, Kolocouris A, Hong M. 2020. Structure and drug binding of the sars-cov-2 envelope protein transmembrane domain in lipid bilayers. Nat Struct Mol Biol. 27(12):1202-1208.

Merad M, Martin JC. 2020. Pathological inflammation in patients with covid-19: A key role for monocytes and macrophages. Nat Rev Immunol. 20(6):355-362.

Merritt JL, 2nd, Norris M, Kanungo S. 2018. Fatty acid oxidation disorders. Ann Transl Med. 6(24):473.

Ni W, Yang X, Yang D, Bao J, Li R, Xiao Y, Hou C, Wang H, Liu J, Yang D et al. 2020. Role of angiotensin-converting enzyme 2 (ace2) in covid-19. Crit Care. 24(1):422.

Qi X, Northridge ME, Hu M, Wu B. 2022. Oral health conditions and covid-19: A systematic review and meta-analysis of the current evidence. Aging Health Res. 2(1):100064.

Satarker S, Nampoothiri M. 2020. Structural proteins in severe acute respiratory syndrome coronavirus-2. Arch Med Res. 51(6):482-491.

Spagnolo P, Balestro E, Aliberti S, Cocconcelli E, Biondini D, Casa GD, Sverzellati N, Maher TM. 2020. Pulmonary fibrosis secondary to covid-19: A call to arms? Lancet Respir Med. 8(8):750-752.

Wang J, Kaperak C, Sato T, Sakuraba A. 2021. Covid-19 reinfection: A rapid systematic review of case reports and case series. J Investig Med. 69(6):1253-1255.

Wang T, Du Z, Zhu F, Cao Z, An Y, Gao Y, Jiang B. 2020. Comorbidities and multi-organ injuries in the treatment of covid-19. Lancet. 395(10228):e52.

Wise J. 2022. Covid-19: Two million people in the uk are estimated to be experiencing long covid, says ons. BMJ. 377:o1391.

Zhang Z, Nomura N, Muramoto Y, Ekimoto T, Uemura T, Liu K, Yui M, Kono N, Aoki J, Ikeguchi M et al. 2022. Structure of sars-cov-2 membrane protein essential for virus assembly. Nat Commun. 13(1):4399.

## Figure legends

**Figure 1. Human periodontal cells express ACE2 and TMPRSS2, and prone to SARS-CoV-2 infection.**

A. Illustration of SARS-CoV-2's key structure proteins;

B and C. Immunofluorescence analysis of ACE2 and TMPRSS2 expression in human periodontal (PDL) tissues (B) and 3D equivalent (C) using specific antibodies and Alexa 568 (red) or Alexa 488 (green) conjugated secondary antibodies. Dotted lines mark epithelia-mesenchymal junctions.

D. Western blotting analysis of ACE2 and TMPRSS2 expression in human periodontal ligament fibroblasts (HPLF) under normal growing condition, and lentiviral mediated ACE2 overexpression. Lamin B1 was used as loading control. All the blots were performed sequentially on the same membrane.

E and F. Normal HPLF or the cells with ACE2 overexpression was treated with His tagged spike (S) protein first then traced using Anti-His Tag APC conjugated antibodies. For controls, the spike protein was omitted (also see Appendix Figure 1B).

G and H: FACS analysis of the samples showed in E and F. Note the anti-His Tag APC antibody did show background but the shifting of the florescence peak could still be visualized (H). n: particle (cell) count.

Bars: 100um

**Figure 2. SARS-CoV-2 envelope and membrane protein could induce PDL fibroblast proliferation, apoptosis and senescence.**

A-D. BrdU incorporation analysis on the PDL fibroblasts treated with indicated conditions and time. Each data dot represent one random field in triplicated samples. Dunnett's test was used for statistical analysis. Representative images can be found from Appendix Figure 2.

E-H. TUNEL analysis on the PDL fibroblasts treated with indicated conditions and time. Each data dot represent one random field in triplicated samples. Dunnett's correction was used for statistical analysis. Representative images can be found from Appendix Figure 3.

I-L. Quantification of senescence-associated β-galactosidase positive cells (for identifying senescence) images on the indicated conditions. Each data dot represent one random field in triplicated samples. Representative images can be found from Appendix Figure 4.

ns: no significance; ** $p<0.01$; ***: $p<0.001$.

**Figure 3. SARS-CoV-2 infection could induce collagen matrix deposition and MMP1 reduction.**

A-F. Western blotting analysis of Collagen I and MMP1 production in the cells under indicated conditions. A shows blotting results. B and C represents statistical analysis (each dot represents a single individual measurement). Dunnett's test was used for statistical analysis.

ns: no significance;

G and H. Real time RT-PCR analysis of Collagen 1 and MMP1 transcription in the indicated conditions.

I-L. Representative three dimensional analysis of Collagen I and MMP1 expression in the indicated conditions at 7 days after seeding the cells and infection in the hydrogel. The gel were stained using anti-Collagen I and MMP1 specific antibodies and developed with Alexa 568 (red) or 488 (Green) conjugated secondary antibodies. Each data dot represent one random field in triplicated samples.

ns: no significance; * $p<0.05$; ** $p<0.01$; ***: $p<0.001$; ****: $p<0.0001$.

Bars: 100um

**Figure 4. Envelope and membrane proteins are responsible to SARS-CoV-2 infection to PDL fibroblasts caused deregulate of mitochondria fatty acid β-oxidation pathway.**

A. Summary of proteomic analysis results of PDL fibroblasts treated with indicated conditions and time points. Only proteins showed <0.50 or >1.5 fold changes were included. For full data analysis please see Appendix Table 1.

B and C. 6 and 48 hours Seahorse palmitate oxidation stress tests under indicated conditions either with vehicle alone or Etomoxir. Note for both time points, envelope group were down-regulated with/without etomoxir treatments, while membrane group also showed down regulation but only in the etomoxir treated samples.

**Figure 5. Mitochondrial fatty acid β-oxidation inhibition mirrored fibrotic degeneration phenotypes in PDL fibroblasts.**

A. Schematic drawing of fatty acid β-oxidation pathway (left) and the Etomoxir functioning mechanism (right).

B and C. BrdU and TUNEL analysis of etomoxir treated cells. For representative images please see Appendix Figure 6. Each data dot represent one random field in triplicated samples.

D and E. Representative senescence-associated β-galactosidase assay on indicated conditions. Note increased senescence in the etomoxir treated samples. Each data dot represent one random field in triplicated samples.

F and G. Western blotting analysis of Collagen I expression in HPLF under etomoxir treatment or vehicle (DMSO) alone. Lamin B1 was used as loading control. All the blots were performed sequentially on the same membrane. G represents statistical analysis (each dot represents a single individual measurement)

H and I. Representative 3D analysis of Collagen I expression in the indicated conditions at 48 hours after seeding the cells and etomoxir treatment in the hydrogel. The gel was stained using

anti-Collagen I specific antibodies and developed with Alexa 568 (red) conjugated secondary antibodies. Each data dot represent one random field in triplicated samples.

* $p<0.05$; ** $p<0.01$; ***: $p<0.001$; ****: $p<0.0001$.

Bars: 100um

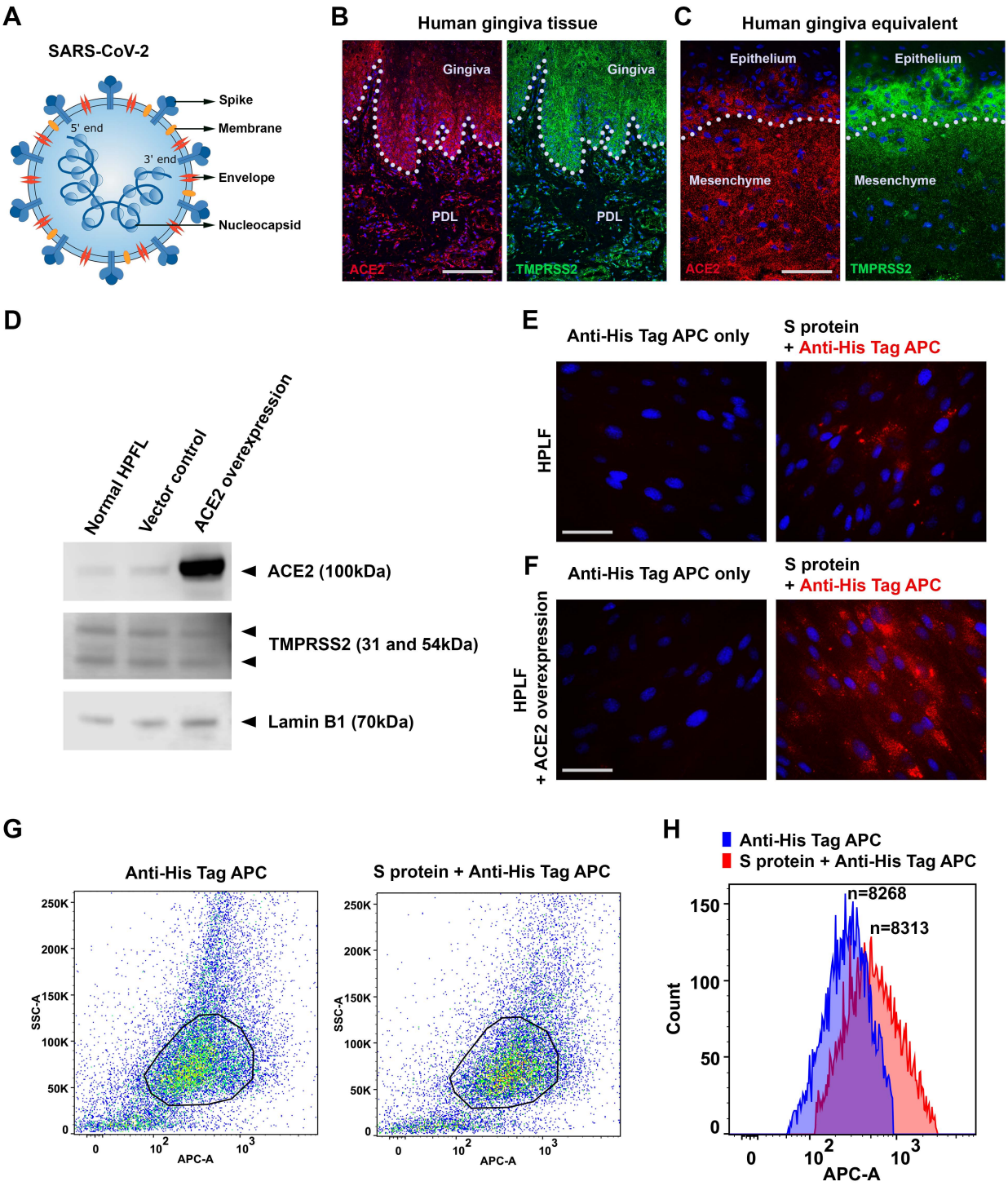
A
SARS-CoV-2
Spike
Membrane
Envelope
Nucleocapsid
5' end
3' end
B
Human gingiva tissue
Gingiva
PDL
ACE2
TMPRSS2
C
Human gingiva equivalent
Epithelium
Mesenchyme
ACE2
TMPRSS2
D
Normal HPFL
Vector control
ACE2 overexpression
ACE2 (100kDa)
TMPRSS2 (31 and 54kDa)
Lamin B1 (70kDa)
E
Anti-His Tag APC only
S protein
+ Anti-His Tag APC
HPLF
F
Anti-His Tag APC only
S protein
+ Anti-His Tag APC
HPLF
+ ACE2 overexpression
G
Anti-His Tag APC
S protein + Anti-His Tag APC
SSC-A
APC-A
250K
200K
150K
100K
50K
0
H
Anti-His Tag APC
S protein + Anti-His Tag APC
n=8268
n=8313
Count
APC-A

Figure 1

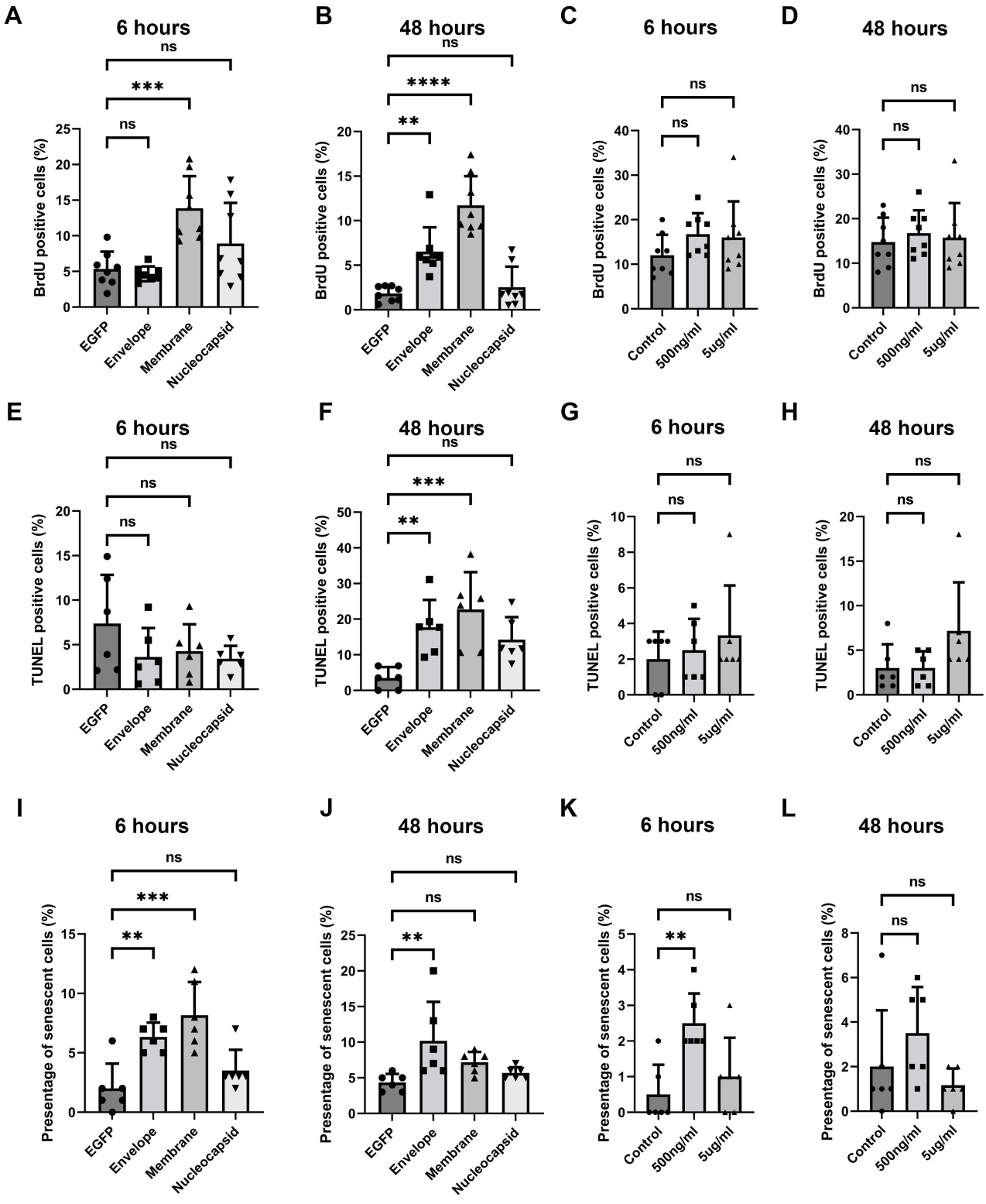
A
6 hours
BrdU positive cells (%)
ns
***
ns
EGFP
Envelope
Membrane
Nucleocapsid
B
48 hours
BrdU positive cells (%)
ns
****
**
EGFP
Envelope
Membrane
Nucleocapsid
C
6 hours
BrdU positive cells (%)
ns
ns
Control
500ng/ml
5ug/ml
D
48 hours
BrdU positive cells (%)
ns
ns
Control
500ng/ml
5ug/ml
E
6 hours
TUNEL positive cells (%)
ns
ns
ns
EGFP
Envelope
Membrane
Nucleocapsid
F
48 hours
TUNEL positive cells (%)
ns
***
**
EGFP
Envelope
Membrane
Nucleocapsid
G
6 hours
TUNEL positive cells (%)
ns
ns
Control
500ng/ml
5ug/ml
H
48 hours
TUNEL positive cells (%)
ns
ns
Control
500ng/ml
5ug/ml
I
6 hours
Presentage of senescent cells (%)
ns
***
**
EGFP
Envelope
Membrane
Nucleocapsid
J
48 hours
Presentage of senescent cells (%)
ns
ns
**
EGFP
Envelope
Membrane
Nucleocapsid
K
6 hours
Presentage of senescent cells (%)
ns
ns
**
Control
500ng/ml
5ug/ml
L
48 hours
Presentage of senescent cells (%)
ns
ns
Control
500ng/ml
5ug/ml

**Figure 2**

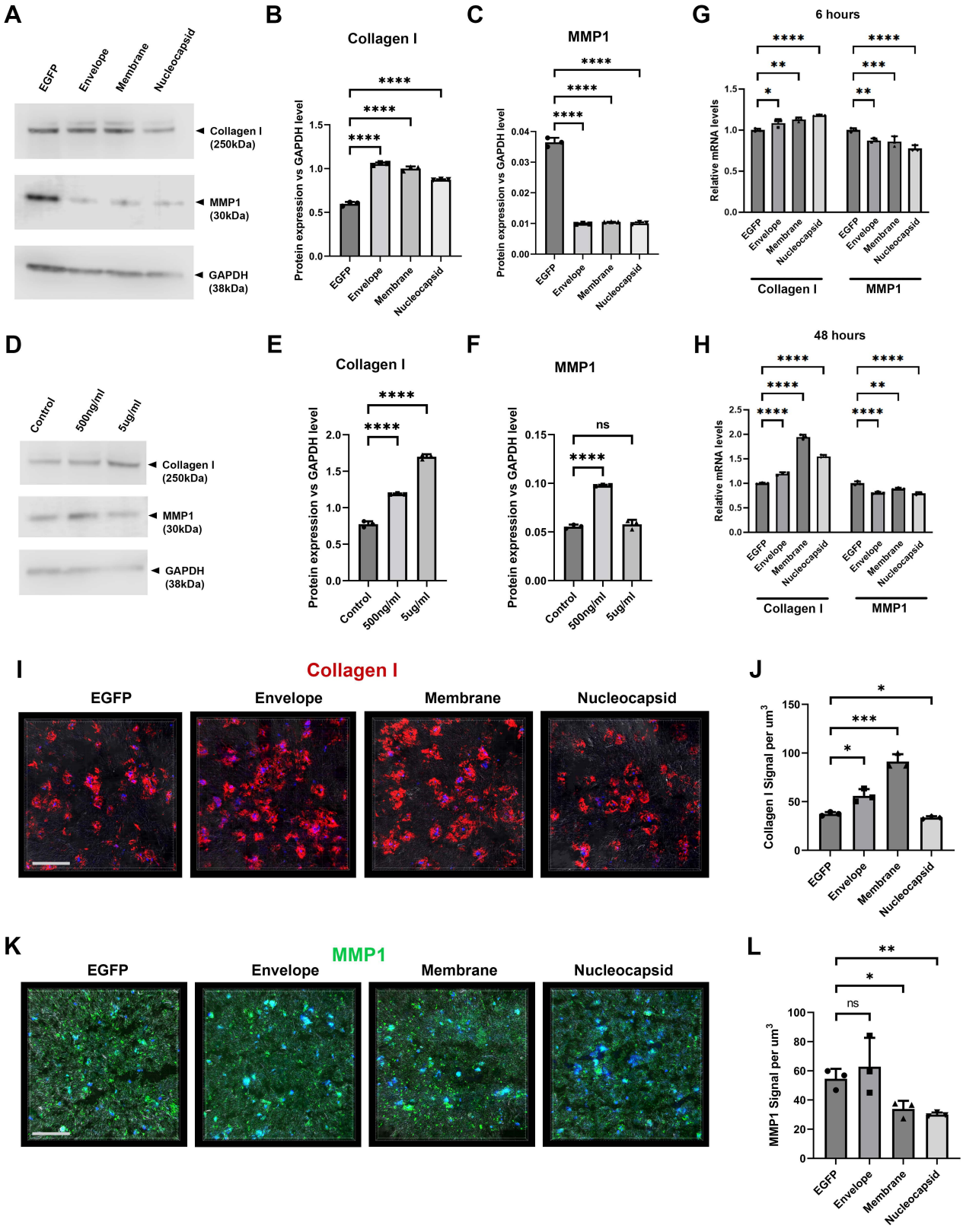
A
EGFP
Envelope
Membrane
Nucleocapsid
Collagen I (250kDa)
MMP1 (30kDa)
GAPDH (38kDa)
B
Collagen I
Protein expression vs GAPDH level
C
MMP1
Protein expression vs GAPDH level
G
6 hours
Relative mRNA levels
Collagen I
MMP1
D
Control
500ng/ml
5ug/ml
Collagen I (250kDa)
MMP1 (30kDa)
GAPDH (38kDa)
E
Collagen I
Protein expression vs GAPDH level
F
MMP1
Protein expression vs GAPDH level
ns
H
48 hours
Relative mRNA levels
Collagen I
MMP1
I
Collagen I
EGFP
Envelope
Membrane
Nucleocapsid
J
Collagen I Signal per um3
K
MMP1
EGFP
Envelope
Membrane
Nucleocapsid
L
MMP1 Signal per um3
ns

Figure 3

**A**

**Protein expression levels (based on proteomic analysis results)**

| | Envelope vs. EGFP | | Membrane vs. EGFP | | Nucleocapsid vs. EGFP | |
|---|---|---|---|---|---|---|
| | 6h | 48h | 6h | 48h | 6h | 48h |
| Proteasome subunit beta type-2 | 0.37 | 0.30 | | | | |
| Trifunctional enzyme subunit alpha | 0.38 | 0.25 | 0.45 | 0.14 | | |
| 60S ribosomal protein L29 | 2.47 | 2.21 | | | | |
| Isoform 2 of Very long-chain specific acyl-CoA dehydrogenase | | | 0.19 | 0.09 | | |
| 60S ribosomal protein L27a | | | 0.22 | 0.16 | | |
| Isoform 2 of Ran-specific GTPase-activating protein | | | 0.34 | 0.43 | | |
| Tubulin beta-2A chain | | | | | 0.36 | 0.36 |
| Cytochrome c oxidase subunit 2 | | | | | 0.37 | 0.21 |
| Isoform Cytoplasmic of Fumarate hydratase | | | | | 0.45 | 0.27 |

**B**

6 hours

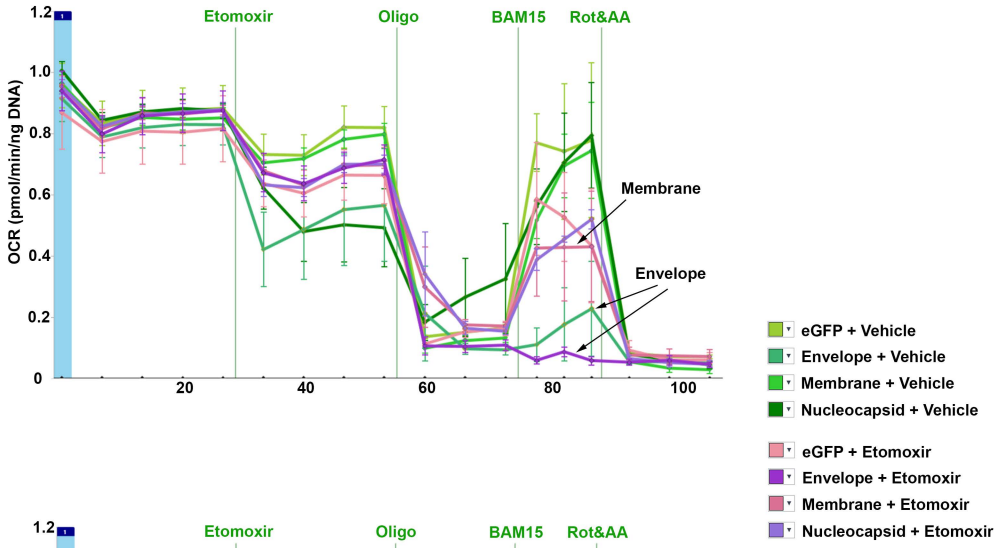


**C**

48 hours

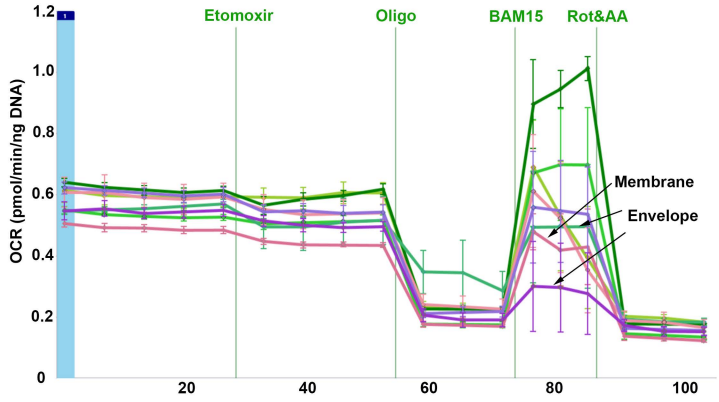


**Figure 4**

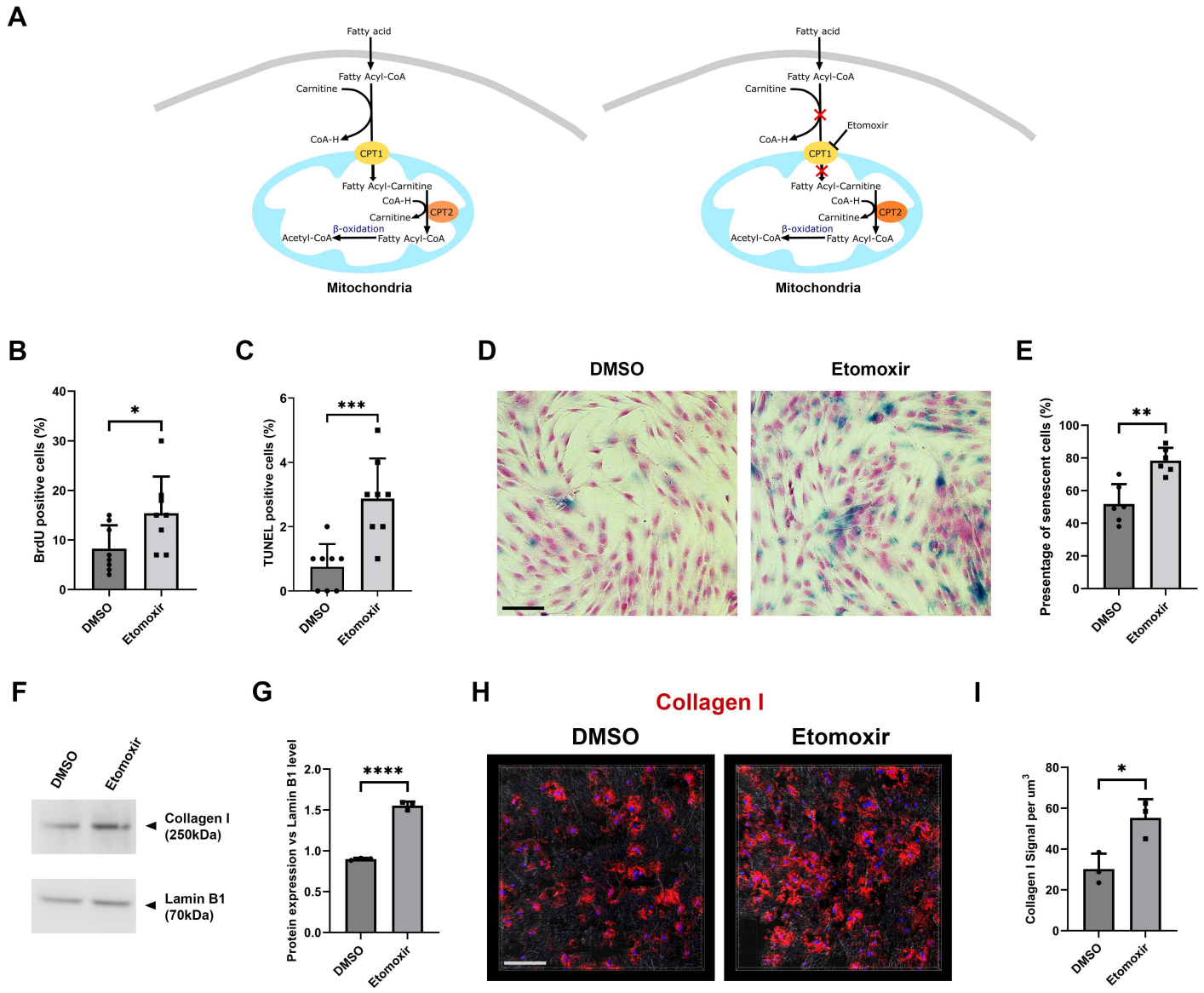
A
Fatty acid
Fatty Acyl-CoA
Carnitine
CoA-H
CPT1
Fatty Acyl-Carnitine
CoA-H
Carnitine
CPT2
β-oxidation
Acetyl-CoA
Fatty Acyl-CoA
Mitochondria
Etomoxir
B
BrdU positive cells (%)
DMSO
Etomoxir
C
TUNEL positive cells (%)
D
DMSO
Etomoxir
E
Presentage of senescent cells (%)
F
Collagen I (250kDa)
Lamin B1 (70kDa)
G
Protein expression vs Lamin B1 level
H
Collagen I
I
Collagen I Signal per um3

Figure 5

# SARS-CoV-2 causes periodontal fibrosis by deregulating mitochondrial β-oxidation

Yan Gao[1], Wai Ling Kok[1], Vikram Sharma[2], Charlotte Sara Illsley[1], Sally Hanks[1], Christopher Tredwin[1], Bing Hu[1*]

1. Stem Cells & Regenerative Medicine Laboratory, Peninsula Dental School, Faculty of Health, University of Plymouth, 16 Research Way, Plymouth, PL6 8BU, UK

2. School of Biomedical Sciences, Faculty of Health, University of Plymouth, 16 Research Way, Plymouth, PL6 8BU, UK

* Corresponding author

Professor Bing Hu

Email: bing.hu@plymouth.ac.uk

**Appendix Materials & Methods**

**Appendix Figure 1 to 6**

**Appendix Table 1 and 2**

## Appendix Materials & Methods

### Immunostaining

Human oral cavity cancer tissue array that contains normal human gingiva tissues, HnTMA108 was purchased from Creative Bioarray. Slides were heated to 60°C for 20 min before being twice washed in xylenes (Sigma Aldrich 534056) for 10 mins. rehydrated with 100% industrial methylated spirit (IMS) (VWR, 23684.360) for 5 min, before being washed for 2 min in 95% IMS and then 70% IMS. Antigen retrieval was performed by 95°C water bath, slide was submerged in pre-warmed 0.01 M citrate buffer solution (citric acid (Sigma Aldrich, C2404) & 0.05% Tween-20 (Sigma Aldrich, P9416)), pH 8.0 for 20 min. Slide was washed briefly in tap water before washed 3 times in phosphate buffered saline (PBS, Sigma, P4417) containing 0.1% Triton-X100, (Sigma, X100) (PBST) for 5 min per wash. Non-Specific binding was blocked by incubation for 60 min with PBST containing 5% Donkey Serum (Sigma, D9663). Primary antibodies were incubated overnight at 4°C. Slide was washed 3 times in PBST before incubation with secondary antibodies for 2 h at room temperature. Nuclei were counterstained with 2 µg/ml DAPI (Sigma Aldrich, D9542) for 10 min then slide was mounted with Dako fluorescent mounting medium (Dako North America Inc., S3023). IF images were captured using a Leica DMI6000 confocal microscope with a Leica TCS SP8 attachment at a scanning thickness of 1 µm per section. The microscope is running LAS X (Leica, Version 3.7.3.23245) software from Leica. Images for comparison were taken using the same settings and post imaging processing was conducted using Adobe Photoshop (Adobe, Version 24.0.1).

For frozen section, the slides were air-dried for 1 h then fixed with 4% paraformaldehyde (PFA; Sigma in PBS) for 30 min, then washed twice with PBST 5 min each. Primary antibodies were incubated overnight at 4°C. Slides were washed three times in PBST before incubation with secondary antibodies for 2 h at room temperature. Nuclei were counterstained with 2 µg/ml DAPI for 10 min.

Images were captured using a Leica DMI6000 confocal microscope with a Leica TCS SP8 attachment. The microscope is running LAS X (Leica, Version 3.7.3.23245) software. Images for

comparison were taken using the same settings and post imaging processing was conducted using Adobe Photoshop (Adobe, Version 24.0.1). Images of 3D equivalents were visualized by Imaris software (Bitplane, Version 9.0.2).

**BrdU incorporation assay**

5*10^3 of HPLFs were seeded into a black 96 well plate (GBO, 655090). After the spike protein treatment or lentiviral infection, BrdU cell prolife labelling reagent (Amersham-GE, RPN201, 1:1000) was diluted in complete cell culture medium then added into dishes for 2-3 h. Cells were washed 3 more times with PBS for 2 min each, then fixed in 4% PFA for 30 min followed by washing twice in PBS. Cells were treated with 100 µl 2N hydrochloric acid (HCl) (Sigma, H1758-100ml) for 30 min before they were stained with anti-BrdU antibody (Abcam, ab6326, 1:500). The antibody staining procedures were exactly as above except that the blocking buffer was prepared with 2.5% bovine serum albumin (BSA) (Sigma. A2153) in PBST. Images were processed in Image J software (National Institutes of Health, Bethesda, MD, USA, Version 1.53k). BrdU-positive cells and total cell number were quantified using 'Analyze Particles' function.

**Terminal deoxynucleotidyl transferase dUTP nick end labelling (TUNEL) assay**

5*10^3 of HPLFs were seeded into black 96 well plate. After the spike protein treatment or lentiviral infection, cells were washed briefly for 5 sec in PBS twice, then fixed in 4% PFA for 30 min and washed twice in PBS 5 min each. Cells were permeabilized by PBST for 2 min on ice then incubated in 50 µl TUNEL mixture (In Situ Cell Death Detection Kit, Fluorescein, version 17, Roche) for 2 h at 37°C in humid atmosphere. After the washing and mounting, images were taken by Leica IM8 conducted using Adobe Photoshop.

**Senescence assay**

5*10^4 of HPLFs were seeded in 24 well plate. After the spike protein treatment or lentiviral infection, cells were washed briefly with PBS, the fixative solution from the senescence kit (Senescence b-galactosidase kit, Cell Signalling, 9860S) was added to each well for 15 min at room temperature. Cells were rinsed 2 times with PBS then β-Galactosidase Staining Solution, pH 6.0, was added into each well, and at the meantime pH 4.0 was added into spare wells as positive control. The plate was incubated at 37°C at least overnight in a dry incubator without $CO_2$. Cells were washed twice with PBS then stained with nuclear fast red solution (Sigma, N8002) for 20 min then washed with distilled $H_2O$. All wells were mounted with 70% glycerol (Sigma, G2025) and images were taken with Leica IM8 conducted using Adobe Photoshop.

**Proteomic analysis**

HPLFs were seeded in 6cm dishes and performed viral infection and protein treatment for 6 h and 48 h. To collect protein after each time points, culture media was removed from the culture dishes and cells were washed in pre-cooled HBSS twice. HBSS was removed and replaced with ice-cold RIPA buffer (ThermoFisher, 89901) supplemented with Halt™ Protease and Phosphatase Inhibitor Cocktail (ThermoFisher , 78440) at 1:100. The cells were detached from the dish using a cell scraper and then collected into an Eppendorf tube on ice then incubated for 30 min with frequent agitation for efficient cell lysis and solubilisation of proteins. Tubes were spun down at 15,000 rpm for 15 min at 4°C so the supernatant containing the protein could be collected and stored at -80°C until ready to load onto a gel. 15 µg protein samples were run on a Nupage 4-12% Bis-Tris protein gel at 200V for 45 min. Gel was rinsed with water before fixing in 40% ethanol and 10% acetic acid for 15 min with gentle agitation. After washing the gel twice in water, the gel was stained overnight in QC colloidal Coomassie Blue G-250 (Biorad, 161-0803). The gel was destained for 1 h with changes of water every 15 min until protein bands were visible. Every sample lane was cut into 4 fractions and each fraction further cut into 1-2 mm cubes for equilibration. In-gel digestion, sample cleanup and mass

spectrometric analysis was carried out as described previously (Dunn, J et al, 2018). All samples were stored at -20°C or analyze directly using mass spectrometry.

## Appendix Figures

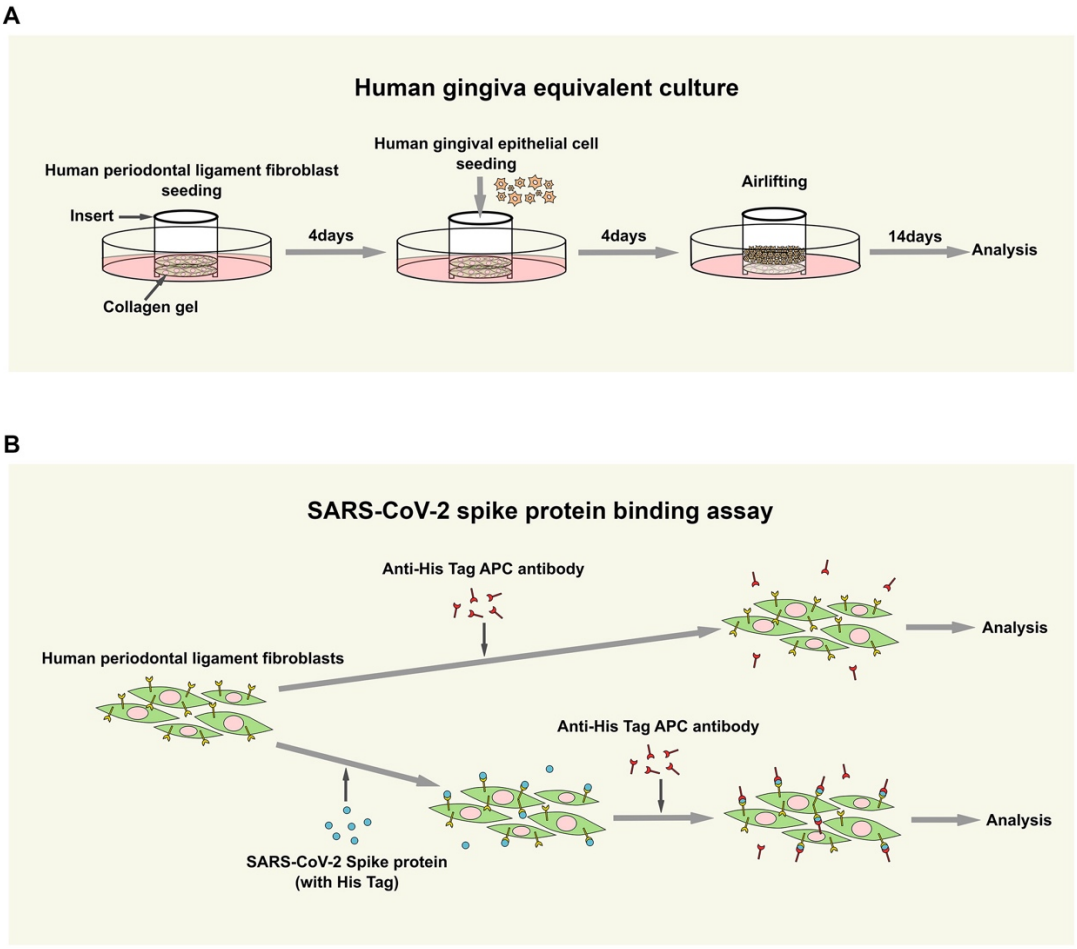


**Appendix Figure 1. Illustration of human gingiva equivalent culture and spike protein binding assay.**

A. For human gingiva equivalent culture, HPLF were seeded into collagen gel supported by a cell culture insert cylinder. 4 days later human gingival epithelial cells were seeded on top of the culture. After a further 4 days, the culture were lifted to air-liquid interface to allow stratification for 14 days before further analysis.

B. To test the binding of spike protein to HPLF cells, the cells were treated with His Tag conjugated spike protein first then traced using anti-His Tag APC conjugated antibodies. For control, the spike proteins were omitted.

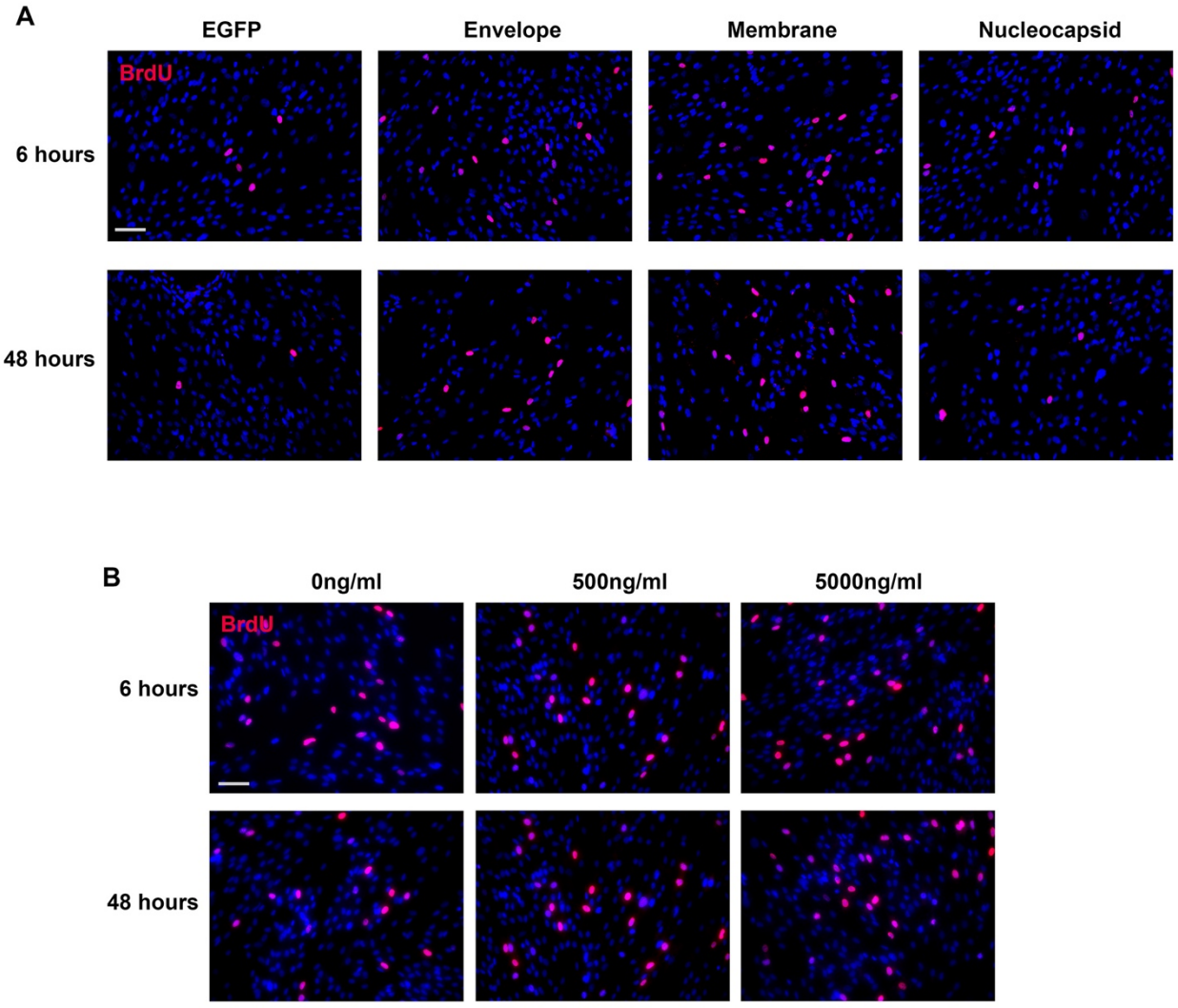


**Appendix Figure 2. SARS-CoV-2 envelope and membrane protein could induce PDL fibroblast proliferation.**

Representative field images of BrdU incorporation analysis in the indicated conditions. Quantitative analysis can be found from Figure 2 A-D.

Bars: 100um

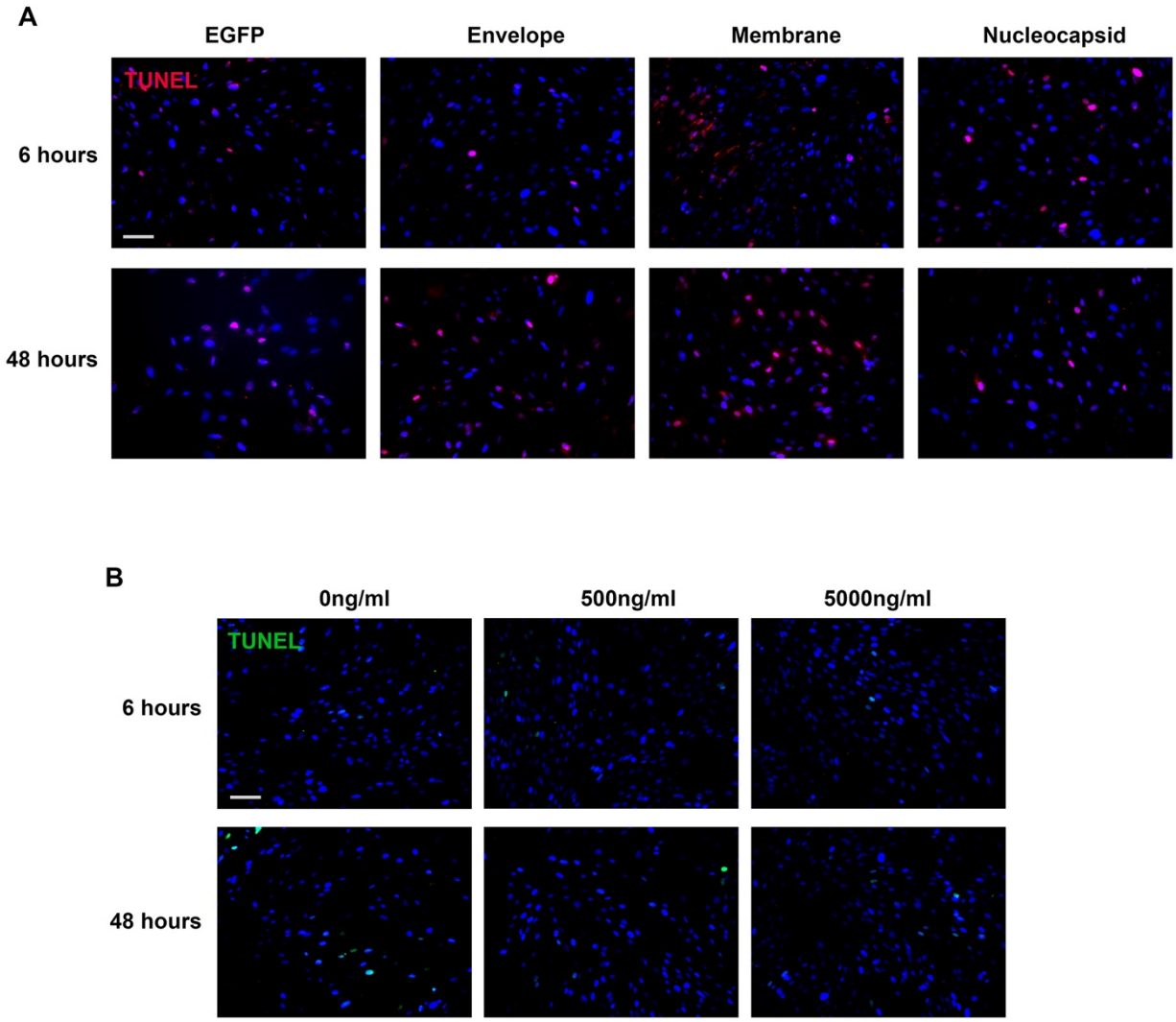


**Appendix Figure 3. SARS-CoV-2 envelope and membrane protein could induce PDL fibroblast apoptosis.**

Representative field images of TUNEL analysis in the indicated conditions. Quantitative analysis can be found from Figure 2 E-H.

Bars: 100um

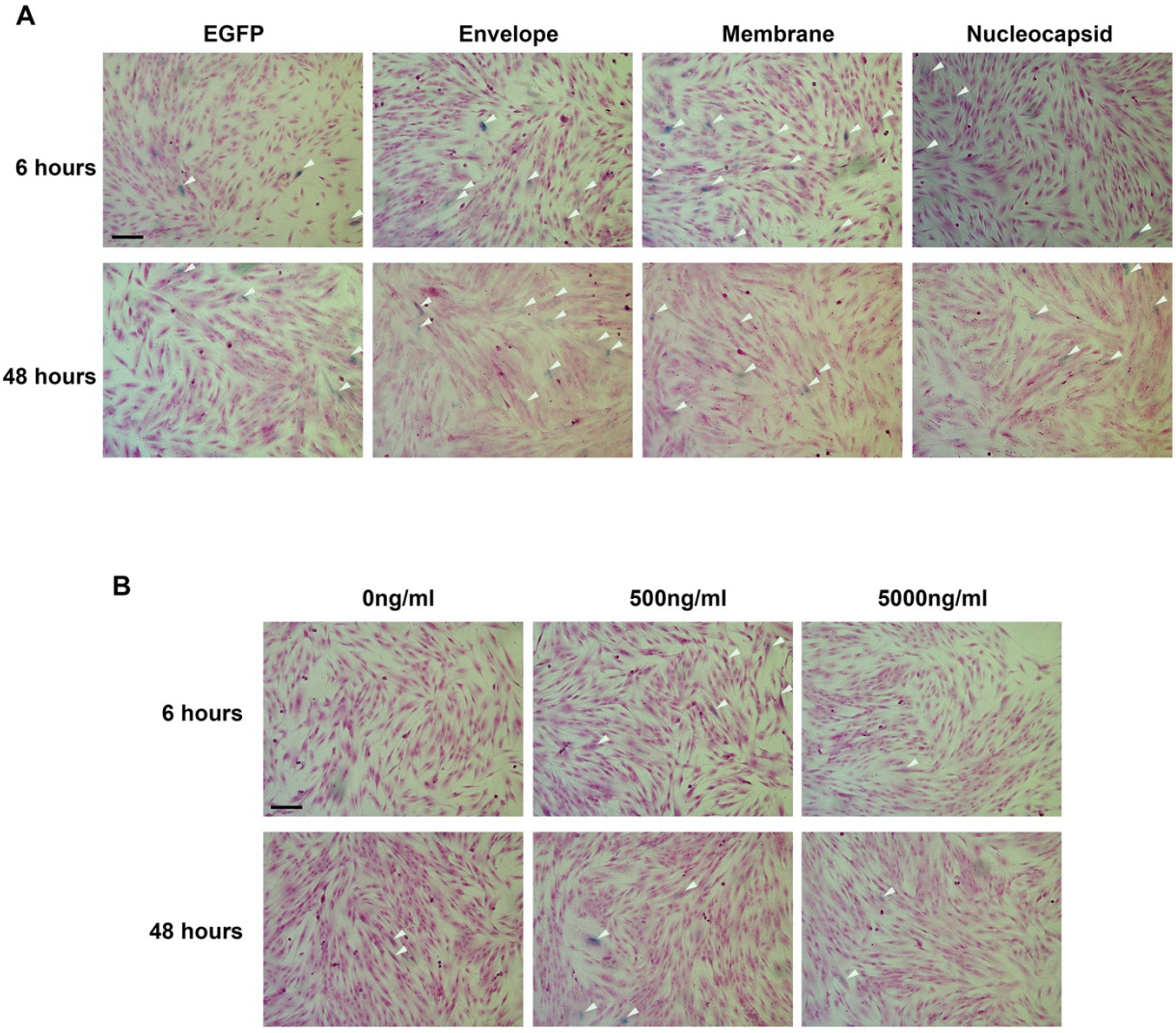


**Appendix Figure 4. SARS-CoV-2 envelope and membrane protein could induce PDL fibroblast senescence.**

Representative field images of senescence analysis in the indicated conditions. The cells were countered stained with nuclear fast red. Note increased blue staining (marking senescent cells) in the envelope and membrane groups. Quantitative analysis can be found from Figure 2 I-L. White arrows indicate representative positive cells.

Bars: 100um

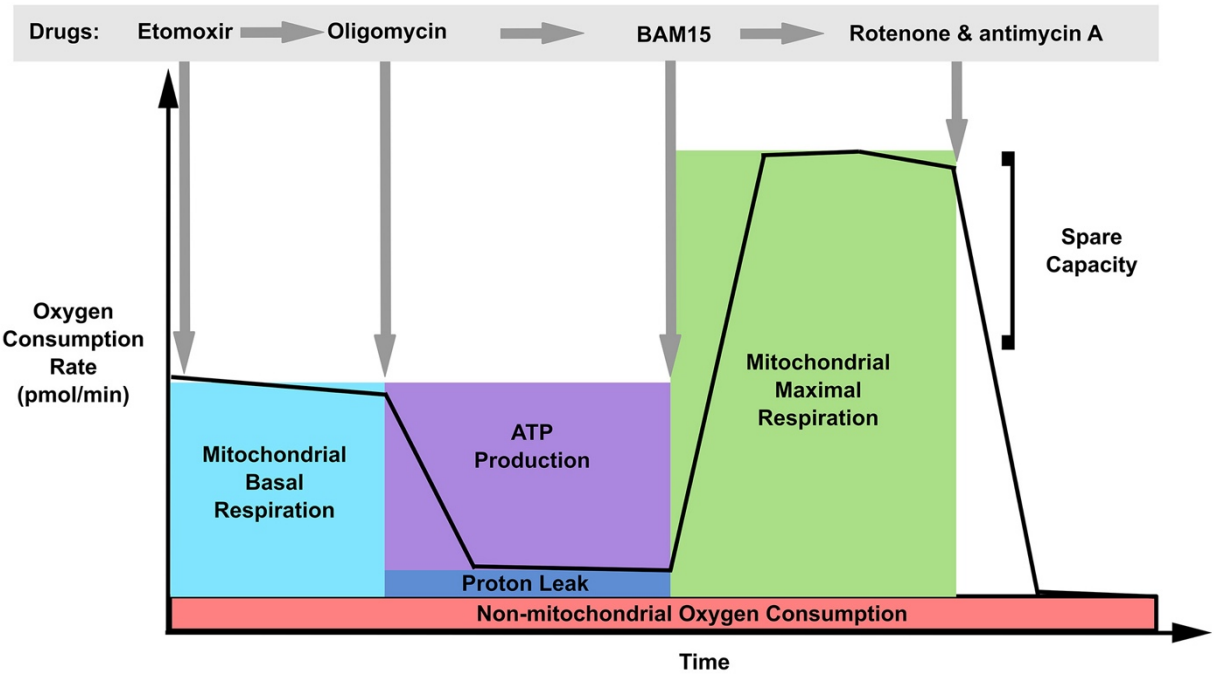


**Appendix Figure 5. Illustration of Seahorse mito stress test, for which drugs were added sequentially into the cell culture and what have been measured by the machine.**

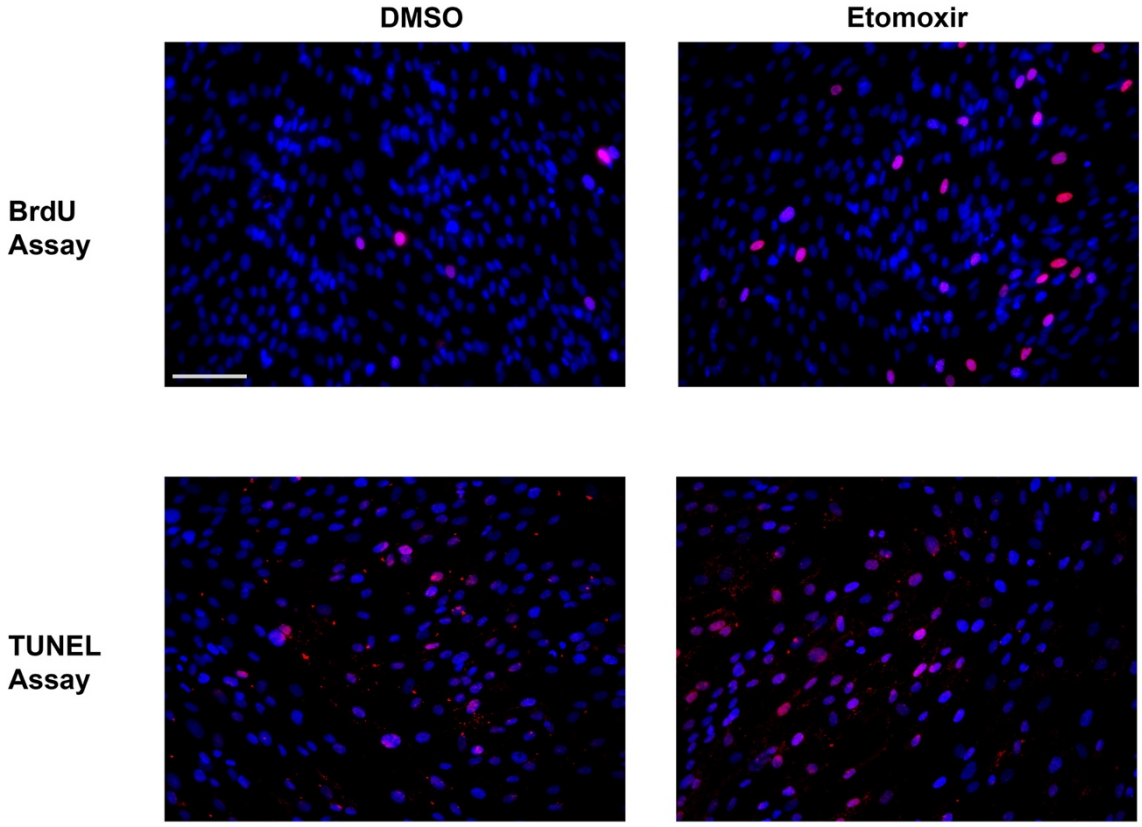


**Appendix Figure 6. Mitochondrial fatty acid β-oxidation inhibition mirrored fibrotic degeneration phenotypes in PDL fibroblasts.**

Representative field images of BrdU incorporation and TUNEL analysis in the indicated conditions. Quantitative analysis can be found from Figure 5 B and C.

## Appendix Table 1

The original proteomic analysis data of the effects of SARS-CoV-2 structural proteins, as showed in Figure 4A.

| Accession | Protein | LFQ intensity EGFP 6hrs | LFQ intensity Envelope 6hrs | LFQ intensity Membrane 6hrs | LFQ intensity Nucleocapsid 6hrs |
|---|---|---|---|---|---|
| H3BTL1 | H3BTL1_HUMAN Microtubule-associated protein 1 light chain 3 beta, isoform CRA_f OS | 20.10239029 | 19.10513687 | 20.0364418 | 20.03939056 |
| Q99613-2 | EIF3C_HUMAN Isoform 2 of Eukaryotic translation initiation factor 3 subunit C OS | 18.629179 | 19.96310425 | 20.06723404 | 20.2131176 |
| F8VZJ2 | F8VZJ2_HUMAN Nascent polypeptide-associated complex subunit alpha OS | 22.0500946 | 21.60272598 | 18.8843956 | 21.94813538 |
| O00148 | DX39A_HUMAN ATP-dependent RNA helicase DDX39A OS | 20.24852562 | 19.92243576 | 20.19075012 | 20.36442184 |
| O00159-2 | MYO1C_HUMAN Isoform 2 of Unconventional myosin-Ic OS | 20.42316437 | 20.65970612 | 21.64368057 | 18.09388161 |
| O00231 | PSD11_HUMAN 26S proteasome non-ATPase regulatory subunit 11 OS | 21.50232315 | 20.77643585 | 18.8217926 | 21.38958359 |
| O00232-2 | PSD12_HUMAN Isoform 2 of 26S proteasome non-ATPase regulatory subunit 12 OS | 19.38958931 | 18.97323799 | 18.15907097 | 19.32212639 |
| O00299 | CLIC1_HUMAN Chloride intracellular channel protein 1 OS | 23.82948685 | 23.17922211 | 23.2844677 | 23.52719116 |
| O00303 | EIF3F_HUMAN Eukaryotic translation initiation factor 3 subunit F OS | 20.16717339 | 19.47286606 | 18.07906342 | 19.43161583 |
| O00410 | IPO5_HUMAN Importin-5 OS | 21.63754654 | 21.14910889 | 21.34261513 | 21.50586319 |
| A0A2R8Y5G6 | A0A2R8Y5G6_HUMAN RNA helicase OS | 20.2237606 | 20.15783119 | 20.38268661 | 20.18555832 |
| O14818 | PSA7_HUMAN Proteasome subunit alpha type-7 OS | 21.17542076 | 21.4470787 | 21.25014496 | 22.0280323 |
| P19105 | ML12A_HUMAN Myosin regulatory light chain 12A OS | 22.9598732 | 22.81103897 | 22.7803669 | 23.33674431 |
| O15143 | ARC1B_HUMAN Actin-related protein 2/3 complex subunit 1B OS | 21.7553997 | 21.41776848 | 20.67959976 | 21.02337074 |
| O15144 | ARPC2_HUMAN Actin-related protein 2/3 complex subunit 2 OS | 21.11825943 | 20.74419022 | 20.81472015 | 20.75881767 |
| A0A286YF22 | A0A286YF22_HUMAN D-3-phosphoglycerate dehydrogenase OS | 22.21483803 | 20.47070313 | 20.90087509 | 21.23543739 |
| O43242 | PSMD3_HUMAN 26S proteasome non-ATPase regulatory subunit 3 OS | 18.42886925 | 19.4923172 | 18.51243401 | 20.35412407 |
| O43707 | ACTN4_HUMAN Alpha-actinin-4 OS | 24.45920181 | 24.34854317 | 24.44373131 | 24.58663368 |
| O43795-2 | MYO1B_HUMAN Isoform 2 of Unconventional myosin-Ib OS | 19.75842857 | 19.13761139 | 19.4098053 | 17.52830315 |
| O43852 | CALU_HUMAN Calumenin OS | 23.00316048 | 23.20448685 | 23.1497612 | 22.97472 |
| O60506-4 | HNRPQ_HUMAN Isoform 4 of Heterogeneous nuclear ribonucleoprotein Q OS | 18.74744225 | 22.43349266 | 21.80931282 | 22.75505257 |
| O60664-4 | PLIN3_HUMAN Isoform 4 of Perilipin-3 OS | 23.39806557 | 22.11977959 | 21.64412117 | 22.92772293 |
| O60701 | UGDH_HUMAN UDP-glucose 6-dehydrogenase OS | 23.65567398 | 23.56685829 | 23.33824158 | 23.71785164 |
| O60763 | USO1_HUMAN General vesicular transport factor p115 OS | 19.5602951 | 20.07678986 | 20.93315506 | 19.38621902 |
| O75083 | WDR1_HUMAN WD repeat-containing protein 1 OS | 22.13138199 | 21.2696228 | 23.37650108 | 23.52037239 |
| E5RIW3 | E5RIW3_HUMAN Tubulin-specific chaperone A OS | 20.52305603 | 19.03895187 | 20.3042984 | 20.24493027 |
| O75369-2 | FLNB_HUMAN Isoform 2 of Filamin-B OS | 23.54580688 | 23.33183289 | 23.51544952 | 23.3334713 |
| B4DJV2 | B4DJV2_HUMAN Citrate synthase OS | 20.92810249 | 20.59532356 | 20.07365608 | 21.55524826 |
| O75396 | SC22B_HUMAN Vesicle-trafficking protein SEC22b OS | 21.74324417 | 21.7069149 | 21.60792542 | 20.76983452 |
| O76003 | GLRX3_HUMAN Glutaredoxin-3 OS | 20.27491951 | 19.94077301 | 18.5617981 | 20.08108902 |
| O94979-3 | SC31A_HUMAN Isoform 3 of Protein transport protein Sec31A OS | 20.96845818 | 21.05278206 | 20.82539749 | 20.87927246 |
| O95373 | IPO7_HUMAN Importin-7 OS | 20.65709114 | 20.65333557 | 21.17102814 | 20.54726791 |
| O95782-2 | AP2A1_HUMAN Isoform B of AP-2 complex subunit alpha-1 OS | 19.28873253 | 18.351408 | 18.48805237 | 19.44828987 |
| O95816 | BAG2_HUMAN BAG family molecular chaperone regulator 2 OS | 19.18461418 | 19.14443588 | 19.68760109 | 19.34550858 |

| | | | | | |
|---|---|---|---|---|---|
| P00338 | LDHA_HUMAN L-lactate dehydrogenase A chain OS | 25.44344711 | 25.19159508 | 25.05527687 | 25.45575714 |
| P00367 | DHE3_HUMAN Glutamate dehydrogenase 1, mitochondrial OS | 20.72550583 | 20.42521667 | 20.81932831 | 20.7519722 |
| P00387-2 | NB5R3_HUMAN Isoform 2 of NADH-cytochrome b5 reductase 3 OS | 21.65530205 | 21.77398491 | 21.40265274 | 22.45176506 |
| P00403 | COX2_HUMAN Cytochrome c oxidase subunit 2 OS | 20.24376869 | 18.19075394 | 20.23958015 | 18.82337379 |
| P00505-2 | AATM_HUMAN Isoform 2 of Aspartate aminotransferase, mitochondrial OS | 20.64368057 | 20.42624092 | 19.4458847 | 19.96225739 |
| P00558 | PGK1_HUMAN Phosphoglycerate kinase 1 OS | 24.08772278 | 23.93939209 | 23.55262375 | 23.79451561 |
| P00568 | KAD1_HUMAN Adenylate kinase isoenzyme 1 OS | 19.53301811 | 20.11629295 | 19.46778107 | 18.75499535 |
| P02452 | CO1A1_HUMAN Collagen alpha-1(I) chain OS | 23.09102058 | 23.28248978 | 23.32072258 | 22.52114105 |
| P02545 | LMNA_HUMAN Prelamin-A/C OS | 25.78877831 | 25.64861488 | 25.65376091 | 25.40311432 |
| P02751-5 | FINC_HUMAN Isoform 5 of Fibronectin OS | 19.21175766 | 20.52219391 | 21.38642883 | 19.76073647 |
| P02786 | TFR1_HUMAN Transferrin receptor protein 1 OS | 19.10517883 | 20.29356194 | 20.46383476 | 18.64682007 |
| P04075 | ALDOA_HUMAN Fructose-bisphosphate aldolase A OS | 25.22262001 | 25.09051132 | 25.17108154 | 25.27159691 |
| P04080 | CYTB_HUMAN Cystatin-B OS | 20.52611732 | 19.50829697 | 20.25234222 | 20.95091438 |
| P04083 | ANXA1_HUMAN Annexin A1 OS | 25.49655724 | 25.25198174 | 25.19745636 | 25.76468658 |
| P04181 | OAT_HUMAN Ornithine aminotransferase, mitochondrial OS | 19.78298378 | 18.27453041 | 19.64839745 | 19.92171097 |
| P04350 | TBB4A_HUMAN Tubulin beta-4A chain OS | 19.22675705 | 18.80141258 | 20.51595306 | 19.99050903 |
| P04406 | G3P_HUMAN Glyceraldehyde-3-phosphate dehydrogenase OS | 25.86968994 | 25.795681 | 25.68059349 | 26.01186371 |
| K7EM73 | K7EM73_HUMAN Calcium-activated neutral proteinase small subunit (Fragment) OS | 20.34028053 | 21.09706306 | 20.18728256 | 21.22464561 |
| A0A6Q8PFK8 | A0A6Q8PFK8_HUMAN Heat shock protein beta-1 OS | 22.90451813 | 23.41905403 | 22.59400177 | 24.08909798 |
| P04843 | RPN1_HUMAN Dolichyl-diphosphooligosaccharide--protein glycosyltransferase subunit 1 OS | 22.59996033 | 22.73931503 | 22.67497635 | 22.67910576 |
| P04844-2 | RPN2_HUMAN Isoform 2 of Dolichyl-diphosphooligosaccharide--protein glycosyltransferase subunit 2 OS | 21.00449753 | 21.7910614 | 21.34098625 | 21.54443932 |
| P05023-3 | AT1A1_HUMAN Isoform 3 of Sodium/potassium-transporting ATPase subunit alpha-1 OS | 21.17102814 | 18.53874207 | 20.76530838 | 19.07042313 |
| P05141 | ADT2_HUMAN ADP/ATP translocase 2 OS | 22.5421505 | 22.79127884 | 22.61236572 | 22.96227455 |
| P05387 | RLA2_HUMAN 60S acidic ribosomal protein P2 OS | 20.0263443 | 19.84896278 | 19.8745079 | 20.33527184 |
| P05388 | RLA0_HUMAN 60S acidic ribosomal protein P0 OS | 22.12786102 | 23.20111084 | 23.83614922 | 22.81395721 |
| P05455 | LA_HUMAN Lupus La protein OS | 20.18555832 | 20.52085304 | 18.54012489 | 20.43267632 |
| H7C4K3 | H7C4K3_HUMAN Integrin beta-1 OS | 22.45108604 | 22.80725098 | 23.01367569 | 22.93646622 |
| P06576 | ATPB_HUMAN ATP synthase subunit beta, mitochondrial OS | 22.97744751 | 23.98988533 | 23.63433647 | 23.94476318 |
| R4GN98 | R4GN98_HUMAN Protein S100 (Fragment) OS | 20.53221893 | 22.26570702 | 22.08384895 | 20.79827881 |
| P06733 | ENOA_HUMAN Alpha-enolase OS | 26.81433296 | 26.25585747 | 25.92379379 | 26.77341652 |
| P06744 | G6PI_HUMAN Glucose-6-phosphate isomerase OS | 21.22564507 | 21.50329399 | 22.13433075 | 21.45317268 |
| P06748-3 | NPM_HUMAN Isoform 3 of Nucleophosmin OS | 23.91488075 | 23.17753601 | 23.01529312 | 23.60625458 |
| P06753-2 | TPM3_HUMAN Isoform 2 of Tropomyosin alpha-3 chain OS | 24.84282875 | 25.24285316 | 24.69620132 | 24.69109726 |
| P07195 | LDHB_HUMAN L-lactate dehydrogenase B chain OS | 23.87483406 | 24.55174446 | 24.20015335 | 24.21489716 |
| P07237 | PDIA1_HUMAN Protein disulfide-isomerase OS | 23.87389565 | 24.38929367 | 24.5389576 | 24.61605072 |
| P07355 | ANXA2_HUMAN Annexin A2 OS | 26.3249855 | 26.16036797 | 26.40963364 | 26.59448624 |
| Q5JP53 | Q5JP53_HUMAN Tubulin beta chain OS | 25.56784439 | 25.24590302 | 24.97814751 | 24.51701164 |
| P07737 | PROF1_HUMAN Profilin-1 OS | 25.31572151 | 24.98984146 | 24.69280052 | 25.51267815 |
| P07741-2 | APT_HUMAN Isoform 2 of Adenine phosphoribosyltransferase OS | 19.49337769 | 19.55965996 | 19.41886902 | 19.26836014 |
| P07814 | SYEP_HUMAN Bifunctional glutamate/proline--tRNA ligase OS | 20.97729111 | 20.52209854 | 20.81158829 | 20.95496559 |
| A0A7I2V668 | A0A7I2V668_HUMAN Cathepsin B OS | 18.59151268 | 19.28309441 | 18.92534637 | 20.0256691 |

| | | | | | |
|---|---|---|---|---|---|
| P07900 | HS90A_HUMAN Heat shock protein HSP 90-alpha OS | 24.97701073 | 24.96798325 | 24.85262489 | 24.31568718 |
| P07954-2 | FUMH_HUMAN Isoform Cytoplasmic of Fumarate hydratase, mitochondrial OS | 21.47427177 | 19.83877563 | 18.75895691 | 20.33145142 |
| A0A087WTA8 | A0A087WTA8_HUMAN Collagen alpha-2(I) chain OS | 19.50655174 | 20.52200317 | 20.08925819 | 18.34784698 |
| P08133-2 | ANXA6_HUMAN Isoform 2 of Annexin A6 OS | 21.31440163 | 20.74706268 | 22.89498711 | 20.61063194 |
| P08195-2 | 4F2_HUMAN Isoform 2 of 4F2 cell-surface antigen heavy chain OS | 20.74369621 | 20.62631416 | 20.87252426 | 21.52616501 |
| P08238 | HS90B_HUMAN Heat shock protein HSP 90-beta OS | 26.66275215 | 26.74239731 | 26.63740921 | 26.3826313 |
| P08670 | VIME_HUMAN Vimentin OS | 28.09763145 | 28.45575714 | 28.18338203 | 28.07418633 |
| P08708 | RS17_HUMAN 40S ribosomal protein S17 OS | 20.42121506 | 20.89081955 | 19.0922699 | 20.2166748 |
| P08758 | ANXA5_HUMAN Annexin A5 OS | 26.03416443 | 25.64617157 | 25.64603424 | 26.01497269 |
| C9J9K3 | C9J9K3_HUMAN 40S ribosomal protein SA (Fragment) OS | 23.82997131 | 23.51689148 | 23.25066566 | 23.94556618 |
| P09211 | GSTP1_HUMAN Glutathione S-transferase P OS | 23.67152405 | 23.38508606 | 23.45989037 | 23.40210533 |
| P09382 | LEG1_HUMAN Galectin-1 OS | 25.39008141 | 24.85357666 | 24.82914734 | 25.43990135 |
| P09493-3 | TPM1_HUMAN Isoform 3 of Tropomyosin alpha-1 chain OS | 23.12140846 | 23.01855659 | 22.72708702 | 23.17525291 |
| P09651-3 | ROA1_HUMAN Isoform 2 of Heterogeneous nuclear ribonucleoprotein A1 OS | 23.24212646 | 23.56790352 | 23.55882454 | 23.16250992 |
| P09936 | UCHL1_HUMAN Ubiquitin carboxyl-terminal hydrolase isozyme L1 OS | 21.78048706 | 21.51016998 | 21.51527977 | 21.37081909 |
| J3QS39 | J3QS39_HUMAN Polyubiquitin-B (Fragment) OS | 25.05804634 | 24.82701683 | 24.93737221 | 25.38742256 |
| P0DMV8-2 | HS71A_HUMAN Isoform 2 of Heat shock 70 kDa protein 1A OS | 22.42190742 | 22.63862991 | 22.50331879 | 22.5267849 |
| P0DP25 | CALM3_HUMAN Calmodulin-3 OS | 21.64552879 | 21.67882729 | 21.98693848 | 21.82629013 |
| P10599 | THIO_HUMAN Thioredoxin OS | 23.13769531 | 22.60306549 | 22.52657127 | 22.82549286 |
| A0A7I2V599 | A0A7I2V599_HUMAN 60 kDa heat shock protein, mitochondrial OS | 23.39479828 | 23.44733238 | 24.19151878 | 24.08172226 |
| P11021 | BIP_HUMAN Endoplasmic reticulum chaperone BiP OS | 25.55800819 | 25.57282639 | 25.71832085 | 25.92592239 |
| P11142 | HSP7C_HUMAN Heat shock cognate 71 kDa protein OS | 26.54789734 | 26.72455406 | 26.61568642 | 26.60724258 |
| P11279 | LAMP1_HUMAN Lysosome-associated membrane glycoprotein 1 OS | 17.32139587 | 19.31709862 | 19.2150135 | 20.2681942 |
| P11413 | G6PD_HUMAN Glucose-6-phosphate 1-dehydrogenase OS | 23.88892555 | 23.74745178 | 23.55168533 | 23.64735222 |
| V9GYY3 | V9GYY3_HUMAN C-1-tetrahydrofolate synthase, cytoplasmic OS | 19.85201454 | 20.60909843 | 17.56593513 | 20.80475235 |
| P11940-2 | PABP1_HUMAN Isoform 2 of Polyadenylate-binding protein 1 OS | 21.51590538 | 22.08718872 | 22.50006294 | 22.46543121 |
| P12004 | PCNA_HUMAN Proliferating cell nuclear antigen OS | 20.3467865 | 18.33042145 | 19.56888008 | 20.10712433 |
| A0A087X0S5 | A0A087X0S5_HUMAN Collagen alpha-1(VI) chain OS | 18.71038246 | 20.07195473 | 20.02998734 | 19.10149193 |
| P12110-3 | CO6A2_HUMAN Isoform 2C2A of Collagen alpha-2(VI) chain OS | 18.38016319 | 18.76461792 | 19.70730209 | 18.65681839 |
| P12111-2 | CO6A3_HUMAN Isoform 2 of Collagen alpha-3(VI) chain OS | 20.01154327 | 18.73948097 | 18.68630219 | 19.30571556 |
| P12236 | ADT3_HUMAN ADP/ATP translocase 3 OS | 21.83865166 | 21.45498085 | 21.2160244 | 21.11667442 |
| E7ETK5 | E7ETK5_HUMAN Inosine-5-monophosphate dehydrogenase 2 OS | 20.26739502 | 19.94535255 | 20.17840195 | 20.36463547 |
| P12814 | ACTN1_HUMAN Alpha-actinin-1 OS | 24.16867256 | 23.90655708 | 24.06923676 | 24.06767845 |
| P12956 | XRCC6_HUMAN X-ray repair cross-complementing protein 6 OS | 22.48537064 | 22.75951004 | 21.96677017 | 22.26014709 |
| P13010 | XRCC5_HUMAN X-ray repair cross-complementing protein 5 OS | 20.98161697 | 21.04693413 | 18.7273922 | 21.02418137 |
| P13489 | RINI_HUMAN Ribonuclease inhibitor OS | 19.07761192 | 19.36923981 | 20.75564384 | 21.56532478 |
| P13639 | EF2_HUMAN Elongation factor 2 OS | 25.42521667 | 25.36131859 | 25.49347496 | 25.31458092 |
| P13667 | PDIA4_HUMAN Protein disulfide-isomerase A4 OS | 22.20329285 | 21.50198364 | 22.4616394 | 22.20401001 |
| P13693 | TCTP_HUMAN Translationally-controlled tumor protein OS | 22.94494057 | 23.02570343 | 22.74299812 | 21.68440247 |
| P13797-3 | PLST_HUMAN Isoform 3 of Plastin-3 OS | 20.80325508 | 21.41012573 | 20.93984032 | 21.11914635 |
| P14314-2 | GLU2B_HUMAN Isoform 2 of Glucosidase 2 subunit beta OS | 20.49462891 | 20.55646515 | 20.94670868 | 20.54952431 |

| | | | | | |
|---|---|---|---|---|---|
| P14618 | KPYM_HUMAN Pyruvate kinase PKM OS | 26.33880234 | 26.30679893 | 26.95038033 | 26.92150307 |
| P14625 | ENPL_HUMAN Endoplasmin OS | 25.14616013 | 24.98215675 | 25.34106064 | 25.01962471 |
| P14868-2 | SYDC_HUMAN Isoform 2 of Aspartate--tRNA ligase, cytoplasmic OS | 20.75808716 | 20.91320229 | 20.63944626 | 20.86052704 |
| P15121 | ALDR_HUMAN Aldo-keto reductase family 1 member B1 OS | 19.60351372 | 20.02106667 | 20.2934494 | 19.91615105 |
| P15170-2 | ERF3A_HUMAN Isoform 2 of Eukaryotic peptide chain release factor GTP-binding subunit ERF3A OS | 18.81366158 | 18.34658432 | 19.01454353 | 19.65240097 |
| E7EQR4 | E7EQR4_HUMAN Ezrin OS | 21.33494568 | 20.75148201 | 21.29288864 | 21.32827568 |
| P15531 | NDKA_HUMAN Nucleoside diphosphate kinase A OS | 20.29949951 | 21.05039406 | 21.42157364 | 20.32256699 |
| B4DLR8 | B4DLR8_HUMAN NAD(P)H dehydrogenase [quinone] 1 OS | 21.96476173 | 22.27486229 | 21.60747528 | 22.14973068 |
| P15880 | RS2_HUMAN 40S ribosomal protein S2 OS | 21.47847557 | 21.86067772 | 21.50489426 | 20.85094643 |
| H0YD13 | H0YD13_HUMAN CD44 antigen OS | 21.84796906 | 21.62055397 | 22.34597397 | 21.94706535 |
| P16152 | CBR1_HUMAN Carbonyl reductase [NADPH] 1 OS | 20.68893242 | 20.65210915 | 20.29670143 | 21.14008522 |
| P16401 | H15_HUMAN Histone H1.5 OS | 20.50445747 | 21.03650856 | 19.98509789 | 20.09106827 |
| P16403 | H12_HUMAN Histone H1.2 OS | 22.56239319 | 23.6404171 | 22.6115551 | 22.15610313 |
| A2A2D0 | A2A2D0_HUMAN Stathmin (Fragment) OS | 22.06766129 | 22.17063141 | 21.99043846 | 22.18546677 |
| P17066 | HSP76_HUMAN Heat shock 70 kDa protein 6 OS | 23.97018051 | 23.79114151 | 24.3663311 | 18.36454964 |
| P17301 | ITA2_HUMAN Integrin alpha-2 OS | 20.62533379 | 18.01978874 | 20.27264404 | 19.34575462 |
| P17844-2 | DDX5_HUMAN Isoform 2 of Probable ATP-dependent RNA helicase DDX5 OS | 21.91779709 | 21.96204567 | 22.16063309 | 22.15893936 |
| P17931 | LEG3_HUMAN Galectin-3 OS | 22.04069519 | 21.6466713 | 21.1992836 | 21.85870743 |
| P17987 | TCPA_HUMAN T-complex protein 1 subunit alpha OS | 21.94663811 | 20.91830635 | 22.14678192 | 22.09316635 |
| P18077 | RL35A_HUMAN 60S ribosomal protein L35a OS | 21.23876381 | 21.20012283 | 20.94927597 | 20.95183945 |
| P18085 | ARF4_HUMAN ADP-ribosylation factor 4 OS | 22.76761436 | 23.49240494 | 22.76050568 | 22.95882797 |
| P18124 | RL7_HUMAN 60S ribosomal protein L7 OS | 22.55255318 | 22.32608223 | 22.11359406 | 22.20711136 |
| P18206-2 | VINC_HUMAN Isoform 1 of Vinculin OS | 25.51270866 | 25.16748619 | 25.25767517 | 25.19121742 |
| A0A087WXM6 | A0A087WXM6_HUMAN 60S ribosomal protein L17 (Fragment) OS | 22.04683495 | 21.91356659 | 21.91914368 | 21.42792892 |
| P18669 | PGAM1_HUMAN Phosphoglycerate mutase 1 OS | 21.50450706 | 22.3384037 | 18.76493454 | 22.02894402 |
| A0A7I2V5M5 | A0A7I2V5M5_HUMAN Nucleolin OS | 23.5639534 | 23.83402824 | 24.17607498 | 23.00643349 |
| P20340-2 | RAB6A_HUMAN Isoform 2 of Ras-related protein Rab-6A OS | 20.68260384 | 20.27082062 | 19.90782928 | 18.33300209 |
| P20618 | PSB1_HUMAN Proteasome subunit beta type-1 OS | 21.38637543 | 20.9909935 | 20.79558563 | 20.46821785 |
| E9PP21 | E9PP21_HUMAN Cysteine and glycine-rich protein 1 OS | 22.33764267 | 22.17621231 | 21.712677 | 22.27121925 |
| P21333-2 | FLNA_HUMAN Isoform 2 of Filamin-A OS | 27.50074005 | 27.26731682 | 27.49845886 | 27.23908806 |
| P21796 | VDAC1_HUMAN Voltage-dependent anion-selective channel protein 1 OS | 20.80317497 | 21.00257683 | 19.18766403 | 21.32289696 |
| P21980 | TGM2_HUMAN Protein-glutamine gamma-glutamyltransferase 2 OS | 21.63706017 | 20.52859879 | 21.82080841 | 21.45973969 |
| P22234 | PUR6_HUMAN Multifunctional protein ADE2 OS | 20.32586288 | 18.53541374 | 18.37940216 | 19.8512516 |
| P22307-6 | SCP2_HUMAN Isoform 6 of Sterol carrier protein 2 OS | 19.93051529 | 18.27853394 | 19.50288582 | 20.16041756 |
| P22314-2 | UBA1_HUMAN Isoform 2 of Ubiquitin-like modifier-activating enzyme 1 OS | 23.46874046 | 23.45148849 | 23.38613892 | 23.43224335 |
| P22392-2 | NDKB_HUMAN Isoform 3 of Nucleoside diphosphate kinase B OS | 24.95557785 | 24.43020248 | 24.24285316 | 24.82561111 |
| A0A7I2V4I6 | A0A7I2V4I6_HUMAN Heterogeneous nuclear ribonucleoproteins A2/B1 OS | 22.79590416 | 22.79405975 | 22.6634903 | 22.38616562 |
| A0A2R8YDM0 | A0A2R8YDM0_HUMAN Prostaglandin-endoperoxide synthase (Fragment) OS | 19.32447243 | 19.92104149 | 20.32586288 | 20.453022 |
| P23246 | SFPQ_HUMAN Splicing factor, proline- and glutamine-rich OS | 21.78572464 | 22.33884048 | 22.07407951 | 19.62455559 |
| P23284 | PPIB_HUMAN Peptidyl-prolyl cis-trans isomerase B OS | 24.42136765 | 23.90334129 | 23.9958477 | 23.69242859 |
| P23381-2 | SYWC_HUMAN Isoform 2 of Tryptophan--tRNA ligase, cytoplasmic OS | 18.65694618 | 18.98865128 | 18.03157043 | 18.45745659 |

| | | | | | |
|---|---|---|---|---|---|
| P23396 | RS3_HUMAN 40S ribosomal protein S3 OS | 23.78096771 | 23.62287903 | 23.62053299 | 23.94708443 |
| P23526 | SAHH_HUMAN Adenosylhomocysteinase OS | 21.50300217 | 21.42700768 | 21.16337013 | 21.25948524 |
| P23528 | COF1_HUMAN Cofilin-1 OS | 24.93597984 | 24.95938683 | 24.94060135 | 25.63765717 |
| P23634-7 | AT2B4_HUMAN Isoform ZB of Plasma membrane calcium-transporting ATPase 4 OS | 20.08498573 | 20.69200325 | 20.50794601 | 18.06524467 |
| P24534 | EF1B_HUMAN Elongation factor 1-beta OS | 22.30502129 | 21.72263336 | 22.14027405 | 22.05857468 |
| Q5QNZ2 | Q5QNZ2_HUMAN ATP synthase F(0) complex subunit B1, mitochondrial OS | 19.32291794 | 20.23958015 | 19.95787239 | 19.57420921 |
| P25398 | RS12_HUMAN 40S ribosomal protein S12 OS | 22.16864204 | 21.38205338 | 21.39037132 | 20.97330284 |
| P25705 | ATPA_HUMAN ATP synthase subunit alpha, mitochondrial OS | 24.05150604 | 24.12273598 | 24.0110321 | 23.74488831 |
| F5GX11 | F5GX11_HUMAN Proteasome subunit alpha type-1 OS | 21.36121178 | 20.17657661 | 20.6032238 | 20.54387474 |
| A0A7I2V2H3 | A0A7I2V2H3_HUMAN UPF0415 protein C7orf25 OS | 20.29299927 | 20.44949913 | 18.5714798 | 17.94278336 |
| P25788-2 | PSA3_HUMAN Isoform 2 of Proteasome subunit alpha type-3 OS | 19.95400429 | 19.35004044 | 18.62101173 | 20.80829239 |
| H0YMZ1 | H0YMZ1_HUMAN Proteasome subunit alpha type (Fragment) OS | 20.44818878 | 18.83518982 | 20.33745193 | 20.11667442 |
| P26038 | MOES_HUMAN Moesin OS | 24.08448219 | 24.15236282 | 24.07667542 | 23.99576187 |
| P26373 | RL13_HUMAN 60S ribosomal protein L13 OS | 21.72088051 | 22.07162666 | 21.93329811 | 22.05596352 |
| A6NLN1 | A6NLN1_HUMAN Polypyrimidine tract-binding protein 1 OS | 21.35498619 | 22.10261536 | 21.91195869 | 22.54333115 |
| P26639 | SYTC_HUMAN Threonine--tRNA ligase 1, cytoplasmic OS | 18.68282509 | 18.14849663 | 20.6827755 | 20.56978226 |
| P26640 | SYVC_HUMAN Valine--tRNA ligase OS | 20.64491272 | 20.36900902 | 19.86188889 | 20.05152321 |
| P26641 | EF1G_HUMAN Elongation factor 1-gamma OS | 24.44909668 | 23.74570847 | 23.42226791 | 23.98589706 |
| P27348 | 1433T_HUMAN 14-3-3 protein theta OS | 21.95311928 | 21.91830635 | 22.69824791 | 21.8007679 |
| F8W7C6 | F8W7C6_HUMAN 60S ribosomal protein L10 OS | 19.95446968 | 20.85041237 | 20.13808632 | 20.4403019 |
| P27797 | CALR_HUMAN Calreticulin OS | 24.27582932 | 24.20321846 | 24.16361618 | 24.06488609 |
| P27816-6 | MAP4_HUMAN Isoform 6 of Microtubule-associated protein 4 OS | 22.30866432 | 22.13295174 | 21.96705246 | 22.24091911 |
| P27824 | CALX_HUMAN Calnexin OS | 22.58545494 | 22.43690109 | 22.57588577 | 22.74349213 |
| P28066 | PSA5_HUMAN Proteasome subunit alpha type-5 OS | 19.54440308 | 21.35697365 | 18.90184212 | 22.0509243 |
| P28072 | PSB6_HUMAN Proteasome subunit beta type-6 OS | 20.35412407 | 20.73537445 | 20.70480537 | 20.0171299 |
| P28074 | PSB5_HUMAN Proteasome subunit beta type-5 OS | 20.54820824 | 20.92918587 | 21.03838539 | 18.24308014 |
| P29373 | RABP2_HUMAN Cellular retinoic acid-binding protein 2 OS | 21.69132042 | 21.58641624 | 21.46218872 | 21.75605202 |
| P29401 | TKT_HUMAN Transketolase OS | 23.89309883 | 23.9358902 | 23.79431725 | 24.02934837 |
| E9PK01 | E9PK01_HUMAN Elongation factor 1-delta (Fragment) OS | 23.84028625 | 24.22140312 | 23.92243195 | 23.40859795 |
| P29966 | MARCS_HUMAN Myristoylated alanine-rich C-kinase substrate OS | 21.43135071 | 21.26441956 | 21.41369438 | 20.4724884 |
| P30040 | ERP29_HUMAN Endoplasmic reticulum resident protein 29 OS | 20.24875641 | 19.04772758 | 19.87669754 | 20.63280678 |
| P30041 | PRDX6_HUMAN Peroxiredoxin-6 OS | 22.81677246 | 22.49831009 | 21.80408287 | 23.03259659 |
| P30044-2 | PRDX5_HUMAN Isoform Cytoplasmic+peroxisomal of Peroxiredoxin-5, mitochondrial OS | 20.55496788 | 19.9026432 | 20.01576805 | 20.35175514 |
| P30048-2 | PRDX3_HUMAN Isoform 2 of Thioredoxin-dependent peroxide reductase, mitochondrial OS | 20.88323021 | 20.84053421 | 20.80207062 | 21.22311401 |
| P30050 | RL12_HUMAN 60S ribosomal protein L12 OS | 22.99602127 | 22.84628677 | 22.77017784 | 23.10616684 |
| P30086 | PEBP1_HUMAN Phosphatidylethanolamine-binding protein 1 OS | 21.17937469 | 20.88226128 | 21.31118965 | 20.51691628 |
| P30101 | PDIA3_HUMAN Protein disulfide-isomerase A3 OS | 24.33892059 | 24.46351051 | 24.36833 | 24.09595299 |
| P30153 | 2AAA_HUMAN Serine/threonine-protein phosphatase 2A 65 kDa regulatory subunit A alpha isoform OS | 20.17438507 | 17.96764565 | 20.35347939 | 20.97889709 |
| P31153-2 | METK2_HUMAN Isoform 2 of S-adenosylmethionine synthase isoform type-2 OS | 21.7015934 | 21.30752563 | 18.02231789 | 19.35296822 |
| P31939 | PUR9_HUMAN Bifunctional purine biosynthesis protein ATIC OS | 19.96395111 | 20.33712578 | 19.75433922 | 19.82289505 |
| P31943 | HNRH1_HUMAN Heterogeneous nuclear ribonucleoprotein H OS | 22.09732056 | 21.65294075 | 21.94141769 | 21.81796265 |

| | | | | | |
|---|---|---|---|---|---|
| P31946-2 | 1433B_HUMAN Isoform Short of 14-3-3 protein beta/alpha OS | 21.12395287 | 22.44609451 | 22.75191116 | 21.69510841 |
| P31948 | STIP1_HUMAN Stress-induced-phosphoprotein 1 OS | 21.68101692 | 21.71586227 | 21.76862335 | 21.52042198 |
| P32119 | PRDX2_HUMAN Peroxiredoxin-2 OS | 21.18083191 | 21.54491234 | 21.79018593 | 21.64059448 |
| D6RAN4 | D6RAN4_HUMAN 60S ribosomal protein L9 (Fragment) OS | 21.75902176 | 21.75474739 | 21.77499008 | 21.77527046 |
| P33176 | KINH_HUMAN Kinesin-1 heavy chain OS | 21.85064125 | 21.33472633 | 21.40135002 | 18.63724709 |
| H0YMM5 | H0YMM5_HUMAN Deoxyuridine 5-triphosphate nucleotidohydrolase OS | 17.98854065 | 19.09668159 | 18.96603775 | 18.76483917 |
| P34932 | HSP74_HUMAN Heat shock 70 kDa protein 4 OS | 20.94005585 | 21.18058968 | 20.53164864 | 20.7768383 |
| C9J0J7 | C9J0J7_HUMAN Profilin OS | 20.86014748 | 20.92998123 | 21.36666298 | 18.95683861 |
| G3XAM7 | G3XAM7_HUMAN Catenin (Cadherin-associated protein), alpha 1, 102kDa, isoform CRA_a OS | 18.23778915 | 19.61126328 | 18.54493904 | 20.20490456 |
| P35232 | PHB_HUMAN Prohibitin OS | 21.47288513 | 21.34759712 | 21.18289375 | 21.02654839 |
| P35241 | RADI_HUMAN Radixin OS | 18.7151165 | 18.15534973 | 19.38460732 | 18.39462662 |
| K7EP65 | K7EP65_HUMAN 60S ribosomal protein L22 (Fragment) OS | 21.8465538 | 22.31024742 | 21.9591465 | 22.57124138 |
| P35579 | MYH9_HUMAN Myosin-9 OS | 27.21946526 | 27.34975815 | 27.44679451 | 27.2035923 |
| P35580 | MYH10_HUMAN Myosin-10 OS | 19.46911812 | 18.07261276 | 19.93718338 | 19.44395065 |
| P35637-2 | FUS_HUMAN Isoform Short of RNA-binding protein FUS OS | 20.26109314 | 20.34527016 | 20.40010071 | 19.83422089 |
| C9JX88 | C9JX88_HUMAN 26S proteasome regulatory subunit 7 OS | 20.30295944 | 18.80281448 | 19.17874146 | 20.59313583 |
| P36578 | RL4_HUMAN 60S ribosomal protein L4 OS | 23.30841446 | 23.01481628 | 22.90056229 | 22.87282562 |
| P37802 | TAGL2_HUMAN Transgelin-2 OS | 22.95617104 | 23.49093819 | 23.52838516 | 22.38687515 |
| P37837 | TALDO_HUMAN Transaldolase OS | 21.21501541 | 21.01120186 | 20.64121246 | 19.90301132 |
| A0A7I2V2G2 | A0A7I2V2G2_HUMAN Stress-70 protein, mitochondrial OS | 22.65066528 | 23.09741592 | 22.98363686 | 23.06202126 |
| P39019 | RS19_HUMAN 40S ribosomal protein S19 OS | 22.94916916 | 23.27696419 | 23.08090973 | 23.17503929 |
| P39023 | RL3_HUMAN 60S ribosomal protein L3 OS | 22.28551292 | 21.49066925 | 21.54707909 | 21.69935036 |
| P39656-3 | OST48_HUMAN Isoform 3 of Dolichyl-diphosphooligosaccharide--protein glycosyltransferase 48 kDa subunit OS | 21.70602798 | 20.82772446 | 21.10014725 | 21.47649956 |
| P40227 | TCPZ_HUMAN T-complex protein 1 subunit zeta OS | 22.43456078 | 22.74435425 | 22.52492142 | 22.80258369 |
| A0A7I2V2L9 | A0A7I2V2L9_HUMAN 60S ribosomal protein L13a OS | 22.31454086 | 22.17834091 | 22.05029297 | 22.66062164 |
| P40925 | MDHC_HUMAN Malate dehydrogenase, cytoplasmic OS | 18.32060432 | 19.06594086 | 20.32597351 | 20.0188961 |
| P40926 | MDHM_HUMAN Malate dehydrogenase, mitochondrial OS | 22.7376442 | 22.84955406 | 22.19084167 | 23.05339622 |
| P40939 | ECHA_HUMAN Trifunctional enzyme subunit alpha, mitochondrial OS | 20.05629349 | 18.65982819 | 18.91164589 | 20.71280289 |
| P41091 | IF2G_HUMAN Eukaryotic translation initiation factor 2 subunit 3 OS | 19.02732849 | 20.92303085 | 20.30374146 | 20.31052399 |
| A0A6Q8PGW4 | A0A6Q8PGW4_HUMAN Diadenosine tetraphosphate synthetase OS | 22.65839958 | 20.50096321 | 22.15035057 | 22.33134079 |
| A0A0A0MSX9 | A0A0A0MSX9_HUMAN Isoleucyl-tRNA synthetase OS | 20.78803635 | 20.23233604 | 18.30582237 | 19.70235252 |
| P42677 | RS27_HUMAN 40S ribosomal protein S27 OS | 21.05291557 | 21.36292458 | 21.74365616 | 21.24103546 |
| P42704 | LPPRC_HUMAN Leucine-rich PPR motif-containing protein, mitochondrial OS | 20.07887459 | 20.15930939 | 19.95375824 | 19.05296326 |
| P42766 | RL35_HUMAN 60S ribosomal protein L35 OS | 20.98530579 | 21.26436234 | 20.98300934 | 20.2877121 |
| D6REM6 | D6REM6_HUMAN Matrin-3 OS | 18.12245369 | 20.94327927 | 20.88807106 | 18.25110435 |
| C9J3L8 | C9J3L8_HUMAN Signal sequence receptor subunit alpha OS | 20.83352661 | 20.42552376 | 19.78462219 | 20.82826614 |
| P43487-2 | RANG_HUMAN Isoform 2 of Ran-specific GTPase-activating protein OS | 19.92619133 | 21.06137848 | 18.36230278 | 20.40851974 |
| A0A0A0MR02 | A0A0A0MR02_HUMAN Outer mitochondrial membrane protein porin 2 (Fragment) OS | 18.93975449 | 18.82051849 | 18.63635254 | 20.91597557 |
| P46060 | RAGP1_HUMAN Ran GTPase-activating protein 1 OS | 20.7369442 | 20.84919167 | 20.60918999 | 20.90771294 |
| E9PLL6 | E9PLL6_HUMAN 60S ribosomal protein L27a OS | 20.7542572 | 19.02553749 | 18.59032059 | 20.97994423 |

| | | | | | |
|---|---|---|---|---|---|
| A0A2R8Y6J3 | A0A2R8Y6J3_HUMAN 60S ribosomal protein L5 (Fragment) OS | 21.16484261 | 20.87919807 | 21.56648636 | 20.66553116 |
| P46779 | RL28_HUMAN 60S ribosomal protein L28 OS | 20.38247681 | 21.68071747 | 22.26384735 | 20.03965759 |
| P46781 | RS9_HUMAN 40S ribosomal protein S9 OS | 22.76727104 | 23.10210228 | 22.92795753 | 22.23549461 |
| P46783 | RS10_HUMAN 40S ribosomal protein S10 OS | 22.1238575 | 21.65560722 | 21.62880898 | 22.79249191 |
| P46821 | MAP1B_HUMAN Microtubule-associated protein 1B OS | 23.13908577 | 22.94111252 | 23.00273132 | 23.0926342 |
| P46940 | IQGA1_HUMAN Ras GTPase-activating-like protein IQGAP1 OS | 24.00821304 | 23.67281914 | 23.76910782 | 23.76708794 |
| P47756-2 | CAPZB_HUMAN Isoform 2 of F-actin-capping protein subunit beta OS | 22.01294136 | 21.34342957 | 21.38758659 | 21.88550377 |
| P47914 | RL29_HUMAN 60S ribosomal protein L29 OS | 19.93747139 | 21.24417496 | 18.78913689 | 19.66221237 |
| P48047 | ATPO_HUMAN ATP synthase subunit O, mitochondrial OS | 20.76700783 | 20.39362144 | 20.49101067 | 20.20179939 |
| P48444 | COPD_HUMAN Coatomer subunit delta OS | 19.20639038 | 18.78091049 | 19.65928841 | 20.10495186 |
| P48643 | TCPE_HUMAN T-complex protein 1 subunit epsilon OS | 19.14135933 | 19.8029232 | 21.50741386 | 21.48978806 |
| P49207 | RL34_HUMAN 60S ribosomal protein L34 OS | 21.11050606 | 21.28133011 | 20.90763855 | 21.49770164 |
| P49257 | LMAN1_HUMAN Protein ERGIC-53 OS | 20.85946465 | 20.31052399 | 18.4568367 | 20.73015785 |
| P49327 | FAS_HUMAN Fatty acid synthase OS | 22.85325241 | 22.78761864 | 22.85325241 | 22.35124207 |
| P49368-2 | TCPG_HUMAN Isoform 2 of T-complex protein 1 subunit gamma OS | 20.64790154 | 22.1076355 | 22.11603928 | 22.52676201 |
| P49411 | EFTU_HUMAN Elongation factor Tu, mitochondrial OS | 20.77209282 | 21.30996895 | 21.29148293 | 21.49389648 |
| A0A6Q8PGR9 | A0A6Q8PGR9_HUMAN Alanine--tRNA ligase OS | 18.80595398 | 20.223526 | 20.52410889 | 20.24435043 |
| P49721 | PSB2_HUMAN Proteasome subunit beta type-2 OS | 20.19002724 | 18.74065781 | 19.61156845 | 18.52177048 |
| P49748-2 | ACADV_HUMAN Isoform 2 of Very long-chain specific acyl-CoA dehydrogenase, mitochondrial OS | 20.55730629 | 20.48492813 | 18.15488434 | 20.70100212 |
| P49755 | TMEDA_HUMAN Transmembrane emp24 domain-containing protein 10 OS | 21.40457535 | 20.70201683 | 20.59322739 | 21.44536209 |
| P50395 | GDIB_HUMAN Rab GDP dissociation inhibitor beta OS | 23.22912598 | 22.87820625 | 22.23777199 | 23.04550171 |
| P50454 | SERPH_HUMAN Serpin H1 OS | 25.6435585 | 25.03980064 | 24.48965263 | 25.09281158 |
| P50502 | F10A1_HUMAN Hsc70-interacting protein OS | 22.07234764 | 21.534832 | 20.55421829 | 21.27537346 |
| P50990 | TCPQ_HUMAN T-complex protein 1 subunit theta OS | 22.16060257 | 23.07182312 | 22.83300591 | 22.91832542 |
| P50991 | TCPD_HUMAN T-complex protein 1 subunit delta OS | 21.31318474 | 21.25112915 | 22.47221565 | 21.98971176 |
| P51148 | RAB5C_HUMAN Ras-related protein Rab-5C OS | 21.26080704 | 21.59514046 | 20.97379303 | 21.83047295 |
| P51149 | RAB7A_HUMAN Ras-related protein Rab-7a OS | 22.71793556 | 22.20158958 | 22.18401527 | 22.25715637 |
| P51571 | SSRD_HUMAN Translocon-associated protein subunit delta OS | 20.67676353 | 19.64981461 | 19.71739578 | 20.84383583 |
| P51572 | BAP31_HUMAN B-cell receptor-associated protein 31 OS | 17.92259598 | 18.25635529 | 19.50223923 | 19.21449471 |
| P52209-2 | 6PGD_HUMAN Isoform 2 of 6-phosphogluconate dehydrogenase, decarboxylating OS | 23.3372879 | 22.33946419 | 21.9394455 | 22.58217239 |
| P52272-2 | HNRPM_HUMAN Isoform 2 of Heterogeneous nuclear ribonucleoprotein M OS | 21.64072609 | 21.08628082 | 22.13599014 | 21.81710434 |
| J3KTF8 | J3KTF8_HUMAN Rho GDP-dissociation inhibitor 1 (Fragment) OS | 23.52133179 | 23.53872108 | 22.55695534 | 23.88874054 |
| P52907 | CAZA1_HUMAN F-actin-capping protein subunit alpha-1 OS | 22.35748482 | 21.97973442 | 22.09413338 | 22.56036568 |
| P53396-2 | ACLY_HUMAN Isoform 2 of ATP-citrate synthase OS | 21.96105766 | 21.92288589 | 22.14724731 | 22.02553368 |
| P53618 | COPB_HUMAN Coatomer subunit beta OS | 19.32070923 | 20.1977253 | 19.00530243 | 20.54434586 |
| P53621 | COPA_HUMAN Coatomer subunit alpha OS | 22.68382454 | 22.54750252 | 22.55025291 | 22.44899559 |
| P54136 | SYRC_HUMAN Arginine--tRNA ligase, cytoplasmic OS | 20.83776665 | 20.80009651 | 20.1692543 | 20.34559631 |
| P55060-4 | XPO2_HUMAN Isoform 4 of Exportin-2 OS | 19.82200813 | 18.66786385 | 17.65454102 | 19.97154999 |
| P55072 | TERA_HUMAN Transitional endoplasmic reticulum ATPase OS | 24.05705452 | 23.39139366 | 23.98771858 | 22.93711281 |
| P55084-2 | ECHB_HUMAN Isoform 2 of Trifunctional enzyme subunit beta, mitochondrial OS | 20.35067558 | 18.85640335 | 19.36937141 | 19.67572975 |
| H0YHC3 | H0YHC3_HUMAN Nucleosome assembly protein 1-like 1 (Fragment) OS | 20.18833733 | 20.7776413 | 20.59623337 | 17.94430542 |

| | | | | | |
|---|---|---|---|---|---|
| P55884 | EIF3B_HUMAN Eukaryotic translation initiation factor 3 subunit B OS | 18.57753944 | 19.83369637 | 19.02816963 | 20.20848274 |
| P59998 | ARPC4_HUMAN Actin-related protein 2/3 complex subunit 4 OS | 22.11470604 | 22.09377861 | 22.12316322 | 22.69166183 |
| P60174 | TPIS_HUMAN Triosephosphate isomerase OS | 23.27639771 | 23.84584618 | 24.09055138 | 24.59718895 |
| B3KW56 | B3KW56_HUMAN Eukaryotic translation initiation factor 3 subunit E OS | 19.91165161 | 19.76900673 | 18.54272652 | 20.17791557 |
| F8W1R7 | F8W1R7_HUMAN Myosin light polypeptide 6 OS | 23.86702919 | 24.01563263 | 23.8969841 | 24.06899071 |
| P60709 | ACTB_HUMAN Actin, cytoplasmic 1 OS | 29.5298996 | 29.50846863 | 29.72000885 | 29.53129578 |
| P60842 | IF4A1_HUMAN Eukaryotic initiation factor 4A-I OS | 25.29862595 | 24.65485382 | 24.5323143 | 24.97631264 |
| P60866 | RS20_HUMAN 40S ribosomal protein S20 OS | 22.93490028 | 23.04278374 | 22.17056847 | 22.09206963 |
| B1ALA9 | B1ALA9_HUMAN Ribose-phosphate pyrophosphokinase 1 OS | 19.31720924 | 18.96899223 | 19.94649506 | 19.62693977 |
| P60900 | PSA6_HUMAN Proteasome subunit alpha type-6 OS | 20.35820961 | 20.8303566 | 20.40883064 | 21.42152214 |
| P60953 | CDC42_HUMAN Cell division control protein 42 homolog OS | 20.50930023 | 20.43806839 | 20.9557457 | 20.54717255 |
| P60981 | DEST_HUMAN Destrin OS | 21.46418381 | 21.45563316 | 21.47516251 | 21.40431595 |
| P61019 | RAB2A_HUMAN Ras-related protein Rab-2A OS | 21.1293087 | 20.28093338 | 20.36324501 | 19.8890667 |
| P61088 | UBE2N_HUMAN Ubiquitin-conjugating enzyme E2 N OS | 20.9978981 | 21.51595306 | 21.42306328 | 21.61162376 |
| P61106 | RAB14_HUMAN Ras-related protein Rab-14 OS | 20.51431656 | 20.53525925 | 20.12325668 | 17.97779083 |
| B4DXW1 | B4DXW1_HUMAN Actin-like protein 3 OS | 22.71753693 | 21.74419022 | 21.8473568 | 22.20660591 |
| P61160 | ARP2_HUMAN Actin-related protein 2 OS | 22.2937851 | 21.52812195 | 22.10354424 | 21.49755478 |
| R4GMT0 | R4GMT0_HUMAN Alpha-centractin OS | 19.0608387 | 19.81391144 | 21.02890968 | 20.02242279 |
| P84077 | ARF1_HUMAN ADP-ribosylation factor 1 OS | 22.76844215 | 22.53793907 | 22.59048843 | 23.07713127 |
| P61224-2 | RAP1B_HUMAN Isoform 2 of Ras-related protein Rap-1b OS | 21.05834389 | 21.05940056 | 21.01678848 | 20.85574532 |
| P61247 | RS3A_HUMAN 40S ribosomal protein S3a OS | 21.88405037 | 22.07309914 | 22.11946297 | 21.52606964 |
| J3QRI7 | J3QRI7_HUMAN 60S ribosomal protein L26 (Fragment) OS | 21.34256172 | 21.26984978 | 21.22552681 | 21.58659935 |
| P61313 | RL15_HUMAN 60S ribosomal protein L15 OS | 19.74180603 | 21.89163589 | 21.21720695 | 19.95475388 |
| P61353 | RL27_HUMAN 60S ribosomal protein L27 OS | 22.93097305 | 22.72698212 | 22.68527985 | 22.77822304 |
| P61586 | RHOA_HUMAN Transforming protein RhoA OS | 20.54736137 | 20.57144928 | 20.46283722 | 18.35413361 |
| P61604 | CH10_HUMAN 10 kDa heat shock protein, mitochondrial OS | 22.73770714 | 22.60387993 | 22.33467293 | 22.72719002 |
| P61619 | S61A1_HUMAN Protein transport protein Sec61 subunit alpha isoform 1 OS | 18.47943306 | 20.18628311 | 20.03442764 | 19.72177315 |
| P61923 | COPZ1_HUMAN Coatomer subunit zeta-1 OS | 18.60433006 | 19.91628265 | 19.40555191 | 17.92468262 |
| P61970 | NTF2_HUMAN Nuclear transport factor 2 OS | 20.49891853 | 20.18531609 | 20.22811317 | 20.33330917 |
| P61978-3 | HNRPK_HUMAN Isoform 3 of Heterogeneous nuclear ribonucleoprotein K OS | 23.09923172 | 23.44037819 | 23.84373856 | 23.63234138 |
| P61981 | 1433G_HUMAN 14-3-3 protein gamma OS | 18.42302132 | 22.27104759 | 17.98696136 | 20.9958992 |
| P62081 | RS7_HUMAN 40S ribosomal protein S7 OS | 22.66921234 | 22.55978203 | 22.36847687 | 22.01127052 |
| E9PMD7 | E9PMD7_HUMAN Serine/threonine-protein phosphatase OS | 20.06539536 | 19.72168922 | 18.28643608 | 20.40395164 |
| P62191-2 | PRS4_HUMAN Isoform 2 of 26S proteasome regulatory subunit 4 OS | 19.5610466 | 20.35487747 | 18.47707939 | 17.67256355 |
| Q5JR95 | Q5JR95_HUMAN 40S ribosomal protein S8 OS | 21.89999199 | 22.16026497 | 22.126791 | 22.73442268 |
| P62244 | RS15A_HUMAN 40S ribosomal protein S15a OS | 22.8121357 | 22.11825943 | 22.24895859 | 22.83686256 |
| P62249 | RS16_HUMAN 40S ribosomal protein S16 OS | 23.02240562 | 23.15893936 | 23.09021187 | 23.08371925 |
| P62258 | 1433E_HUMAN 14-3-3 protein epsilon OS | 24.48179245 | 24.88599777 | 25.01069069 | 24.21385956 |
| A0A2R8Y811 | A0A2R8Y811_HUMAN 40S ribosomal protein S14 (Fragment) OS | 22.64425278 | 22.63916016 | 22.63143158 | 23.099617 |
| P62266 | RS23_HUMAN 40S ribosomal protein S23 OS | 19.49882126 | 20.69515038 | 20.42141914 | 20.35928154 |
| P62269 | RS18_HUMAN 40S ribosomal protein S18 OS | 22.16429138 | 22.85625839 | 22.96545029 | 22.22022247 |
| P62277 | RS13_HUMAN 40S ribosomal protein S13 OS | 22.54196167 | 23.03071213 | 22.88016891 | 23.04660225 |

| | | | | | |
|---|---|---|---|---|---|
| P62280 | RS11_HUMAN 40S ribosomal protein S11 OS | 21.46956062 | 22.00963211 | 22.20203781 | 21.24150085 |
| P62424 | RL7A_HUMAN 60S ribosomal protein L7a OS | 22.38474464 | 22.31705475 | 22.33772469 | 22.15927887 |
| P62495-2 | ERF1_HUMAN Isoform 2 of Eukaryotic peptide chain release factor subunit 1 OS | 19.9813385 | 19.69171333 | 18.8434906 | 19.57411385 |
| P62701 | RS4X_HUMAN 40S ribosomal protein S4, X isoform OS | 22.05480385 | 22.29698181 | 22.86287308 | 21.86619759 |
| P62750 | RL23A_HUMAN 60S ribosomal protein L23a OS | 22.6637516 | 22.13868141 | 22.56320763 | 22.01767349 |
| P62805 | H4_HUMAN Histone H4 OS | 20.7542572 | 19.5152607 | 18.8754425 | 19.59492302 |
| P62826 | RAN_HUMAN GTP-binding nuclear protein Ran OS | 23.31575584 | 23.00792313 | 23.3066082 | 24.03263092 |
| P62829 | RL23_HUMAN 60S ribosomal protein L23 OS | 21.55032349 | 22.20275497 | 19.74606705 | 21.30991364 |
| S4R456 | S4R456_HUMAN 40S ribosomal protein S15 (Fragment) OS | 18.76415825 | 18.87331963 | 18.88997269 | 18.95011711 |
| P62847-2 | RS24_HUMAN Isoform 2 of 40S ribosomal protein S24 OS | 18.87836456 | 20.34256172 | 20.33690834 | 21.84049606 |
| P62851 | RS25_HUMAN 40S ribosomal protein S25 OS | 22.20263481 | 22.06822014 | 21.82018471 | 22.31688881 |
| P62857 | RS28_HUMAN 40S ribosomal protein S28 OS | 19.75593758 | 20.7923336 | 20.42613792 | 20.1043129 |
| E5RI99 | E5RI99_HUMAN 60S ribosomal protein L30 (Fragment) OS | 19.77177048 | 20.74336815 | 20.14532089 | 20.04473495 |
| P62899 | RL31_HUMAN 60S ribosomal protein L31 OS | 21.02472305 | 21.78508568 | 21.93844032 | 21.34321213 |
| P62906 | RL10A_HUMAN 60S ribosomal protein L10a OS | 22.63526726 | 22.59279442 | 21.74996948 | 22.84684181 |
| D3YTB1 | D3YTB1_HUMAN 60S ribosomal protein L32 (Fragment) OS | 19.16825104 | 19.68024254 | 20.77531052 | 19.93445015 |
| P62913 | RL11_HUMAN 60S ribosomal protein L11 OS | 22.14099121 | 22.10126877 | 22.33279037 | 21.17907143 |
| P62917 | RL8_HUMAN 60S ribosomal protein L8 OS | 20.62220955 | 20.93660927 | 21.90142822 | 21.3046875 |
| P62937 | PPIA_HUMAN Peptidyl-prolyl cis-trans isomerase A OS | 25.39584541 | 25.18899345 | 25.30002213 | 25.47966576 |
| P63000 | RAC1_HUMAN Ras-related C3 botulinum toxin substrate 1 OS | 22.02259064 | 22.02323532 | 21.77213287 | 21.61445618 |
| P63104 | 1433Z_HUMAN 14-3-3 protein zeta/delta OS | 23.11859131 | 24.02478981 | 24.46967125 | 23.54427528 |
| P63173 | RL38_HUMAN 60S ribosomal protein L38 OS | 19.12953377 | 19.08990479 | 18.94283485 | 19.35309029 |
| I3L397 | I3L397_HUMAN Eukaryotic translation initiation factor 5A (Fragment) OS | 23.20315933 | 22.88628578 | 22.66001129 | 22.99548531 |
| P63244 | RACK1_HUMAN Receptor of activated protein C kinase 1 OS | 22.68769455 | 22.40223503 | 22.33057594 | 22.37904167 |
| P67809 | YBOX1_HUMAN Y-box-binding protein 1 OS | 22.74765587 | 22.75920486 | 22.52561569 | 22.25600433 |
| H0YNG3 | H0YNG3_HUMAN Signal peptidase complex catalytic subunit SEC11 OS | 18.22343063 | 19.51091194 | 19.41544914 | 19.53732872 |
| P67936 | TPM4_HUMAN Tropomyosin alpha-4 chain OS | 24.36084938 | 24.38007355 | 23.59434319 | 24.00547409 |
| P68032 | ACTC_HUMAN Actin, alpha cardiac muscle 1 OS | 24.74088097 | 25.19869232 | 24.25659561 | 25.02643776 |
| P68036-2 | UB2L3_HUMAN Isoform 2 of Ubiquitin-conjugating enzyme E2 L3 OS | 20.16619301 | 20.69557571 | 20.87395096 | 20.99196243 |
| A0A7I2V659 | A0A7I2V659_HUMAN Elongation factor 1-alpha 1 OS | 28.44517708 | 28.03574753 | 27.33125305 | 28.28034019 |
| P68363 | TBA1B_HUMAN Tubulin alpha-1B chain OS | 27.3512764 | 26.94826508 | 27.13359451 | 27.01393127 |
| P68371 | TBB4B_HUMAN Tubulin beta-4B chain OS | 27.17560005 | 26.76268578 | 26.85697556 | 26.43130302 |
| P78371 | TCPB_HUMAN T-complex protein 1 subunit beta OS | 21.93524361 | 22.83682251 | 22.53661156 | 22.74796295 |
| P78417 | GSTO1_HUMAN Glutathione S-transferase omega-1 OS | 22.47114944 | 21.69782448 | 21.38331985 | 22.29299927 |
| P78527 | PRKDC_HUMAN DNA-dependent protein kinase catalytic subunit OS | 21.67137337 | 21.07391739 | 19.96395111 | 19.34712219 |
| C9JXB8 | C9JXB8_HUMAN 60S ribosomal protein L24 OS | 21.07110405 | 20.63979912 | 20.12830162 | 19.10333824 |
| J3QR09 | J3QR09_HUMAN Ribosomal protein L19 OS | 18.86495018 | 17.8894558 | 18.10998154 | 19.38549232 |
| P84103-2 | SRSF3_HUMAN Isoform 2 of Serine/arginine-rich splicing factor 3 OS | 19.94692421 | 18.28826523 | 20.18180275 | 20.56010818 |
| P98179 | RBM3_HUMAN RNA-binding protein 3 OS | 20.84375763 | 20.35810089 | 20.57800865 | 21.36719704 |
| C9JFR7 | C9JFR7_HUMAN Cytochrome c (Fragment) OS | 20.96613693 | 21.44475555 | 21.244524 | 21.09841347 |
| F8VVM2 | F8VVM2_HUMAN Phosphate carrier protein, mitochondrial OS | 17.60062599 | 18.42212296 | 21.98811722 | 22.12107658 |
| A0A024R4E5 | A0A024R4E5_HUMAN High density lipoprotein binding protein (Vigilin), isoform CRA_a OS | 22.63045311 | 21.8818512 | 22.13062859 | 21.87927246 |

| | | | | | |
|---|---|---|---|---|---|
| Q00610-2 | CLH1_HUMAN Isoform 2 of Clathrin heavy chain 1 OS | 24.28333855 | 24.4599514 | 24.52348709 | 24.4379673 |
| A0A1W2PPS1 | A0A1W2PPS1_HUMAN Heterogeneous nuclear ribonucleoprotein U OS | 22.81362534 | 22.8461132 | 22.21252441 | 22.80616951 |
| Q01082 | SPTB2_HUMAN Spectrin beta chain, non-erythrocytic 1 OS | 20.09377861 | 20.3208046 | 20.39110565 | 19.40790939 |
| Q01105-3 | SET_HUMAN Isoform 3 of Protein SET OS | 22.15761375 | 21.89371109 | 21.63688278 | 21.83174896 |
| Q01469 | FABP5_HUMAN Fatty acid-binding protein 5 OS | 19.76960945 | 19.52793121 | 19.37285995 | 19.24328041 |
| Q01518-2 | CAP1_HUMAN Isoform 2 of Adenylyl cyclase-associated protein 1 OS | 23.38811111 | 22.81166649 | 22.88028145 | 22.88689995 |
| Q01813 | PFKAP_HUMAN ATP-dependent 6-phosphofructokinase, platelet type OS | 21.26161003 | 20.82593918 | 20.44929695 | 20.34667778 |
| Q01995 | TAGL_HUMAN Transgelin OS | 25.09583282 | 24.96128654 | 25.1590786 | 24.31264496 |
| M0R3D6 | M0R3D6_HUMAN 60S ribosomal protein L18a (Fragment) OS | 19.75468254 | 20.95659828 | 21.43043137 | 19.5927887 |
| Q02878 | RL6_HUMAN 60S ribosomal protein L6 OS | 22.6342926 | 22.74763489 | 22.59573364 | 22.70256615 |
| Q03135 | CAV1_HUMAN Caveolin-1 OS | 22.41717529 | 22.91661263 | 22.47375298 | 21.99565887 |
| Q04637-6 | IF4G1_HUMAN Isoform E of Eukaryotic translation initiation factor 4 gamma 1 OS | 18.87566185 | 21.64891052 | 21.73309898 | 21.32668686 |
| Q04917 | 1433F_HUMAN 14-3-3 protein eta OS | 22.33043861 | 21.76672554 | 21.66422844 | 21.3857975 |
| Q05682-5 | CALD1_HUMAN Isoform 5 of Caldesmon OS | 23.44695282 | 23.52324867 | 23.57957458 | 23.55145073 |
| A0A6I8PTT9 | A0A6I8PTT9_HUMAN Glutamine--fructose-6-phosphate transaminase (isomerizing) OS | 19.03189087 | 18.82517242 | 19.52383232 | 20.12578201 |
| Q06323 | PSME1_HUMAN Proteasome activator complex subunit 1 OS | 20.07313156 | 18.79440498 | 18.25384521 | 19.6867466 |
| Q06830 | PRDX1_HUMAN Peroxiredoxin-1 OS | 24.96035957 | 24.15398598 | 24.34448624 | 24.11791039 |
| Q07020 | RL18_HUMAN 60S ribosomal protein L18 OS | 23.02531433 | 23.17790031 | 22.8281498 | 21.97819901 |
| Q07065 | CKAP4_HUMAN Cytoskeleton-associated protein 4 OS | 25.25666618 | 25.28957748 | 25.32717896 | 25.23553276 |
| Q08211 | DHX9_HUMAN ATP-dependent RNA helicase A OS | 20.98454094 | 20.9061718 | 21.01065636 | 21.02614212 |
| Q09666 | AHNK_HUMAN Neuroblast differentiation-associated protein AHNAK OS | 26.62100792 | 26.41356087 | 26.47032356 | 25.94518661 |
| Q12792 | TWF1_HUMAN Twinfilin-1 OS | 19.92853546 | 19.87456703 | 19.09229469 | 19.71100426 |
| Q13162 | PRDX4_HUMAN Peroxiredoxin-4 OS | 18.68662453 | 20.78700066 | 18.63160133 | 21.92972755 |
| Q13200 | PSMD2_HUMAN 26S proteasome non-ATPase regulatory subunit 2 OS | 20.86831093 | 20.59623337 | 20.59614182 | 21.10174942 |
| A0A7I2YQU2 | A0A7I2YQU2_HUMAN Eukaryotic translation initiation factor 3 subunit I OS | 18.56655884 | 19.83174896 | 18.65626717 | 19.56917 |
| Q13404 | UB2V1_HUMAN Ubiquitin-conjugating enzyme E2 variant 1 OS | 24.62405205 | 24.62823105 | 24.45481682 | 24.98215675 |
| Q13509 | TBB3_HUMAN Tubulin beta-3 chain OS | 20.71665955 | 20.27344131 | 20.58306885 | 19.21914864 |
| Q13813-3 | SPTN1_HUMAN Isoform 3 of Spectrin alpha chain, non-erythrocytic 1 OS | 20.70902061 | 21.31744194 | 20.69905472 | 20.48424149 |
| Q13885 | TBB2A_HUMAN Tubulin beta-2A chain OS | 21.21365166 | 20.09377861 | 20.43857574 | 19.739748 |
| Q14019 | COTL1_HUMAN Coactosin-like protein OS | 21.77386284 | 21.90142822 | 22.01573563 | 21.13652229 |
| H0YA96 | H0YA96_HUMAN Heterogeneous nuclear ribonucleoprotein D0 (Fragment) OS | 22.32750893 | 21.78656197 | 21.28799438 | 22.0921669 |
| Q14152 | EIF3A_HUMAN Eukaryotic translation initiation factor 3 subunit A OS | 20.89245033 | 21.60462761 | 20.39508629 | 20.68970108 |
| Q14203-5 | DCTN1_HUMAN Isoform 5 of Dynactin subunit 1 OS | 17.61199188 | 19.21425819 | 17.94719696 | 18.45355988 |
| Q14204 | DYHC1_HUMAN Cytoplasmic dynein 1 heavy chain 1 OS | 23.90113258 | 23.65403366 | 23.85908508 | 23.16855049 |
| Q14315 | FLNC_HUMAN Filamin-C OS | 27.09194374 | 26.97421265 | 26.98185349 | 26.87244034 |
| Q14697 | GANAB_HUMAN Neutral alpha-glucosidase AB OS | 22.99762344 | 23.51941299 | 23.18717575 | 23.43529892 |
| Q14764 | MVP_HUMAN Major vault protein OS | 20.39058113 | 22.77344131 | 19.33424759 | 21.94510269 |
| Q14847 | LASP1_HUMAN LIM and SH3 domain protein 1 OS | 21.31290817 | 21.60688782 | 22.53036308 | 21.82325935 |
| Q14974 | IMB1_HUMAN Importin subunit beta-1 OS | 22.30866432 | 21.90517998 | 22.1890316 | 21.7320652 |
| Q15019 | SEPT2_HUMAN Septin-2 OS | 22.23861885 | 21.11362457 | 21.44985199 | 21.60765457 |
| Q15056-2 | IF4H_HUMAN Isoform Short of Eukaryotic translation initiation factor 4H OS | 20.77305794 | 20.79827881 | 18.79834366 | 21.32558823 |

| | | | | | |
|---|---|---|---|---|---|
| Q15084-3 | PDIA6_HUMAN Isoform 3 of Protein disulfide-isomerase A6 OS | 22.83953667 | 22.79237175 | 22.26224136 | 23.43338966 |
| Q15149-4 | PLEC_HUMAN Isoform 4 of Plectin OS | 24.71711922 | 24.969347 | 24.830019 | 24.10181427 |
| Q15293 | RCN1_HUMAN Reticulocalbin-1 OS | 21.11977959 | 21.70150948 | 21.04353523 | 20.97784996 |
| Q15365 | PCBP1_HUMAN Poly(rC)-binding protein 1 OS | 21.63732529 | 22.02799988 | 22.22914124 | 22.05135727 |
| Q15366-6 | PCBP2_HUMAN Isoform 6 of Poly(rC)-binding protein 2 OS | 20.50057411 | 18.698452 | 20.46483231 | 20.68294716 |
| B8ZZU8 | B8ZZU8_HUMAN Elongin-B OS | 19.77781677 | 19.90050697 | 19.78297615 | 20.01876068 |
| F5H365 | F5H365_HUMAN Protein transport protein SEC23 OS | 17.96944618 | 18.96937752 | 18.12153816 | 21.32542419 |
| Q15691 | MARE1_HUMAN Microtubule-associated protein RP/EB family member 1 OS | 17.83308029 | 20.34884071 | 19.53636169 | 20.24504662 |
| Q15758 | AAAT_HUMAN Neutral amino acid transporter B(0) OS | 20.70379257 | 20.43705368 | 20.63856316 | 20.75971222 |
| Q15907 | RB11B_HUMAN Ras-related protein Rab-11B OS | 22.26252937 | 22.26258659 | 22.11524582 | 22.28587914 |
| Q15942 | ZYX_HUMAN Zyxin OS | 22.23613739 | 22.16287804 | 22.59201813 | 22.23567009 |
| E7ES33 | E7ES33_HUMAN Septin OS | 21.20794678 | 21.85269928 | 20.24562645 | 21.16195679 |
| Q16222-3 | UAP1_HUMAN Isoform 3 of UDP-N-acetylhexosamine pyrophosphorylase OS | 19.39533806 | 19.98273277 | 20.26670837 | 20.1983242 |
| Q16527 | CSRP2_HUMAN Cysteine and glycine-rich protein 2 OS | 19.78471756 | 20.29165268 | 19.84460068 | 18.88469315 |
| Q16555-2 | DPYL2_HUMAN Isoform 2 of Dihydropyrimidinase-related protein 2 OS | 22.42393494 | 22.52125931 | 22.51662636 | 22.7605648 |
| Q16658 | FSCN1_HUMAN Fascin OS | 23.51905441 | 23.55461693 | 23.22679138 | 23.33197021 |
| A0A7I2YQ74 | A0A7I2YQ74_HUMAN UTP--glucose-1-phosphate uridylyltransferase OS | 20.23350716 | 20.25118637 | 20.38004684 | 20.29949951 |
| E9PIR7 | E9PIR7_HUMAN Thioredoxin-disulfide reductase OS | 20.91590309 | 20.79867363 | 18.58206558 | 19.95005989 |
| Q6NZI2 | CAVN1_HUMAN Caveolae-associated protein 1 OS | 22.70372963 | 23.40080261 | 23.39309692 | 23.35272408 |
| Q6UVK1 | CSPG4_HUMAN Chondroitin sulfate proteoglycan 4 OS | 19.39962006 | 19.93574715 | 20.68671227 | 19.50047684 |
| Q70UQ0-4 | IKIP_HUMAN Isoform 4 of Inhibitor of nuclear factor kappa-B kinase-interacting protein OS | 19.40643692 | 18.23005867 | 19.04209328 | 20.60503387 |
| Q7KZF4 | SND1_HUMAN Staphylococcal nuclease domain-containing protein 1 OS | 22.73789215 | 22.74517441 | 23.06307602 | 22.70459366 |
| Q86VP6 | CAND1_HUMAN Cullin-associated NEDD8-dissociated protein 1 OS | 20.53782082 | 20.93026924 | 20.72050476 | 20.99444962 |
| Q8NBS9-2 | TXND5_HUMAN Isoform 2 of Thioredoxin domain-containing protein 5 OS | 21.11273384 | 20.36879539 | 20.0941658 | 20.95496559 |
| Q8TED1 | GPX8_HUMAN Probable glutathione peroxidase 8 OS | 20.08485603 | 19.09341431 | 19.99507141 | 19.04289818 |
| Q8WUM4 | PDC6I_HUMAN Programmed cell death 6-interacting protein OS | 21.28455353 | 19.92161369 | 18.27128601 | 20.72533989 |
| Q92499-3 | DDX1_HUMAN Isoform 3 of ATP-dependent RNA helicase DDX1 OS | 18.12132645 | 20.40613365 | 18.52245331 | 18.84397888 |
| Q92598-2 | HS105_HUMAN Isoform Beta of Heat shock protein 105 kDa OS | 18.6023674 | 20.34797668 | 18.33521271 | 20.21643829 |
| Q92616 | GCN1_HUMAN eIF-2-alpha kinase activator GCN1 OS | 18.45020676 | 19.38721085 | 20.10098076 | 18.54070282 |
| A0A087WTP3 | A0A087WTP3_HUMAN Far upstream element-binding protein 2 OS | 21.17169952 | 20.74197006 | 20.79891205 | 20.47704315 |
| Q92973-2 | TNPO1_HUMAN Isoform 2 of Transportin-1 OS | 18.61182785 | 20.31959343 | 18.71065712 | 18.6649456 |
| Q969G5 | CAVN3_HUMAN Caveolae-associated protein 3 OS | 21.30969238 | 21.17846298 | 20.51595306 | 21.67878342 |
| Q969H8 | MYDGF_HUMAN Myeloid-derived growth factor OS | 21.56365013 | 21.38337326 | 21.09847641 | 21.35143089 |
| Q96AE4 | FUBP1_HUMAN Far upstream element-binding protein 1 OS | 20.86883736 | 20.4691124 | 20.22646904 | 19.21940613 |
| Q96AG4 | LRC59_HUMAN Leucine-rich repeat-containing protein 59 OS | 21.9192524 | 22.20353127 | 22.36327171 | 22.0500946 |
| Q96AY3 | FKB10_HUMAN Peptidyl-prolyl cis-trans isomerase FKBP10 OS | 20.18410492 | 19.36252594 | 20.24933624 | 19.78151894 |
| Q96HC4 | PDLI5_HUMAN PDZ and LIM domain protein 5 OS | 18.70390511 | 19.27682877 | 19.87273407 | 19.69335556 |
| Q96QK1 | VPS35_HUMAN Vacuolar protein sorting-associated protein 35 OS | 18.32221222 | 19.24896812 | 19.19289398 | 20.00990486 |
| Q96TA1-2 | NIBA2_HUMAN Isoform 2 of Protein Niban 2 OS | 19.14989853 | 20.91086197 | 20.85376549 | 20.61387253 |
| A0A087X271 | A0A087X271_HUMAN Calponin (Fragment) OS | 23.69699669 | 23.3259449 | 21.96183395 | 22.62075615 |

| | | | | | |
|---|---|---|---|---|---|
| A0A7I2V641 | A0A7I2V641_HUMAN 26S proteasome non-ATPase regulatory subunit 1 OS | 18.28941727 | 19.67624664 | 19.57581902 | 18.32927704 |
| Q99497 | PARK7_HUMAN Parkinson disease protein 7 OS | 22.21092033 | 22.30401993 | 22.20490456 | 21.77193069 |
| Q99536 | VAT1_HUMAN Synaptic vesicle membrane protein VAT-1 homolog OS | 22.63396072 | 22.03795052 | 19.75020599 | 21.72317505 |
| F5GY37 | F5GY37_HUMAN Prohibitin OS | 21.92788506 | 21.71962738 | 20.81550217 | 21.71895981 |
| Q99715-4 | COCA1_HUMAN Isoform 4 of Collagen alpha-1(XII) chain OS | 19.68501854 | 19.96253967 | 19.78284836 | 18.75119781 |
| Q99832 | TCPH_HUMAN T-complex protein 1 subunit eta OS | 21.34884071 | 20.57800865 | 21.46856689 | 21.84352875 |
| Q9BRA2 | TXD17_HUMAN Thioredoxin domain-containing protein 17 OS | 19.84862518 | 19.68291283 | 20.00675964 | 20.44717979 |
| Q9BSJ8 | ESYT1_HUMAN Extended synaptotagmin-1 OS | 20.17803764 | 20.97673225 | 20.32223701 | 20.76773453 |
| Q9BUF5 | TBB6_HUMAN Tubulin beta-6 chain OS | 23.14765167 | 22.41423607 | 22.6908741 | 22.16459846 |
| Q9BVK6 | TMED9_HUMAN Transmembrane emp24 domain-containing protein 9 OS | 19.98036194 | 20.52008629 | 19.68292999 | 20.33712578 |
| Q9H0U4 | RAB1B_HUMAN Ras-related protein Rab-1B OS | 22.75906181 | 22.75963211 | 22.9252243 | 22.09326363 |
| Q5T123 | Q5T123_HUMAN SH3 domain-binding glutamic acid-rich-like protein 3 OS | 21.15189934 | 18.7892971 | 18.71455956 | 20.36292458 |
| Q9H3N1 | TMX1_HUMAN Thioredoxin-related transmembrane protein 1 OS | 18.19048309 | 20.78668213 | 19.18562889 | 17.42985535 |
| Q9H4M9 | EHD1_HUMAN EH domain-containing protein 1 OS | 18.41928482 | 19.01069069 | 20.92672729 | 21.23502731 |
| Q9HB71 | CYBP_HUMAN Calcyclin-binding protein OS | 18.70917511 | 20.5643959 | 18.91725349 | 18.86560249 |
| A0A087X163 | A0A087X163_HUMAN Ras-related protein Rab-18 OS | 18.61141777 | 19.37511063 | 18.93945313 | 18.47066879 |
| Q9NQC3-2 | RTN4_HUMAN Isoform B of Reticulon-4 OS | 23.34272385 | 22.8412838 | 22.71078682 | 23.19751549 |
| Q9NR12 | PDLI7_HUMAN PDZ and LIM domain protein 7 OS | 18.79019356 | 19.67226219 | 19.06404877 | 19.15857887 |
| Q9NRV9 | HEBP1_HUMAN Heme-binding protein 1 OS | 18.67448997 | 18.21212578 | 19.93890762 | 18.86046219 |
| D6RGI3 | D6RGI3_HUMAN Septin OS | 22.12164688 | 21.77996635 | 21.67998695 | 21.34651566 |
| Q9NZM1-6 | MYOF_HUMAN Isoform 6 of Myoferlin OS | 23.84957314 | 23.01350403 | 23.11109543 | 22.56048203 |
| Q9NZN4 | EHD2_HUMAN EH domain-containing protein 2 OS | 22.09329414 | 21.28421402 | 21.56644058 | 21.16373825 |
| Q9P0L0 | VAPA_HUMAN Vesicle-associated membrane protein-associated protein A OS | 19.88254547 | 19.76885033 | 19.23502541 | 18.76872063 |
| Q9P2E9 | RRBP1_HUMAN Ribosome-binding protein 1 OS | 23.50178909 | 23.40911674 | 23.15705872 | 23.19231606 |
| F8VQE1 | F8VQE1_HUMAN LIM domain and actin-binding protein 1 OS | 21.16974449 | 20.71749496 | 18.20223618 | 20.70480537 |
| Q9UHD8-7 | SEPT9_HUMAN Isoform 7 of Septin-9 OS | 22.38955688 | 22.09026146 | 22.11565781 | 22.17273712 |
| Q9ULV4 | COR1C_HUMAN Coronin-1C OS | 20.39267731 | 20.36591721 | 21.1221199 | 20.94320679 |
| Q9UQ80-2 | PA2G4_HUMAN Isoform 2 of Proliferation-associated protein 2G4 OS | 21.8764267 | 21.51931763 | 21.58664513 | 21.97620773 |
| Q9Y230 | RUVB2_HUMAN RuvB-like 2 OS | 18.30500984 | 18.33820915 | 20.23128128 | 19.30720139 |
| Q9Y265 | RUVB1_HUMAN RuvB-like 1 OS | 18.55114746 | 20.03335381 | 20.45100975 | 20.28557014 |
| Q9Y266 | NUDC_HUMAN Nuclear migration protein nudC OS | 19.0090847 | 19.68888283 | 17.75411606 | 18.9045372 |
| Q9Y3U8 | RL36_HUMAN 60S ribosomal protein L36 OS | 20.48197746 | 21.4355793 | 20.8459034 | 20.64570427 |
| Q9Y490 | TLN1_HUMAN Talin-1 OS | 24.84388351 | 24.7702179 | 24.88920403 | 24.74180603 |
| A0A087X054 | A0A087X054_HUMAN Hypoxia up-regulated protein 1 OS | 20.05642509 | 20.02485847 | 21.03106499 | 19.64225197 |
| Q9Y617-2 | SERC_HUMAN Isoform 2 of Phosphoserine aminotransferase OS | 21.74176407 | 21.5323143 | 21.55982971 | 21.35681343 |
| Q9Y678 | COPG1_HUMAN Coatomer subunit gamma-1 OS | 21.22640991 | 21.85551643 | 21.95521355 | 21.34705734 |
| Q9Y696 | CLIC4_HUMAN Chloride intracellular channel protein 4 OS | 22.36956787 | 22.27673721 | 21.01277161 | 21.85365295 |

| **Accession** | **Protein** | **LFQ intensity eGFP 48hrs** | **LFQ intensity Envelope 48hrs** | **LFQ intensity Membrane 48hrs** | **LFQ intensity Nucleocapsid 48hrs** |
|---|---|---|---|---|---|
| H3BTL1 | H3BTL1_HUMAN Microtubule-associated protein 1 light chain 3 beta, isoform CRA_f OS | 20.61602783 | 19.31570053 | 20.51749229 | 20.4514122 |

| | | | | | |
|---|---|---|---|---|---|
| Q99613-2 | EIF3C_HUMAN Isoform 2 of Eukaryotic translation initiation factor 3 subunit C OS | 20.29052734 | 20.32695961 | 20.18664551 | 20.28263092 |
| F8VZJ2 | F8VZJ2_HUMAN Nascent polypeptide-associated complex subunit alpha OS | 21.19904518 | 18.63215828 | 21.84230042 | 22.28022575 |
| O00148 | DX39A_HUMAN ATP-dependent RNA helicase DDX39A OS | 20.31118965 | 20.01835251 | 20.09571075 | 18.59388924 |
| O00159-2 | MYO1C_HUMAN Isoform 2 of Unconventional myosin-Ic OS | 22.21106911 | 21.78320694 | 21.85733986 | 22.21380043 |
| O00231 | PSD11_HUMAN 26S proteasome non-ATPase regulatory subunit 11 OS | 21.21406746 | 20.9754734 | 21.56899261 | 21.15480614 |
| O00232-2 | PSD12_HUMAN Isoform 2 of 26S proteasome non-ATPase regulatory subunit 12 OS | 20.46513176 | 19.75865555 | 19.89496803 | 18.77387047 |
| O00299 | CLIC1_HUMAN Chloride intracellular channel protein 1 OS | 24.23066711 | 24.3347683 | 24.61071014 | 23.91988945 |
| O00303 | EIF3F_HUMAN Eukaryotic translation initiation factor 3 subunit F OS | 19.38295746 | 18.56738091 | 20.39571381 | 18.66461372 |
| O00410 | IPO5_HUMAN Importin-5 OS | 21.32849503 | 21.32350159 | 21.36890221 | 21.21204948 |
| A0A2R8Y5G6 | A0A2R8Y5G6_HUMAN RNA helicase OS | 21.15684319 | 21.00915337 | 20.47040558 | 20.73859406 |
| O14818 | PSA7_HUMAN Proteasome subunit alpha type-7 OS | 22.06785774 | 22.11581802 | 22.22925949 | 22.20669556 |
| P19105 | ML12A_HUMAN Myosin regulatory light chain 12A OS | 23.62399483 | 23.00559425 | 23.69508553 | 23.48000526 |
| O15143 | ARC1B_HUMAN Actin-related protein 2/3 complex subunit 1B OS | 21.59700775 | 20.73809814 | 21.18755341 | 21.15455818 |
| O15144 | ARPC2_HUMAN Actin-related protein 2/3 complex subunit 2 OS | 20.68628502 | 18.87779427 | 21.54858398 | 21.10232735 |
| A0A286YF22 | A0A286YF22_HUMAN D-3-phosphoglycerate dehydrogenase OS | 22.08229065 | 21.99603844 | 21.67499733 | 21.21092033 |
| O43242 | PSMD3_HUMAN 26S proteasome non-ATPase regulatory subunit 3 OS | 20.24411774 | 20.6088295 | 20.23899651 | 20.32794762 |
| O43707 | ACTN4_HUMAN Alpha-actinin-4 OS | 23.97561264 | 23.64603424 | 23.7552166 | 24.17119598 |
| O43795-2 | MYO1B_HUMAN Isoform 2 of Unconventional myosin-Ib OS | 20.40114212 | 19.9607029 | 19.70079803 | 20.30529976 |
| O43852 | CALU_HUMAN Calumenin OS | 23.17360687 | 23.74375916 | 23.61862946 | 22.98340988 |
| O60506-4 | HNRPQ_HUMAN Isoform 4 of Heterogeneous nuclear ribonucleoprotein Q OS | 23.01831818 | 21.88136482 | 21.81979561 | 22.45603371 |
| O60664-4 | PLIN3_HUMAN Isoform 4 of Perilipin-3 OS | 22.88912964 | 22.62209702 | 22.99765778 | 22.50491905 |
| O60701 | UGDH_HUMAN UDP-glucose 6-dehydrogenase OS | 23.14577103 | 23.81723976 | 23.6198616 | 23.17949677 |
| O60763 | USO1_HUMAN General vesicular transport factor p115 OS | 20.40062141 | 19.94377899 | 19.95503616 | 20.12338448 |
| O75083 | WDR1_HUMAN WD repeat-containing protein 1 OS | 23.52169228 | 23.40483665 | 23.53575897 | 23.6003685 |
| E5RIW3 | E5RIW3_HUMAN Tubulin-specific chaperone A OS | 20.54745483 | 20.4355278 | 20.63129807 | 18.83438873 |
| O75369-2 | FLNB_HUMAN Isoform 2 of Filamin-B OS | 23.62878609 | 23.7702179 | 23.60614204 | 23.62667084 |
| B4DJV2 | B4DJV2_HUMAN Citrate synthase OS | 21.43903351 | 20.50106049 | 21.43786621 | 21.09029388 |
| O75396 | SC22B_HUMAN Vesicle-trafficking protein SEC22b OS | 22.06887627 | 21.81323242 | 21.65285301 | 22.25245667 |
| O76003 | GLRX3_HUMAN Glutaredoxin-3 OS | 18.77362633 | 19.87885284 | 18.01993942 | 18.97174072 |
| O94979-3 | SC31A_HUMAN Isoform 3 of Protein transport protein Sec31A OS | 21.21501541 | 20.64640808 | 21.30123138 | 21.05867386 |
| O95373 | IPO7_HUMAN Importin-7 OS | 21.0726738 | 20.87882233 | 20.47050476 | 20.38479614 |
| O95782-2 | AP2A1_HUMAN Isoform B of AP-2 complex subunit alpha-1 OS | 19.65579987 | 19.41734505 | 19.11441422 | 18.37331772 |
| O95816 | BAG2_HUMAN BAG family molecular chaperone regulator 2 OS | 20.03778267 | 19.60074043 | 19.6768322 | 19.50629997 |
| P00338 | LDHA_HUMAN L-lactate dehydrogenase A chain OS | 25.59931946 | 24.21178246 | 25.64121819 | 25.35194969 |
| P00367 | DHE3_HUMAN Glutamate dehydrogenase 1, mitochondrial OS | 20.1382122 | 21.23257065 | 20.90771294 | 21.21199036 |
| P00387-2 | NB5R3_HUMAN Isoform 2 of NADH-cytochrome b5 reductase 3 OS | 22.25161934 | 20.54113388 | 22.09635544 | 22.2870369 |
| P00403 | COX2_HUMAN Cytochrome c oxidase subunit 2 OS | 20.18519402 | 20.31030273 | 20.06276321 | 17.92194557 |
| P00505-2 | AATM_HUMAN Isoform 2 of Aspartate aminotransferase, mitochondrial OS | 20.38711357 | 19.84133339 | 19.64602089 | 20.5334549 |

| | | | | | |
|---|---|---|---|---|---|
| P00558 | PGK1_HUMAN Phosphoglycerate kinase 1 OS | 23.70038795 | 24.01077652 | 23.98085022 | 23.66231728 |
| P00568 | KAD1_HUMAN Adenylate kinase isoenzyme 1 OS | 20.12691689 | 19.76556778 | 19.90935326 | 20.07156181 |
| P02452 | CO1A1_HUMAN Collagen alpha-1(I) chain OS | 25.26054955 | 25.17157745 | 25.11787033 | 25.20407677 |
| P02545 | LMNA_HUMAN Prelamin-A/C OS | 25.40291786 | 25.47512627 | 25.71319008 | 25.26456261 |
| P02751-5 | FINC_HUMAN Isoform 5 of Fibronectin OS | 21.25902557 | 21.49921227 | 20.68551445 | 21.11426163 |
| P02786 | TFR1_HUMAN Transferrin receptor protein 1 OS | 21.27685165 | 20.27161789 | 20.21714783 | 21.07365608 |
| P04075 | ALDOA_HUMAN Fructose-bisphosphate aldolase A OS | 25.17352295 | 25.48793602 | 24.71093369 | 25.2035923 |
| P04080 | CYTB_HUMAN Cystatin-B OS | 21.09596825 | 20.51152039 | 20.36099625 | 21.31986809 |
| P04083 | ANXA1_HUMAN Annexin A1 OS | 25.85984421 | 25.46245003 | 25.31451225 | 25.27191734 |
| P04181 | OAT_HUMAN Ornithine aminotransferase, mitochondrial OS | 19.77516747 | 20.05576515 | 20.26899338 | 18.02760124 |
| P04350 | TBB4A_HUMAN Tubulin beta-4A chain OS | 21.51821327 | 20.98974609 | 21.78831482 | 20.72966003 |
| P04406 | G3P_HUMAN Glyceraldehyde-3-phosphate dehydrogenase OS | 26.29617691 | 25.36649704 | 25.45741844 | 25.5820179 |
| K7EM73 | K7EM73_HUMAN Calcium-activated neutral proteinase small subunit (Fragment) OS | 21.22205162 | 21.29473877 | 21.43822098 | 21.59363747 |
| A0A6Q8PFK8 | A0A6Q8PFK8_HUMAN Heat shock protein beta-1 OS | 24.37245369 | 24.6660614 | 24.20254517 | 24.95628738 |
| P04843 | RPN1_HUMAN Dolichyl-diphosphooligosaccharide--protein glycosyltransferase subunit 1 OS | 23.33046532 | 23.2104454 | 22.76013947 | 23.20088577 |
| P04844-2 | RPN2_HUMAN Isoform 2 of Dolichyl-diphosphooligosaccharide--protein glycosyltransferase subunit 2 OS | 22.18365097 | 21.64403152 | 21.6032238 | 21.49658012 |
| P05023-3 | AT1A1_HUMAN Isoform 3 of Sodium/potassium-transporting ATPase subunit alpha-1 OS | 21.11057091 | 21.35525513 | 20.99113083 | 21.16263199 |
| P05141 | ADT2_HUMAN ADP/ATP translocase 2 OS | 21.48365021 | 22.39949989 | 22.11069679 | 22.44609451 |
| P05387 | RLA2_HUMAN 60S acidic ribosomal protein P2 OS | 20.08770561 | 20.49589729 | 19.80579185 | 20.27514648 |
| P05388 | RLA0_HUMAN 60S acidic ribosomal protein P0 OS | 22.57147217 | 22.75007057 | 22.37530708 | 22.33992767 |
| P05455 | LA_HUMAN Lupus La protein OS | 20.00429153 | 21.74291611 | 20.257761 | 20.50193405 |
| H7C4K3 | H7C4K3_HUMAN Integrin beta-1 OS | 22.8581562 | 23.02396202 | 23.01133919 | 22.98018837 |
| P06576 | ATPB_HUMAN ATP synthase subunit beta, mitochondrial OS | 24.12344742 | 23.96410942 | 23.83740044 | 24.01996422 |
| R4GN98 | R4GN98_HUMAN Protein S100 (Fragment) OS | 20.72208977 | 21.599823 | 20.35906792 | 20.35767174 |
| P06733 | ENOA_HUMAN Alpha-enolase OS | 26.74111176 | 26.54545403 | 26.79426765 | 26.75684547 |
| P06744 | G6PI_HUMAN Glucose-6-phosphate isomerase OS | 22.42864418 | 22.34499931 | 22.41763878 | 22.10261536 |
| P06748-3 | NPM_HUMAN Isoform 3 of Nucleophosmin OS | 22.79336548 | 22.7108078 | 22.87464523 | 23.0128746 |
| P06753-2 | TPM3_HUMAN Isoform 2 of Tropomyosin alpha-3 chain OS | 24.54250526 | 25.21337891 | 24.96886253 | 24.77700806 |
| P07195 | LDHB_HUMAN L-lactate dehydrogenase B chain OS | 23.85880089 | 23.40002251 | 23.93409157 | 23.63289642 |
| P07237 | PDIA1_HUMAN Protein disulfide-isomerase OS | 24.70054626 | 24.93111801 | 24.70677757 | 24.89254379 |
| P07355 | ANXA2_HUMAN Annexin A2 OS | 26.59733009 | 26.1086483 | 26.18290901 | 26.60865402 |
| Q5JP53 | Q5JP53_HUMAN Tubulin beta chain OS | 25.12904167 | 25.62220955 | 25.58840752 | 25.11521339 |
| P07737 | PROF1_HUMAN Profilin-1 OS | 25.58626175 | 25.19636726 | 25.59391594 | 25.46323013 |
| P07741-2 | APT_HUMAN Isoform 2 of Adenine phosphoribosyltransferase OS | 19.62508392 | 19.3804493 | 19.40645027 | 18.29244232 |
| P07814 | SYEP_HUMAN Bifunctional glutamate/proline--tRNA ligase OS | 21.41245461 | 21.20251656 | 21.11711884 | 20.71498299 |
| A0A7I2V668 | A0A7I2V668_HUMAN Cathepsin B OS | 21.01352119 | 21.11222649 | 18.72297287 | 21.22864342 |
| P07900 | HS90A_HUMAN Heat shock protein HSP 90-alpha OS | 25.17866135 | 25.23066711 | 25.19490433 | 25.04485321 |
| P07954-2 | FUMH_HUMAN Isoform Cytoplasmic of Fumarate hydratase, mitochondrial OS | 20.41069603 | 20.77940559 | 20.80970573 | 18.50860214 |

| | | | | | |
|---|---|---|---|---|---|
| A0A087WTA8 | A0A087WTA8_HUMAN Collagen alpha-2(I) chain OS | 24.04009247 | 24.18971062 | 23.89050484 | 23.835186 |
| P08133-2 | ANXA6_HUMAN Isoform 2 of Annexin A6 OS | 23.14861298 | 22.47397614 | 22.0764637 | 23.00011826 |
| P08195-2 | 4F2_HUMAN Isoform 2 of 4F2 cell-surface antigen heavy chain OS | 21.80278206 | 21.16545677 | 18.55701637 | 21.57846832 |
| P08238 | HS90B_HUMAN Heat shock protein HSP 90-beta OS | 26.72103691 | 27.03601074 | 26.61259651 | 26.97278976 |
| P08670 | VIME_HUMAN Vimentin OS | 27.92643166 | 27.78144264 | 27.94642639 | 27.59967422 |
| P08708 | RS17_HUMAN 40S ribosomal protein S17 OS | 19.34197617 | 20.06999016 | 20.12401581 | 20.2693367 |
| P08758 | ANXA5_HUMAN Annexin A5 OS | 25.90728951 | 24.90370941 | 26.21661949 | 25.90274429 |
| C9J9K3 | C9J9K3_HUMAN 40S ribosomal protein SA (Fragment) OS | 22.93883514 | 22.66955757 | 22.58297539 | 23.36932945 |
| P09211 | GSTP1_HUMAN Glutathione S-transferase P OS | 23.5114727 | 24.15506744 | 24.5366478 | 24.07879448 |
| P09382 | LEG1_HUMAN Galectin-1 OS | 24.75139046 | 25.20910645 | 25.52966499 | 25.35910797 |
| P09493-3 | TPM1_HUMAN Isoform 3 of Tropomyosin alpha-1 chain OS | 23.28686714 | 22.82801437 | 23.23216057 | 23.02414894 |
| P09651-3 | ROA1_HUMAN Isoform 2 of Heterogeneous nuclear ribonucleoprotein A1 OS | 22.3688221 | 23.61031723 | 22.52075768 | 22.28940201 |
| P09936 | UCHL1_HUMAN Ubiquitin carboxyl-terminal hydrolase isozyme L1 OS | 22.0267849 | 21.69947815 | 21.65302849 | 22.27463531 |
| J3QS39 | J3QS39_HUMAN Polyubiquitin-B (Fragment) OS | 25.43083954 | 25.14230728 | 25.24793243 | 25.28866386 |
| P0DMV8-2 | HS71A_HUMAN Isoform 2 of Heat shock 70 kDa protein 1A OS | 23.30480003 | 22.37289238 | 22.56043625 | 23.17430878 |
| P0DP25 | CALM3_HUMAN Calmodulin-3 OS | 22.3113842 | 21.35563087 | 22.31705475 | 21.82609558 |
| P10599 | THIO_HUMAN Thioredoxin OS | 23.29516029 | 22.97388077 | 22.84155273 | 22.73783112 |
| A0A7I2V599 | A0A7I2V599_HUMAN 60 kDa heat shock protein, mitochondrial OS | 23.77655602 | 24.07373619 | 24.05191994 | 24.16629982 |
| P11021 | BIP_HUMAN Endoplasmic reticulum chaperone BiP OS | 26.22101593 | 26.02892685 | 25.72832298 | 26.22131157 |
| P11142 | HSP7C_HUMAN Heat shock cognate 71 kDa protein OS | 26.54633713 | 26.52459335 | 26.42298889 | 26.63339424 |
| P11279 | LAMP1_HUMAN Lysosome-associated membrane glycoprotein 1 OS | 21.02884293 | 21.24504662 | 18.07195663 | 18.31446075 |
| P11413 | G6PD_HUMAN Glucose-6-phosphate 1-dehydrogenase OS | 23.51159286 | 23.81303787 | 23.84249306 | 23.78954887 |
| V9GYY3 | V9GYY3_HUMAN C-1-tetrahydrofolate synthase, cytoplasmic OS | 20.76902771 | 20.7466526 | 20.46463394 | 20.99133873 |
| P11940-2 | PABP1_HUMAN Isoform 2 of Polyadenylate-binding protein 1 OS | 22.49689674 | 22.47951126 | 21.75678444 | 22.63325119 |
| P12004 | PCNA_HUMAN Proliferating cell nuclear antigen OS | 19.69995117 | 19.57966614 | 19.51034355 | 19.98189545 |
| A0A087X0S5 | A0A087X0S5_HUMAN Collagen alpha-1(VI) chain OS | 20.94756508 | 20.67796707 | 20.38131523 | 20.73900604 |
| P12110-3 | CO6A2_HUMAN Isoform 2C2A of Collagen alpha-2(VI) chain OS | 20.41379738 | 19.88619614 | 19.87937737 | 19.74571609 |
| P12111-2 | CO6A3_HUMAN Isoform 2 of Collagen alpha-3(VI) chain OS | 21.92321205 | 22.11158943 | 22.16177177 | 21.7786026 |
| P12236 | ADT3_HUMAN ADP/ATP translocase 3 OS | 20.45402527 | 20.4596405 | 21.09699821 | 21.72953606 |
| E7ETK5 | E7ETK5_HUMAN Inosine-5-monophosphate dehydrogenase 2 OS | 19.78273582 | 20.56504631 | 20.41751099 | 20.21204948 |
| P12814 | ACTN1_HUMAN Alpha-actinin-1 OS | 23.76698685 | 23.12697983 | 23.49191666 | 23.29516029 |
| P12956 | XRCC6_HUMAN X-ray repair cross-complementing protein 6 OS | 22.56695175 | 22.32465553 | 21.75319672 | 22.34519005 |
| P13010 | XRCC5_HUMAN X-ray repair cross-complementing protein 5 OS | 21.67856979 | 21.08582687 | 20.87199783 | 21.24736595 |
| P13489 | RINI_HUMAN Ribonuclease inhibitor OS | 21.70446777 | 18.20135307 | 21.84804535 | 21.52387047 |
| P13639 | EF2_HUMAN Elongation factor 2 OS | 25.30218697 | 25.73259735 | 26.16109848 | 25.58972359 |
| P13667 | PDIA4_HUMAN Protein disulfide-isomerase A4 OS | 22.57482529 | 22.61261368 | 22.5365181 | 22.94567299 |
| P13693 | TCTP_HUMAN Translationally-controlled tumor protein OS | 22.15591812 | 21.87428856 | 21.91148376 | 22.06292725 |
| P13797-3 | PLST_HUMAN Isoform 3 of Plastin-3 OS | 21.77096367 | 21.26080704 | 20.74098396 | 21.45347404 |

| | | | | | |
|---|---|---|---|---|---|
| P14314-2 | GLU2B_HUMAN Isoform 2 of Glucosidase 2 subunit beta OS | 21.38047028 | 21.60086823 | 22.08255005 | 21.5177803 |
| P14618 | KPYM_HUMAN Pyruvate kinase PKM OS | 27.30426025 | 27.35951042 | 26.99269676 | 27.45615005 |
| P14625 | ENPL_HUMAN Endoplasmin OS | 25.62522316 | 25.66901207 | 25.58588982 | 25.55218506 |
| P14868-2 | SYDC_HUMAN Isoform 2 of Aspartate--tRNA ligase, cytoplasmic OS | 20.97568321 | 21.10290337 | 20.97098732 | 21.48084259 |
| P15121 | ALDR_HUMAN Aldo-keto reductase family 1 member B1 OS | 20.20012283 | 19.66695213 | 20.00072098 | 20.58710289 |
| P15170-2 | ERF3A_HUMAN Isoform 2 of Eukaryotic peptide chain release factor GTP-binding subunit ERF3A OS | 19.17871857 | 18.8816967 | 18.65241432 | 18.97840881 |
| E7EQR4 | E7EQR4_HUMAN Ezrin OS | 21.62408447 | 21.44637299 | 21.66353416 | 21.60648155 |
| P15531 | NDKA_HUMAN Nucleoside diphosphate kinase A OS | 20.1347065 | 20.28353691 | 19.48254776 | 20.32454491 |
| B4DLR8 | B4DLR8_HUMAN NAD(P)H dehydrogenase [quinone] 1 OS | 22.44753265 | 21.86578369 | 22.30376816 | 22.73442268 |
| P15880 | RS2_HUMAN 40S ribosomal protein S2 OS | 21.24411774 | 18.87893677 | 21.9693718 | 21.77503014 |
| H0YD13 | H0YD13_HUMAN CD44 antigen OS | 22.43895721 | 23.2060833 | 23.46063995 | 22.74071503 |
| P16152 | CBR1_HUMAN Carbonyl reductase [NADPH] 1 OS | 20.7833271 | 20.15400314 | 20.06276321 | 21.21957207 |
| P16401 | H15_HUMAN Histone H1.5 OS | 18.7462368 | 19.19828224 | 20.49921227 | 18.50682259 |
| P16403 | H12_HUMAN Histone H1.2 OS | 22.38640213 | 18.74824715 | 22.90209007 | 22.68478775 |
| A2A2D0 | A2A2D0_HUMAN Stathmin (Fragment) OS | 22.34226227 | 22.94529915 | 22.71406174 | 22.72735596 |
| P17066 | HSP76_HUMAN Heat shock 70 kDa protein 6 OS | 24.61397362 | 18.26551056 | 24.45437813 | 23.79897118 |
| P17301 | ITA2_HUMAN Integrin alpha-2 OS | 20.31406975 | 20.44505882 | 21.03624153 | 19.52389908 |
| P17844-2 | DDX5_HUMAN Isoform 2 of Probable ATP-dependent RNA helicase DDX5 OS | 21.87075806 | 21.69782448 | 21.48718834 | 22.00747681 |
| P17931 | LEG3_HUMAN Galectin-3 OS | 21.06651306 | 20.39863968 | 20.80388451 | 21.38120842 |
| P17987 | TCPA_HUMAN T-complex protein 1 subunit alpha OS | 22.82805443 | 22.23224831 | 22.20341301 | 21.87271309 |
| P18077 | RL35A_HUMAN 60S ribosomal protein L35a OS | 21.2151947 | 20.62952042 | 20.89533806 | 18.39235115 |
| P18085 | ARF4_HUMAN ADP-ribosylation factor 4 OS | 23.32635689 | 23.1848774 | 23.47691917 | 23.37491035 |
| P18124 | RL7_HUMAN 60S ribosomal protein L7 OS | 22.77858353 | 22.86116982 | 22.92049026 | 21.71276093 |
| P18206-2 | VINC_HUMAN Isoform 1 of Vinculin OS | 25.69399643 | 25.5762043 | 25.60995102 | 25.6798687 |
| A0A087WXM6 | A0A087WXM6_HUMAN 60S ribosomal protein L17 (Fragment) OS | 21.83194351 | 22.09371376 | 22.00915337 | 22.17660713 |
| P18669 | PGAM1_HUMAN Phosphoglycerate mutase 1 OS | 22.57996559 | 22.89827538 | 22.50629997 | 22.94472694 |
| A0A7I2V5M5 | A0A7I2V5M5_HUMAN Nucleolin OS | 24.28376198 | 24.15305901 | 23.8727684 | 24.26492119 |
| P20340-2 | RAB6A_HUMAN Isoform 2 of Ras-related protein Rab-6A OS | 20.35035133 | 20.64728546 | 19.22706413 | 20.53772736 |
| P20618 | PSB1_HUMAN Proteasome subunit beta type-1 OS | 21.58879662 | 21.0796566 | 21.55314064 | 21.32756424 |
| E9PP21 | E9PP21_HUMAN Cysteine and glycine-rich protein 1 OS | 22.84471703 | 22.3922596 | 22.31274033 | 23.36546326 |
| P21333-2 | FLNA_HUMAN Isoform 2 of Filamin-A OS | 27.62086868 | 27.82468796 | 27.72916603 | 27.72227478 |
| P21796 | VDAC1_HUMAN Voltage-dependent anion-selective channel protein 1 OS | 20.6687355 | 18.72044563 | 21.33848572 | 21.56583595 |
| P21980 | TGM2_HUMAN Protein-glutamine gamma-glutamyltransferase 2 OS | 21.30513382 | 21.54787827 | 20.48079491 | 21.22193336 |
| P22234 | PUR6_HUMAN Multifunctional protein ADE2 OS | 19.85329437 | 20.30039215 | 20.32926178 | 19.82730484 |
| P22307-6 | SCP2_HUMAN Isoform 6 of Sterol carrier protein 2 OS | 20.27605629 | 20.05999374 | 19.90847397 | 19.79895973 |
| P22314-2 | UBA1_HUMAN Isoform 2 of Ubiquitin-like modifier-activating enzyme 1 OS | 23.89458084 | 23.74201202 | 23.80262375 | 23.73923302 |
| P22392-2 | NDKB_HUMAN Isoform 3 of Nucleoside diphosphate kinase B OS | 24.87084198 | 24.58703423 | 25.027071 | 24.5736351 |
| A0A7I2V4I6 | A0A7I2V4I6_HUMAN Heterogeneous nuclear ribonucleoproteins A2/B1 OS | 22.01185036 | 21.45728683 | 22.39076424 | 21.95822716 |

| | | | | | |
|---|---|---|---|---|---|
| A0A2R8YDM0 | A0A2R8YDM0_HUMAN Prostaglandin-endoperoxide synthase (Fragment) OS | 20.32586288 | 20.18046761 | 18.31494141 | 20.08160782 |
| P23246 | SFPQ_HUMAN Splicing factor, proline- and glutamine-rich OS | 21.93700409 | 22.39204979 | 22.44929695 | 22.170784 |
| P23284 | PPIB_HUMAN Peptidyl-prolyl cis-trans isomerase B OS | 24.49307823 | 24.43083954 | 24.33203888 | 24.61801338 |
| P23381-2 | SYWC_HUMAN Isoform 2 of Tryptophan--tRNA ligase, cytoplasmic OS | 19.58361816 | 19.61547089 | 19.94206238 | 19.09093857 |
| P23396 | RS3_HUMAN 40S ribosomal protein S3 OS | 24.05589676 | 23.84661102 | 24.10717392 | 23.0134201 |
| P23526 | SAHH_HUMAN Adenosylhomocysteinase OS | 21.42639351 | 21.24341965 | 21.40374374 | 21.49896812 |
| P23528 | COF1_HUMAN Cofilin-1 OS | 25.63425446 | 25.41902351 | 25.51023483 | 25.02356529 |
| P23634-7 | AT2B4_HUMAN Isoform ZB of Plasma membrane calcium-transporting ATPase 4 OS | 19.09305573 | 18.99697495 | 19.97070694 | 19.05999374 |
| P24534 | EF1B_HUMAN Elongation factor 1-beta OS | 22.53945541 | 22.28398895 | 23.46699905 | 18.71809959 |
| Q5QNZ2 | Q5QNZ2_HUMAN ATP synthase F(0) complex subunit B1, mitochondrial OS | 19.74175644 | 19.88176727 | 19.82468224 | 20.20717239 |
| P25398 | RS12_HUMAN 40S ribosomal protein S12 OS | 21.24010468 | 21.19111252 | 20.75702858 | 21.18960571 |
| P25705 | ATPA_HUMAN ATP synthase subunit alpha, mitochondrial OS | 24.06899071 | 24.1180687 | 24.17554283 | 23.322649 |
| F5GX11 | F5GX11_HUMAN Proteasome subunit alpha type-1 OS | 20.89326668 | 21.15776825 | 21.75991631 | 20.15721321 |
| A0A7I2V2H3 | A0A7I2V2H3_HUMAN UPF0415 protein C7orf25 OS | 18.28251839 | 20.25395775 | 20.9078598 | 21.27560234 |
| P25788-2 | PSA3_HUMAN Isoform 2 of Proteasome subunit alpha type-3 OS | 21.40504456 | 21.23473549 | 20.93437958 | 18.14051628 |
| H0YMZ1 | H0YMZ1_HUMAN Proteasome subunit alpha type (Fragment) OS | 20.68918991 | 20.87342644 | 20.73355484 | 20.08511543 |
| P26038 | MOES_HUMAN Moesin OS | 24.19355011 | 24.49405479 | 24.2624855 | 24.43338966 |
| P26373 | RL13_HUMAN 60S ribosomal protein L13 OS | 22.53971481 | 22.312603 | 22.59839249 | 22.6654644 |
| A6NLN1 | A6NLN1_HUMAN Polypyrimidine tract-binding protein 1 OS | 21.72538185 | 22.15412521 | 21.51383591 | 22.02242279 |
| P26639 | SYTC_HUMAN Threonine--tRNA ligase 1, cytoplasmic OS | 20.62551308 | 20.51951027 | 20.79177666 | 21.08634567 |
| P26640 | SYVC_HUMAN Valine--tRNA ligase OS | 20.20836258 | 20.69752693 | 20.3126297 | 20.14307976 |
| P26641 | EF1G_HUMAN Elongation factor 1-gamma OS | 23.89993668 | 23.68474579 | 24.16851997 | 23.83026123 |
| P27348 | 1433T_HUMAN 14-3-3 protein theta OS | 22.66890907 | 22.60295296 | 22.68429565 | 22.8053627 |
| F8W7C6 | F8W7C6_HUMAN 60S ribosomal protein L10 OS | 20.09777069 | 20.208601 | 20.27491951 | 20.58737755 |
| P27797 | CALR_HUMAN Calreticulin OS | 24.5749054 | 23.92524338 | 23.95287132 | 24.04518509 |
| P27816-6 | MAP4_HUMAN Isoform 6 of Microtubule-associated protein 4 OS | 22.35584641 | 22.31890297 | 21.99334526 | 22.26524925 |
| P27824 | CALX_HUMAN Calnexin OS | 23.38640213 | 22.6495018 | 22.55510712 | 22.92092514 |
| P28066 | PSA5_HUMAN Proteasome subunit alpha type-5 OS | 22.57500839 | 22.02958298 | 21.85919952 | 22.3742733 |
| P28072 | PSB6_HUMAN Proteasome subunit beta type-6 OS | 21.40836525 | 21.35380173 | 21.3002243 | 21.63878441 |
| P28074 | PSB5_HUMAN Proteasome subunit beta type-5 OS | 20.89548683 | 20.46093941 | 20.28973961 | 20.46303749 |
| P29373 | RABP2_HUMAN Cellular retinoic acid-binding protein 2 OS | 19.99479485 | 21.08102226 | 18.70096016 | 18.61837006 |
| P29401 | TKT_HUMAN Transketolase OS | 24.20776749 | 24.15282631 | 24.09884644 | 24.58141327 |
| E9PK01 | E9PK01_HUMAN Elongation factor 1-delta (Fragment) OS | 23.50324631 | 23.40379715 | 23.96895027 | 23.96956635 |
| P29966 | MARCS_HUMAN Myristoylated alanine-rich C-kinase substrate OS | 21.71082878 | 21.66674423 | 22.72317505 | 21.75747681 |
| P30040 | ERP29_HUMAN Endoplasmic reticulum resident protein 29 OS | 20.35423279 | 20.56987381 | 20.70716667 | 20.00030899 |
| P30041 | PRDX6_HUMAN Peroxiredoxin-6 OS | 22.99870872 | 22.94952583 | 22.97891426 | 23.0866375 |
| P30044-2 | PRDX5_HUMAN Isoform Cytoplasmic+peroxisomal of Peroxiredoxin-5, mitochondrial OS | 20.39424896 | 20.23911285 | 20.7653904 | 20.62871933 |
| P30048-2 | PRDX3_HUMAN Isoform 2 of Thioredoxin-dependent peroxide reductase, mitochondrial OS | 21.37225533 | 21.13570976 | 21.50533104 | 20.64755058 |

| | | | | | |
|---|---|---|---|---|---|
| P30050 | RL12_HUMAN 60S ribosomal protein L12 OS | 23.00829887 | 22.51156998 | 23.46687508 | 22.59689331 |
| P30086 | PEBP1_HUMAN Phosphatidylethanolamine-binding protein 1 OS | 21.32652092 | 21.54429817 | 21.36442184 | 21.65983772 |
| P30101 | PDIA3_HUMAN Protein disulfide-isomerase A3 OS | 24.80548096 | 24.68051338 | 24.6496563 | 24.82914734 |
| P30153 | 2AAA_HUMAN Serine/threonine-protein phosphatase 2A 65 kDa regulatory subunit A alpha isoform OS | 21.11946297 | 21.01950645 | 20.6721077 | 20.49355507 |
| P31153-2 | METK2_HUMAN Isoform 2 of S-adenosylmethionine synthase isoform type-2 OS | 20.46223831 | 18.66385651 | 20.77442741 | 20.27013588 |
| P31939 | PUR9_HUMAN Bifunctional purine biosynthesis protein ATIC OS | 20.63023186 | 20.10674095 | 18.97669983 | 20.52878952 |
| P31943 | HNRH1_HUMAN Heterogeneous nuclear ribonucleoprotein H OS | 22.08086014 | 21.91002083 | 21.93419838 | 21.38184357 |
| P31946-2 | 1433B_HUMAN Isoform Short of 14-3-3 protein beta/alpha OS | 22.59208679 | 22.45312119 | 22.50772858 | 22.56241608 |
| P31948 | STIP1_HUMAN Stress-induced-phosphoprotein 1 OS | 21.73326492 | 21.64601135 | 21.98728561 | 21.84712791 |
| P32119 | PRDX2_HUMAN Peroxiredoxin-2 OS | 21.55093384 | 21.07515717 | 21.79970169 | 21.80872345 |
| D6RAN4 | D6RAN4_HUMAN 60S ribosomal protein L9 (Fragment) OS | 21.66657066 | 21.72671127 | 22.05543327 | 21.66882324 |
| P33176 | KINH_HUMAN Kinesin-1 heavy chain OS | 21.65136528 | 21.56090164 | 21.58627892 | 21.76987457 |
| H0YMM5 | H0YMM5_HUMAN Deoxyuridine 5-triphosphate nucleotidohydrolase OS | 19.21546173 | 19.30972672 | 18.38822746 | 19.26233101 |
| P34932 | HSP74_HUMAN Heat shock 70 kDa protein 4 OS | 20.9091053 | 20.69845963 | 21.35186195 | 21.7148571 |
| C9J0J7 | C9J0J7_HUMAN Profilin OS | 21.2540741 | 20.90793228 | 21.47990608 | 20.59194946 |
| G3XAM7 | G3XAM7_HUMAN Catenin (Cadherin-associated protein), alpha 1, 102kDa, isoform CRA_a OS | 19.64450836 | 19.77747917 | 18.35654449 | 19.63878632 |
| P35232 | PHB_HUMAN Prohibitin OS | 20.84597969 | 21.70281982 | 22.01991463 | 21.68589973 |
| P35241 | RADI_HUMAN Radixin OS | 19.45977974 | 18.48234367 | 19.02935028 | 19.17589569 |
| K7EP65 | K7EP65_HUMAN 60S ribosomal protein L22 (Fragment) OS | 21.96232796 | 22.31664085 | 21.82442665 | 21.80778122 |
| P35579 | MYH9_HUMAN Myosin-9 OS | 27.69298744 | 27.68772507 | 27.64972496 | 27.52260399 |
| P35580 | MYH10_HUMAN Myosin-10 OS | 19.84689903 | 20.07169342 | 20.23467636 | 19.03425407 |
| P35637-2 | FUS_HUMAN Isoform Short of RNA-binding protein FUS OS | 20.17621231 | 19.37597466 | 20.66005516 | 18.87025833 |
| C9JX88 | C9JX88_HUMAN 26S proteasome regulatory subunit 7 OS | 20.50494385 | 20.25925636 | 20.85916138 | 20.70708275 |
| P36578 | RL4_HUMAN 60S ribosomal protein L4 OS | 23.41066933 | 22.97846031 | 23.07975388 | 23.05467224 |
| P37802 | TAGL2_HUMAN Transgelin-2 OS | 23.55894279 | 23.16295433 | 23.46737289 | 23.71931458 |
| P37837 | TALDO_HUMAN Transaldolase OS | 21.08679962 | 19.02413177 | 20.32860565 | 20.90719795 |
| A0A7I2V2G2 | A0A7I2V2G2_HUMAN Stress-70 protein, mitochondrial OS | 23.15665817 | 22.81215668 | 22.90218353 | 23.21714783 |
| P39019 | RS19_HUMAN 40S ribosomal protein S19 OS | 23.29810143 | 22.96102142 | 23.22679138 | 23.2208271 |
| P39023 | RL3_HUMAN 60S ribosomal protein L3 OS | 21.65757179 | 21.20717239 | 21.90216446 | 21.84892464 |
| P39656-3 | OST48_HUMAN Isoform 3 of Dolichyl-diphosphooligosaccharide--protein glycosyltransferase 48 kDa subunit OS | 21.79780388 | 21.1774292 | 21.31942749 | 22.05870628 |
| P40227 | TCPZ_HUMAN T-complex protein 1 subunit zeta OS | 23.08307076 | 22.75735474 | 23.01816559 | 23.13899231 |
| A0A7I2V2L9 | A0A7I2V2L9_HUMAN 60S ribosomal protein L13a OS | 22.39610672 | 22.25571632 | 22.15625763 | 21.81225395 |
| P40925 | MDHC_HUMAN Malate dehydrogenase, cytoplasmic OS | 20.48000526 | 19.65826797 | 20.6313858 | 17.91763306 |
| P40926 | MDHM_HUMAN Malate dehydrogenase, mitochondrial OS | 22.90459251 | 21.84318352 | 22.86039352 | 22.60844612 |
| P40939 | ECHA_HUMAN Trifunctional enzyme subunit alpha, mitochondrial OS | 20.74032402 | 18.74769402 | 17.91740227 | 20.55496788 |
| P41091 | IF2G_HUMAN Eukaryotic translation initiation factor 2 subunit 3 OS | 20.78268814 | 20.32816696 | 19.31460571 | 18.8465004 |
| A0A6Q8PGW4 | A0A6Q8PGW4_HUMAN Diadenosine tetraphosphate synthetase OS | 22.81164742 | 22.85264397 | 22.54077911 | 22.37007523 |
| A0A0A0MSX9 | A0A0A0MSX9_HUMAN Isoleucyl-tRNA synthetase OS | 20.7786026 | 20.84766388 | 20.14631462 | 20.0578804 |

| | | | | | |
|---|---|---|---|---|---|
| P42677 | RS27_HUMAN 40S ribosomal protein S27 OS | 21.11457825 | 20.45813751 | 20.52238655 | 20.73297501 |
| P42704 | LPPRC_HUMAN Leucine-rich PPR motif-containing protein, mitochondrial OS | 19.63912964 | 19.58732414 | 19.86545753 | 20.08692932 |
| P42766 | RL35_HUMAN 60S ribosomal protein L35 OS | 21.38621902 | 21.34992027 | 21.19502449 | 19.02222824 |
| D6REM6 | D6REM6_HUMAN Matrin-3 OS | 20.65132141 | 20.34353638 | 20.30016899 | 20.57837677 |
| C9J3L8 | C9J3L8_HUMAN Signal sequence receptor subunit alpha OS | 20.50037956 | 18.08462524 | 19.95730591 | 18.94451141 |
| P43487-2 | RANG_HUMAN Isoform 2 of Ran-specific GTPase-activating protein OS | 20.61486053 | 21.50828362 | 19.3814888 | 19.36341476 |
| A0A0A0MR02 | A0A0A0MR02_HUMAN Outer mitochondrial membrane protein porin 2 (Fragment) OS | 21.10053062 | 18.61115074 | 21.37655449 | 20.70682907 |
| P46060 | RAGP1_HUMAN Ran GTPase-activating protein 1 OS | 21.03113365 | 21.17292023 | 21.28551292 | 21.48074532 |
| E9PLL6 | E9PLL6_HUMAN 60S ribosomal protein L27a OS | 20.7218399 | 20.5857296 | 18.10736084 | 20.9452095 |
| A0A2R8Y6J3 | A0A2R8Y6J3_HUMAN 60S ribosomal protein L5 (Fragment) OS | 21.12704277 | 20.5799427 | 21.10437584 | 21.60580254 |
| P46779 | RL28_HUMAN 60S ribosomal protein L28 OS | 19.70502472 | 20.13583374 | 19.93286705 | 20.12376213 |
| P46781 | RS9_HUMAN 40S ribosomal protein S9 OS | 22.77623558 | 22.41799927 | 22.1380558 | 22.41975021 |
| P46783 | RS10_HUMAN 40S ribosomal protein S10 OS | 22.18255997 | 22.0206604 | 22.16977501 | 22.31843376 |
| P46821 | MAP1B_HUMAN Microtubule-associated protein 1B OS | 22.97861862 | 23.17653084 | 23.35649109 | 22.91104507 |
| P46940 | IQGA1_HUMAN Ras GTPase-activating-like protein IQGAP1 OS | 24.22956657 | 24.04301643 | 24.16415215 | 24.13124084 |
| P47756-2 | CAPZB_HUMAN Isoform 2 of F-actin-capping protein subunit beta OS | 21.83491516 | 18.75108147 | 21.58765221 | 21.50455475 |
| P47914 | RL29_HUMAN 60S ribosomal protein L29 OS | 18.63410187 | 19.77980232 | 20.04072762 | 19.09104729 |
| P48047 | ATPO_HUMAN ATP synthase subunit O, mitochondrial OS | 21.42290878 | 20.24458313 | 20.49823761 | 21.00819588 |
| P48444 | COPD_HUMAN Coatomer subunit delta OS | 19.85680771 | 19.67188263 | 20.21608353 | 20.0283699 |
| P48643 | TCPE_HUMAN T-complex protein 1 subunit epsilon OS | 22.21299934 | 21.5017395 | 21.18095398 | 22.19628525 |
| P49207 | RL34_HUMAN 60S ribosomal protein L34 OS | 21.33707047 | 21.1965847 | 20.83622551 | 21.05979538 |
| P49257 | LMAN1_HUMAN Protein ERGIC-53 OS | 20.11120605 | 20.76571274 | 20.66908264 | 20.18131638 |
| P49327 | FAS_HUMAN Fatty acid synthase OS | 23.05225182 | 22.79459572 | 22.67712784 | 22.94050407 |
| P49368-2 | TCPG_HUMAN Isoform 2 of T-complex protein 1 subunit gamma OS | 23.14796066 | 22.38255501 | 22.19117165 | 22.48458481 |
| P49411 | EFTU_HUMAN Elongation factor Tu, mitochondrial OS | 21.58476639 | 21.36959457 | 21.82578468 | 21.39503479 |
| A0A6Q8PGR9 | A0A6Q8PGR9_HUMAN Alanine--tRNA ligase OS | 22.0797863 | 22.1624794 | 21.7981987 | 22.03415871 |
| P49721 | PSB2_HUMAN Proteasome subunit beta type-2 OS | 20.43440819 | 18.70707512 | 20.25418854 | 20.5731144 |
| P49748-2 | ACADV_HUMAN Isoform 2 of Very long-chain specific acyl-CoA dehydrogenase, mitochondrial OS | 21.2420826 | 20.63174248 | 17.81671143 | 20.72284126 |
| P49755 | TMEDA_HUMAN Transmembrane emp24 domain-containing protein 10 OS | 21.50949287 | 21.12905693 | 20.75066376 | 20.81464195 |
| P50395 | GDIB_HUMAN Rab GDP dissociation inhibitor beta OS | 23.33483696 | 23.04206467 | 23.48775291 | 23.14231682 |
| P50454 | SERPH_HUMAN Serpin H1 OS | 25.20258331 | 25.42825508 | 25.41969872 | 25.27831268 |
| P50502 | F10A1_HUMAN Hsc70-interacting protein OS | 21.56267357 | 20.98516655 | 21.51200294 | 20.1685524 |
| P50990 | TCPQ_HUMAN T-complex protein 1 subunit theta OS | 23.54557228 | 23.41209221 | 23.56115913 | 23.53990555 |
| P50991 | TCPD_HUMAN T-complex protein 1 subunit delta OS | 23.07407951 | 22.80142021 | 22.39876938 | 22.98285294 |
| P51148 | RAB5C_HUMAN Ras-related protein Rab-5C OS | 21.3372879 | 21.36693001 | 21.72121429 | 21.43119812 |
| P51149 | RAB7A_HUMAN Ras-related protein Rab-7a OS | 22.55817032 | 22.36644936 | 22.36946297 | 22.44447899 |
| P51571 | SSRD_HUMAN Translocon-associated protein subunit delta OS | 18.66031456 | 20.03684425 | 20.51422119 | 19.06433678 |
| P51572 | BAP31_HUMAN B-cell receptor-associated protein 31 OS | 19.22668076 | 19.28956032 | 19.14118385 | 19.75802231 |

| | | | | | |
|---|---|---|---|---|---|
| P52209-2 | 6PGD_HUMAN Isoform 2 of 6-phosphogluconate dehydrogenase, decarboxylating OS | 22.70541763 | 22.59386444 | 22.85699844 | 22.75509453 |
| P52272-2 | HNRPM_HUMAN Isoform 2 of Heterogeneous nuclear ribonucleoprotein M OS | 21.94966888 | 22.02789879 | 21.52257729 | 21.77916527 |
| J3KTF8 | J3KTF8_HUMAN Rho GDP-dissociation inhibitor 1 (Fragment) OS | 23.87201691 | 24.0578804 | 24.23118019 | 23.78835487 |
| P52907 | CAZA1_HUMAN F-actin-capping protein subunit alpha-1 OS | 22.37268066 | 21.3631382 | 22.77495003 | 22.74015999 |
| P53396-2 | ACLY_HUMAN Isoform 2 of ATP-citrate synthase OS | 22.4673233 | 22.21912956 | 22.16695786 | 22.45645905 |
| P53618 | COPB_HUMAN Coatomer subunit beta OS | 21.08290863 | 18.38897133 | 17.43130112 | 20.36303139 |
| P53621 | COPA_HUMAN Coatomer subunit alpha OS | 22.91932678 | 22.40603065 | 22.80846786 | 22.60731697 |
| P54136 | SYRC_HUMAN Arginine--tRNA ligase, cytoplasmic OS | 20.94877815 | 20.63156509 | 20.39100075 | 20.99748611 |
| P55060-4 | XPO2_HUMAN Isoform 4 of Exportin-2 OS | 20.3780365 | 20.3042984 | 20.11895561 | 20.2455101 |
| P55072 | TERA_HUMAN Transitional endoplasmic reticulum ATPase OS | 24.27362633 | 24.4832077 | 24.09361649 | 24.43224335 |
| P55084-2 | ECHB_HUMAN Isoform 2 of Trifunctional enzyme subunit beta, mitochondrial OS | 19.71219826 | 19.80769539 | 20.84176445 | 18.28129005 |
| H0YHC3 | H0YHC3_HUMAN Nucleosome assembly protein 1-like 1 (Fragment) OS | 20.54425049 | 20.63147545 | 20.22387886 | 21.2160244 |
| P55884 | EIF3B_HUMAN Eukaryotic translation initiation factor 3 subunit B OS | 20.8956337 | 19.67891312 | 18.57518959 | 19.43682861 |
| P59998 | ARPC4_HUMAN Actin-related protein 2/3 complex subunit 4 OS | 22.28813553 | 22.78680038 | 22.48726273 | 22.39286232 |
| P60174 | TPIS_HUMAN Triosephosphate isomerase OS | 24.44556427 | 24.71088028 | 24.43942642 | 24.62934303 |
| B3KW56 | B3KW56_HUMAN Eukaryotic translation initiation factor 3 subunit E OS | 19.85682297 | 20.29221344 | 19.07779694 | 18.93789291 |
| F8W1R7 | F8W1R7_HUMAN Myosin light polypeptide 6 OS | 24.57894135 | 24.75409508 | 24.40210533 | 24.60438919 |
| P60709 | ACTB_HUMAN Actin, cytoplasmic 1 OS | 29.33001328 | 29.86727905 | 28.66478729 | 29.2647686 |
| P60842 | IF4A1_HUMAN Eukaryotic initiation factor 4A-I OS | 24.70872498 | 24.78875351 | 25.12892342 | 24.72108841 |
| P60866 | RS20_HUMAN 40S ribosomal protein S20 OS | 22.42526627 | 22.77039909 | 22.66459656 | 22.66938591 |
| B1ALA9 | B1ALA9_HUMAN Ribose-phosphate pyrophosphokinase 1 OS | 18.88178253 | 19.33992577 | 19.43888092 | 18.15581894 |
| P60900 | PSA6_HUMAN Proteasome subunit alpha type-6 OS | 21.58536148 | 21.45156288 | 21.56369781 | 21.6724968 |
| P60953 | CDC42_HUMAN Cell division control protein 42 homolog OS | 20.10200691 | 20.73908806 | 20.56941032 | 20.01848793 |
| P60981 | DEST_HUMAN Destrin OS | 21.72313309 | 21.87286186 | 21.45256996 | 21.26384735 |
| P61019 | RAB2A_HUMAN Ras-related protein Rab-2A OS | 20.43135071 | 20.34992027 | 20.78612328 | 21.72454834 |
| P61088 | UBE2N_HUMAN Ubiquitin-conjugating enzyme E2 N OS | 21.16637611 | 21.61108208 | 21.29916382 | 21.65403366 |
| P61106 | RAB14_HUMAN Ras-related protein Rab-14 OS | 21.25638008 | 20.82010651 | 20.78420639 | 20.41565514 |
| B4DXW1 | B4DXW1_HUMAN Actin-like protein 3 OS | 22.37387466 | 21.79665565 | 22.07910347 | 22.25179291 |
| P61160 | ARP2_HUMAN Actin-related protein 2 OS | 21.78783798 | 22.01410103 | 18.80467796 | 21.74394417 |
| R4GMT0 | R4GMT0_HUMAN Alpha-centractin OS | 20.42224121 | 20.82314301 | 19.00419807 | 20.38426971 |
| P84077 | ARF1_HUMAN ADP-ribosylation factor 1 OS | 22.8700428 | 22.76237106 | 22.99137306 | 22.64961243 |
| P61224-2 | RAP1B_HUMAN Isoform 2 of Ras-related protein Rap-1b OS | 21.52367783 | 21.00374222 | 20.86944008 | 20.72275734 |
| P61247 | RS3A_HUMAN 40S ribosomal protein S3a OS | 21.48301125 | 21.54382706 | 21.85064125 | 21.55669785 |
| J3QRI7 | J3QRI7_HUMAN 60S ribosomal protein L26 (Fragment) OS | 21.39634132 | 21.09384346 | 20.63927078 | 21.47867203 |
| P61313 | RL15_HUMAN 60S ribosomal protein L15 OS | 20.59541321 | 19.92959023 | 20.48709106 | 20.49394608 |
| P61353 | RL27_HUMAN 60S ribosomal protein L27 OS | 22.97445869 | 22.77056122 | 22.63060951 | 22.8403244 |
| P61586 | RHOA_HUMAN Transforming protein RhoA OS | 19.98759651 | 20.52305603 | 20.76449966 | 20.54283524 |
| P61604 | CH10_HUMAN 10 kDa heat shock protein, mitochondrial OS | 22.4226265 | 22.30744171 | 22.5920639 | 22.50717163 |

| | | | | | |
|---|---|---|---|---|---|
| P61619 | S61A1_HUMAN Protein transport protein Sec61 subunit alpha isoform 1 OS | 19.67051888 | 19.80440521 | 19.67796707 | 19.7062397 |
| P61923 | COPZ1_HUMAN Coatomer subunit zeta-1 OS | 20.11540413 | 20.36559677 | 20.05814552 | 19.71450615 |
| P61970 | NTF2_HUMAN Nuclear transport factor 2 OS | 21.28427124 | 20.87530327 | 20.36581039 | 20.86135864 |
| P61978-3 | HNRPK_HUMAN Isoform 3 of Heterogeneous nuclear ribonucleoprotein K OS | 23.69338608 | 24.02622604 | 23.7654705 | 23.6595974 |
| P61981 | 1433G_HUMAN 14-3-3 protein gamma OS | 22.70366478 | 21.37623596 | 22.02516174 | 18.85562325 |
| P62081 | RS7_HUMAN 40S ribosomal protein S7 OS | 22.80146027 | 21.96789551 | 21.70977783 | 22.33535385 |
| E9PMD7 | E9PMD7_HUMAN Serine/threonine-protein phosphatase OS | 20.32025337 | 18.63227081 | 20.4649334 | 20.40405655 |
| P62191-2 | PRS4_HUMAN Isoform 2 of 26S proteasome regulatory subunit 4 OS | 19.86011696 | 20.93409157 | 20.52707291 | 20.58113861 |
| Q5JR95 | Q5JR95_HUMAN 40S ribosomal protein S8 OS | 22.29476738 | 22.55027771 | 22.76634026 | 23.05617714 |
| P62244 | RS15A_HUMAN 40S ribosomal protein S15a OS | 22.37276077 | 22.1238575 | 22.46480751 | 22.78208733 |
| P62249 | RS16_HUMAN 40S ribosomal protein S16 OS | 23.22833443 | 23.08633041 | 23.2766819 | 22.66839027 |
| P62258 | 1433E_HUMAN 14-3-3 protein epsilon OS | 24.36452866 | 24.86258888 | 25.07246971 | 24.43898201 |
| A0A2R8Y811 | A0A2R8Y811_HUMAN 40S ribosomal protein S14 (Fragment) OS | 22.77832222 | 22.81025505 | 22.53226662 | 22.7710247 |
| P62266 | RS23_HUMAN 40S ribosomal protein S23 OS | 19.91680717 | 19.80626297 | 19.22837257 | 18.28453445 |
| P62269 | RS18_HUMAN 40S ribosomal protein S18 OS | 22.22270012 | 22.41444206 | 22.35568428 | 22.2277317 |
| P62277 | RS13_HUMAN 40S ribosomal protein S13 OS | 22.7966156 | 23.0280323 | 22.61820412 | 22.66405487 |
| P62280 | RS11_HUMAN 40S ribosomal protein S11 OS | 20.74246407 | 21.16796875 | 20.88106537 | 21.46313667 |
| P62424 | RL7A_HUMAN 60S ribosomal protein L7a OS | 22.42378044 | 18.94994545 | 22.51169014 | 22.22290611 |
| P62495-2 | ERF1_HUMAN Isoform 2 of Eukaryotic peptide chain release factor subunit 1 OS | 19.04307556 | 19.20320129 | 20.02512932 | 20.0318737 |
| P62701 | RS4X_HUMAN 40S ribosomal protein S4, X isoform OS | 22.58244705 | 22.62417412 | 22.77918434 | 21.74505234 |
| P62750 | RL23A_HUMAN 60S ribosomal protein L23a OS | 22.83425903 | 22.25822067 | 22.62305832 | 22.96326447 |
| P62805 | H4_HUMAN Histone H4 OS | 18.8910141 | 18.83523941 | 18.29583359 | 18.90744781 |
| P62826 | RAN_HUMAN GTP-binding nuclear protein Ran OS | 24.46176338 | 24.08675194 | 24.00204468 | 24.21393394 |
| P62829 | RL23_HUMAN 60S ribosomal protein L23 OS | 21.83140182 | 21.14948082 | 21.43623924 | 21.33276176 |
| S4R456 | S4R456_HUMAN 40S ribosomal protein S15 (Fragment) OS | 18.87330055 | 18.98317909 | 18.99887657 | 19.39975548 |
| P62847-2 | RS24_HUMAN Isoform 2 of 40S ribosomal protein S24 OS | 20.687397 | 20.51902962 | 20.27775955 | 20.34212685 |
| P62851 | RS25_HUMAN 40S ribosomal protein S25 OS | 22.21341515 | 22.18392372 | 22.04143143 | 22.04383469 |
| P62857 | RS28_HUMAN 40S ribosomal protein S28 OS | 19.09625053 | 19.2377243 | 20.52764511 | 18.82063293 |
| E5RI99 | E5RI99_HUMAN 60S ribosomal protein L30 (Fragment) OS | 19.09628296 | 19.47548103 | 19.1880722 | 18.9431839 |
| P62899 | RL31_HUMAN 60S ribosomal protein L31 OS | 21.51287079 | 21.52960014 | 21.51566505 | 21.56034279 |
| P62906 | RL10A_HUMAN 60S ribosomal protein L10a OS | 23.07394981 | 22.79193497 | 23.26742363 | 23.41557693 |
| D3YTB1 | D3YTB1_HUMAN 60S ribosomal protein L32 (Fragment) OS | 19.64353943 | 19.51476097 | 19.31690025 | 20.50988007 |
| P62913 | RL11_HUMAN 60S ribosomal protein L11 OS | 21.7864418 | 22.02482414 | 21.53957367 | 22.34472847 |
| P62917 | RL8_HUMAN 60S ribosomal protein L8 OS | 21.62894249 | 21.89788818 | 21.69459724 | 21.11114311 |
| P62937 | PPIA_HUMAN Peptidyl-prolyl cis-trans isomerase A OS | 24.97683716 | 25.02812576 | 25.21404457 | 25.09904671 |
| P63000 | RAC1_HUMAN Ras-related C3 botulinum toxin substrate 1 OS | 21.93102837 | 21.89285851 | 21.86351585 | 22.38924217 |
| P63104 | 1433Z_HUMAN 14-3-3 protein zeta/delta OS | 24.56778717 | 24.90577698 | 24.856287 | 24.80626678 |
| P63173 | RL38_HUMAN 60S ribosomal protein L38 OS | 18.49188423 | 18.88479614 | 19.83377266 | 17.66793251 |

| | | | | | |
|---|---|---|---|---|---|
| I3L397 | I3L397_HUMAN Eukaryotic translation initiation factor 5A (Fragment) OS | 22.95351028 | 22.89330292 | 22.57346153 | 22.53803444 |
| P63244 | RACK1_HUMAN Receptor of activated protein C kinase 1 OS | 21.35024452 | 21.170784 | 22.76941109 | 22.2841301 |
| P67809 | YBOX1_HUMAN Y-box-binding protein 1 OS | 22.65237236 | 22.907547 | 22.40080261 | 22.9051609 |
| H0YNG3 | H0YNG3_HUMAN Signal peptidase complex catalytic subunit SEC11 OS | 19.40270424 | 19.7603302 | 19.68708801 | 19.88902283 |
| P67936 | TPM4_HUMAN Tropomyosin alpha-4 chain OS | 24.1532917 | 24.04901505 | 24.21252441 | 24.52007294 |
| P68032 | ACTC_HUMAN Actin, alpha cardiac muscle 1 OS | 25.18899345 | 24.83465576 | 24.26076317 | 25.29858971 |
| P68036-2 | UB2L3_HUMAN Isoform 2 of Ubiquitin-conjugating enzyme E2 L3 OS | 20.33745193 | 20.60421944 | 20.35863876 | 20.6382103 |
| A0A7I2V659 | A0A7I2V659_HUMAN Elongation factor 1-alpha 1 OS | 28.03396416 | 27.76287651 | 28.18669128 | 28.00961304 |
| P68363 | TBA1B_HUMAN Tubulin alpha-1B chain OS | 27.35766602 | 27.515028 | 27.62247467 | 27.29640388 |
| P68371 | TBB4B_HUMAN Tubulin beta-4B chain OS | 27.19788742 | 26.8773632 | 27.41264153 | 27.12129402 |
| P78371 | TCPB_HUMAN T-complex protein 1 subunit beta OS | 22.8313427 | 23.25364113 | 23.14559937 | 23.05617714 |
| P78417 | GSTO1_HUMAN Glutathione S-transferase omega-1 OS | 22.32882309 | 22.48089218 | 22.40794945 | 22.57431602 |
| P78527 | PRKDC_HUMAN DNA-dependent protein kinase catalytic subunit OS | 21.72587967 | 21.63214111 | 21.56630135 | 21.7286644 |
| C9JXB8 | C9JXB8_HUMAN 60S ribosomal protein L24 OS | 21.09680557 | 21.11190796 | 20.88524437 | 21.43806839 |
| J3QR09 | J3QR09_HUMAN Ribosomal protein L19 OS | 19.01748276 | 19.72578812 | 19.72573853 | 20.3035183 |
| P84103-2 | SRSF3_HUMAN Isoform 2 of Serine/arginine-rich splicing factor 3 OS | 18.7894001 | 20.36474228 | 20.44384575 | 20.59705162 |
| P98179 | RBM3_HUMAN RNA-binding protein 3 OS | 20.38131523 | 20.97477341 | 19.7901535 | 20.52735901 |
| C9JFR7 | C9JFR7_HUMAN Cytochrome c (Fragment) OS | 21.03999329 | 21.10935974 | 20.71129036 | 21.25257301 |
| F8VVM2 | F8VVM2_HUMAN Phosphate carrier protein, mitochondrial OS | 21.65123367 | 22.38389969 | 22.223526 | 21.95840454 |
| A0A024R4E5 | A0A024R4E5_HUMAN High density lipoprotein binding protein (Vigilin), isoform CRA_a OS | 22.42157364 | 22.21563911 | 21.96490288 | 22.32011604 |
| Q00610-2 | CLH1_HUMAN Isoform 2 of Clathrin heavy chain 1 OS | 24.97928238 | 24.67298126 | 24.81972694 | 24.59576607 |
| A0A1W2PPS1 | A0A1W2PPS1_HUMAN Heterogeneous nuclear ribonucleoprotein U OS | 22.69313049 | 22.85212898 | 23.09529305 | 22.65429688 |
| Q01082 | SPTB2_HUMAN Spectrin beta chain, non-erythrocytic 1 OS | 21.80770302 | 21.04853249 | 21.25919914 | 20.98607063 |
| Q01105-3 | SET_HUMAN Isoform 3 of Protein SET OS | 18.95907784 | 19.06279373 | 21.68461609 | 22.34600258 |
| Q01469 | FABP5_HUMAN Fatty acid-binding protein 5 OS | 19.00317574 | 18.85256577 | 18.67992592 | 18.67603683 |
| Q01518-2 | CAP1_HUMAN Isoform 2 of Adenylyl cyclase-associated protein 1 OS | 22.56090164 | 23.20096016 | 23.59479904 | 22.99465752 |
| Q01813 | PFKAP_HUMAN ATP-dependent 6-phosphofructokinase, platelet type OS | 22.05208588 | 21.34212685 | 21.14033508 | 21.37607574 |
| Q01995 | TAGL_HUMAN Transgelin OS | 24.7683506 | 24.65518188 | 24.50609398 | 24.88539314 |
| M0R3D6 | M0R3D6_HUMAN 60S ribosomal protein L18a (Fragment) OS | 19.92990875 | 19.86867142 | 20.1021347 | 20.40062141 |
| Q02878 | RL6_HUMAN 60S ribosomal protein L6 OS | 22.42675209 | 22.08929062 | 22.28757095 | 22.91342163 |
| Q03135 | CAV1_HUMAN Caveolin-1 OS | 22.72075462 | 22.38677025 | 22.3856926 | 22.21545982 |
| Q04637-6 | IF4G1_HUMAN Isoform E of Eukaryotic translation initiation factor 4 gamma 1 OS | 21.82915688 | 21.39131546 | 21.84586525 | 21.52061272 |
| Q04917 | 1433F_HUMAN 14-3-3 protein eta OS | 22.6102047 | 22.48047447 | 22.50006294 | 22.64180756 |
| Q05682-5 | CALD1_HUMAN Isoform 5 of Caldesmon OS | 22.96497345 | 23.71408272 | 23.85367203 | 23.31340599 |
| A0A6I8PTT9 | A0A6I8PTT9_HUMAN Glutamine--fructose-6-phosphate transaminase (isomerizing) OS | 20.48404312 | 20.22470284 | 20.57653236 | 20.77828217 |
| Q06323 | PSME1_HUMAN Proteasome activator complex subunit 1 OS | 18.18373871 | 19.07732773 | 19.4559536 | 20.34460831 |
| Q06830 | PRDX1_HUMAN Peroxiredoxin-1 OS | 25.09470558 | 24.84536743 | 24.84856987 | 25.20018959 |
| Q07020 | RL18_HUMAN 60S ribosomal protein L18 OS | 22.49071693 | 22.67646217 | 22.55506134 | 22.72008705 |

| | | | | | |
|---|---|---|---|---|---|
| Q07065 | CKAP4_HUMAN Cytoskeleton-associated protein 4 OS | 25.88105774 | 25.56537819 | 25.3656292 | 25.76638031 |
| Q08211 | DHX9_HUMAN ATP-dependent RNA helicase A OS | 20.88554192 | 20.41586113 | 20.59841537 | 20.43298149 |
| Q09666 | AHNK_HUMAN Neuroblast differentiation-associated protein AHNAK OS | 26.80919075 | 26.82784081 | 26.60752487 | 26.89585114 |
| Q12792 | TWF1_HUMAN Twinfilin-1 OS | 19.77402496 | 19.71676636 | 19.71513367 | 18.12091637 |
| Q13162 | PRDX4_HUMAN Peroxiredoxin-4 OS | 21.9103508 | 21.42147064 | 21.97952652 | 21.31523132 |
| Q13200 | PSMD2_HUMAN 26S proteasome non-ATPase regulatory subunit 2 OS | 20.71833229 | 20.72974396 | 20.90778542 | 20.67719269 |
| A0A7I2YQU2 | A0A7I2YQU2_HUMAN Eukaryotic translation initiation factor 3 subunit I OS | 20.01031494 | 18.65255928 | 19.58714485 | 19.62633324 |
| Q13404 | UB2V1_HUMAN Ubiquitin-conjugating enzyme E2 variant 1 OS | 25.04034424 | 25.15054321 | 24.50536728 | 24.32244301 |
| Q13509 | TBB3_HUMAN Tubulin beta-3 chain OS | 20.62729454 | 21.03704643 | 20.46293831 | 20.93919373 |
| Q13813-3 | SPTN1_HUMAN Isoform 3 of Spectrin alpha chain, non-erythrocytic 1 OS | 22.29094887 | 22.0790062 | 22.85004997 | 21.93340683 |
| Q13885 | TBB2A_HUMAN Tubulin beta-2A chain OS | 20.257761 | 20.23139954 | 20.50067139 | 18.76807785 |
| Q14019 | COTL1_HUMAN Coactosin-like protein OS | 21.47476768 | 21.88110352 | 21.42188263 | 21.59609604 |
| H0YA96 | H0YA96_HUMAN Heterogeneous nuclear ribonucleoprotein D0 (Fragment) OS | 21.51460648 | 21.17053795 | 21.23800659 | 21.82178116 |
| Q14152 | EIF3A_HUMAN Eukaryotic translation initiation factor 3 subunit A OS | 21.46453285 | 21.34044266 | 21.08679962 | 21.03402519 |
| Q14203-5 | DCTN1_HUMAN Isoform 5 of Dynactin subunit 1 OS | 19.51335335 | 19.29692459 | 19.15960503 | 19.35968971 |
| Q14204 | DYHC1_HUMAN Cytoplasmic dynein 1 heavy chain 1 OS | 24.34435081 | 24.31035805 | 24.19730568 | 24.18714523 |
| Q14315 | FLNC_HUMAN Filamin-C OS | 27.12149239 | 27.11723709 | 27.25349617 | 27.0048542 |
| Q14697 | GANAB_HUMAN Neutral alpha-glucosidase AB OS | 23.36292458 | 22.8890934 | 22.88393974 | 23.58060837 |
| Q14764 | MVP_HUMAN Major vault protein OS | 22.82702637 | 22.94881439 | 22.78640175 | 23.10726929 |
| Q14847 | LASP1_HUMAN LIM and SH3 domain protein 1 OS | 21.25678253 | 22.18474007 | 21.33788681 | 21.2075882 |
| Q14974 | IMB1_HUMAN Importin subunit beta-1 OS | 22.3130188 | 22.37877655 | 22.22552681 | 22.31893158 |
| Q15019 | SEPT2_HUMAN Septin-2 OS | 21.82667732 | 21.78524399 | 20.0318737 | 21.30557823 |
| Q15056-2 | IF4H_HUMAN Isoform Short of Eukaryotic translation initiation factor 4H OS | 21.22146225 | 21.41622162 | 21.5228653 | 22.01229477 |
| Q15084-3 | PDIA6_HUMAN Isoform 3 of Protein disulfide-isomerase A6 OS | 23.18219757 | 23.13641357 | 23.43948936 | 23.43109512 |
| Q15149-4 | PLEC_HUMAN Isoform 4 of Plectin OS | 25.25093269 | 24.91988945 | 25.1126709 | 25.1349659 |
| Q15293 | RCN1_HUMAN Reticulocalbin-1 OS | 20.77378273 | 21.71234131 | 17.98793602 | 21.14108467 |
| Q15365 | PCBP1_HUMAN Poly(rC)-binding protein 1 OS | 21.73677826 | 21.9072361 | 21.34472847 | 21.80565643 |
| Q15366-6 | PCBP2_HUMAN Isoform 6 of Poly(rC)-binding protein 2 OS | 20.30106354 | 20.06736565 | 20.74131203 | 20.65499687 |
| B8ZZU8 | B8ZZU8_HUMAN Elongin-B OS | 18.43782806 | 18.92963982 | 19.85376549 | 20.35638237 |
| F5H365 | F5H365_HUMAN Protein transport protein SEC23 OS | 21.41926003 | 21.0653286 | 20.91568375 | 21.73454666 |
| Q15691 | MARE1_HUMAN Microtubule-associated protein RP/EB family member 1 OS | 18.58977509 | 19.15172577 | 19.41030312 | 18.99092293 |
| Q15758 | AAAT_HUMAN Neutral amino acid transporter B(0) OS | 20.91210556 | 21.30374146 | 21.05629349 | 21.60082245 |
| Q15907 | RB11B_HUMAN Ras-related protein Rab-11B OS | 22.33606339 | 22.42513847 | 22.12543488 | 22.69670105 |
| Q15942 | ZYX_HUMAN Zyxin OS | 22.87152863 | 22.36383247 | 22.08916283 | 22.49947929 |
| E7ES33 | E7ES33_HUMAN Septin OS | 21.02823448 | 21.39937019 | 21.57740744 | 20.84544373 |
| Q16222-3 | UAP1_HUMAN Isoform 3 of UDP-N-acetylhexosamine pyrophosphorylase OS | 20.71774673 | 20.5890255 | 21.29092026 | 20.81362534 |
| Q16527 | CSRP2_HUMAN Cysteine and glycine-rich protein 2 OS | 20.24898911 | 19.03178215 | 20.2585659 | 20.15177536 |
| Q16555-2 | DPYL2_HUMAN Isoform 2 of Dihydropyrimidinase-related protein 2 OS | 22.89191437 | 22.48387146 | 22.51535225 | 22.79141808 |

| | | | | | |
|---|---|---|---|---|---|
| Q16658 | FSCN1_HUMAN Fascin OS | 23.12012863 | 23.95774841 | 23.68880463 | 23.29151154 |
| A0A7I2YQ74 | A0A7I2YQ74_HUMAN UTP--glucose-1-phosphate uridylyltransferase OS | 20.73040771 | 20.23572922 | 20.22599792 | 20.52821732 |
| E9PIR7 | E9PIR7_HUMAN Thioredoxin-disulfide reductase OS | 20.13520813 | 22.20421982 | 20.66031647 | 20.95347404 |
| Q6NZI2 | CAVN1_HUMAN Caveolae-associated protein 1 OS | 23.55027771 | 23.35231972 | 23.77846336 | 23.37583733 |
| Q6UVK1 | CSPG4_HUMAN Chondroitin sulfate proteoglycan 4 OS | 22.93912315 | 22.35345078 | 22.73419571 | 22.38031006 |
| Q70UQ0-4 | IKIP_HUMAN Isoform 4 of Inhibitor of nuclear factor kappa-B kinase-interacting protein OS | 20.96169281 | 20.2250576 | 19.98814011 | 20.65970612 |
| Q7KZF4 | SND1_HUMAN Staphylococcal nuclease domain-containing protein 1 OS | 23.31686211 | 23.32649422 | 23.29291534 | 23.51544952 |
| Q86VP6 | CAND1_HUMAN Cullin-associated NEDD8-dissociated protein 1 OS | 20.88084221 | 20.96027946 | 20.43338966 | 20.77313995 |
| Q8NBS9-2 | TXND5_HUMAN Isoform 2 of Thioredoxin domain-containing protein 5 OS | 20.94105911 | 20.64702225 | 21.04286766 | 20.72916222 |
| Q8TED1 | GPX8_HUMAN Probable glutathione peroxidase 8 OS | 18.95015335 | 20.26796532 | 20.07535362 | 20.22776222 |
| Q8WUM4 | PDC6I_HUMAN Programmed cell death 6-interacting protein OS | 21.52750206 | 21.55651093 | 21.44924736 | 20.98523521 |
| Q92499-3 | DDX1_HUMAN Isoform 3 of ATP-dependent RNA helicase DDX1 OS | 21.01780891 | 20.79344368 | 20.19544411 | 20.9557457 |
| Q92598-2 | HS105_HUMAN Isoform Beta of Heat shock protein 105 kDa OS | 20.23642921 | 20.25234222 | 20.68208885 | 19.83480835 |
| Q92616 | GCN1_HUMAN eIF-2-alpha kinase activator GCN1 OS | 19.96268082 | 19.60320663 | 19.48883629 | 18.87059975 |
| A0A087WTP3 | A0A087WTP3_HUMAN Far upstream element-binding protein 2 OS | 21.19490433 | 21.02018547 | 21.56917953 | 21.09732056 |
| Q92973-2 | TNPO1_HUMAN Isoform 2 of Transportin-1 OS | 20.04566956 | 20.53402519 | 18.87665558 | 20.35315514 |
| Q969G5 | CAVN3_HUMAN Caveolae-associated protein 3 OS | 21.82442665 | 20.65438461 | 21.56267357 | 21.22334862 |
| Q969H8 | MYDGF_HUMAN Myeloid-derived growth factor OS | 21.44091034 | 21.9212532 | 21.48394585 | 21.342453 |
| Q96AE4 | FUBP1_HUMAN Far upstream element-binding protein 1 OS | 20.93272209 | 20.83684158 | 20.31506538 | 21.13345337 |
| Q96AG4 | LRC59_HUMAN Leucine-rich repeat-containing protein 59 OS | 22.75144196 | 21.95095062 | 22.62464333 | 22.54898453 |
| Q96AY3 | FKB10_HUMAN Peptidyl-prolyl cis-trans isomerase FKBP10 OS | 20.19568443 | 20.47447014 | 20.399683 | 20.26132393 |
| Q96HC4 | PDLI5_HUMAN PDZ and LIM domain protein 5 OS | 19.94792175 | 19.39408112 | 19.55939865 | 19.54916763 |
| Q96QK1 | VPS35_HUMAN Vacuolar protein sorting-associated protein 35 OS | 20.62987518 | 20.65831184 | 20.38900566 | 21.01726532 |
| Q96TA1-2 | NIBA2_HUMAN Isoform 2 of Protein Niban 2 OS | 21.71686745 | 20.96402168 | 20.68157387 | 21.38052177 |
| A0A087X271 | A0A087X271_HUMAN Calponin (Fragment) OS | 23.08953476 | 22.62776184 | 22.79120064 | 22.18797493 |
| A0A7I2V641 | A0A7I2V641_HUMAN 26S proteasome non-ATPase regulatory subunit 1 OS | 20.179739 | 19.58616829 | 19.29665565 | 20.6661377 |
| Q99497 | PARK7_HUMAN Parkinson disease protein 7 OS | 22.87517166 | 22.71793556 | 22.83803558 | 22.54533577 |
| Q99536 | VAT1_HUMAN Synaptic vesicle membrane protein VAT-1 homolog OS | 21.73098755 | 21.59368324 | 22.00295448 | 21.65678596 |
| F5GY37 | F5GY37_HUMAN Prohibitin OS | 21.46203804 | 18.62091637 | 21.73525047 | 21.64891052 |
| Q99715-4 | COCA1_HUMAN Isoform 4 of Collagen alpha-1(XII) chain OS | 23.96322823 | 24.28029633 | 23.71826935 | 23.67012024 |
| Q99832 | TCPH_HUMAN T-complex protein 1 subunit eta OS | 22.27301407 | 22.31215858 | 21.68286133 | 22.31942749 |
| Q9BRA2 | TXD17_HUMAN Thioredoxin domain-containing protein 17 OS | 20.04393578 | 20.12754631 | 19.92491722 | 20.79519081 |
| Q9BSJ8 | ESYT1_HUMAN Extended synaptotagmin-1 OS | 21.77591324 | 21.3288784 | 21.09029388 | 21.22605705 |
| Q9BUF5 | TBB6_HUMAN Tubulin beta-6 chain OS | 22.85214806 | 22.76218987 | 22.93560219 | 22.94660187 |
| Q9BVK6 | TMED9_HUMAN Transmembrane emp24 domain-containing protein 9 OS | 20.93358612 | 20.93574715 | 21.05231857 | 21.12647438 |
| Q9H0U4 | RAB1B_HUMAN Ras-related protein Rab-1B OS | 22.43270111 | 22.57503319 | 22.97305679 | 22.72486115 |
| Q5T123 | Q5T123_HUMAN SH3 domain-binding glutamic acid-rich-like protein 3 OS | 20.5874691 | 20.44748306 | 20.63484573 | 20.56458092 |
| Q9H3N1 | TMX1_HUMAN Thioredoxin-related transmembrane protein 1 OS | 20.38553429 | 20.24435043 | 19.96592522 | 18.50144386 |

| | | | | | |
|---|---|---|---|---|---|
| Q9H4M9 | EHD1_HUMAN EH domain-containing protein 1 OS | 21.21626091 | 21.05609512 | 21.66209984 | 21.61800194 |
| Q9HB71 | CYBP_HUMAN Calcyclin-binding protein OS | 21.07012177 | 21.29193306 | 21.10667801 | 21.24196625 |
| A0A087X163 | A0A087X163_HUMAN Ras-related protein Rab-18 OS | 19.9343071 | 19.69951057 | 18.67591667 | 19.63078308 |
| Q9NQC3-2 | RTN4_HUMAN Isoform B of Reticulon-4 OS | 22.88684464 | 22.36828995 | 23.12352562 | 22.69799423 |
| Q9NR12 | PDLI7_HUMAN PDZ and LIM domain protein 7 OS | 19.44159889 | 19.90405464 | 20.33527184 | 20.15003967 |
| Q9NRV9 | HEBP1_HUMAN Heme-binding protein 1 OS | 20.5460434 | 20.23923111 | 19.58080673 | 18.86299706 |
| D6RGI3 | D6RGI3_HUMAN Septin OS | 22.09519577 | 21.59099007 | 22.53848457 | 21.22364426 |
| Q9NZM1-6 | MYOF_HUMAN Isoform 6 of Myoferlin OS | 23.33456421 | 23.35930824 | 23.51941299 | 23.40561485 |
| Q9NZN4 | EHD2_HUMAN EH domain-containing protein 2 OS | 21.6853447 | 21.87582779 | 22.1516819 | 21.82842255 |
| Q9P0L0 | VAPA_HUMAN Vesicle-associated membrane protein-associated protein A OS | 20.19111252 | 20.65377235 | 21.08173752 | 19.89276123 |
| Q9P2E9 | RRBP1_HUMAN Ribosome-binding protein 1 OS | 23.14600372 | 23.28489113 | 23.42598343 | 23.22552681 |
| F8VQE1 | F8VQE1_HUMAN LIM domain and actin-binding protein 1 OS | 20.20669556 | 20.37708282 | 20.42419052 | 20.58884239 |
| Q9UHD8-7 | SEPT9_HUMAN Isoform 7 of Septin-9 OS | 22.22393799 | 22.41959572 | 22.67260361 | 22.53791618 |
| Q9ULV4 | COR1C_HUMAN Coronin-1C OS | 20.28059387 | 21.59382057 | 20.74935532 | 20.60855865 |
| Q9UQ80-2 | PA2G4_HUMAN Isoform 2 of Proliferation-associated protein 2G4 OS | 21.73144341 | 21.54198456 | 22.05075836 | 21.95191002 |
| Q9Y230 | RUVB2_HUMAN RuvB-like 2 OS | 20.31572914 | 20.23186874 | 20.65342331 | 20.00360489 |
| Q9Y265 | RUVB1_HUMAN RuvB-like 1 OS | 20.3109684 | 20.10174942 | 19.86678696 | 19.98036194 |
| Q9Y266 | NUDC_HUMAN Nuclear migration protein nudC OS | 19.5786705 | 20.15721321 | 19.76089859 | 19.83787346 |
| Q9Y3U8 | RL36_HUMAN 60S ribosomal protein L36 OS | 20.25614929 | 20.49882126 | 20.18652534 | 18.73384285 |
| Q9Y490 | TLN1_HUMAN Talin-1 OS | 24.98315811 | 25.01260948 | 25.03216743 | 24.93251419 |
| A0A087X054 | A0A087X054_HUMAN Hypoxia up-regulated protein 1 OS | 21.84796906 | 21.17876625 | 20.70235443 | 21.04979515 |
| Q9Y617-2 | SERC_HUMAN Isoform 2 of Phosphoserine aminotransferase OS | 21.61265755 | 21.64315224 | 21.30635834 | 21.52750206 |
| Q9Y678 | COPG1_HUMAN Coatomer subunit gamma-1 OS | 22.16438293 | 21.94998932 | 21.65744019 | 22.20573997 |
| Q9Y696 | CLIC4_HUMAN Chloride intracellular channel protein 4 OS | 22.25942802 | 22.63710403 | 22.63955688 | 22.24251938 |

**Appendix Table 2**

The key materials and reagents used in the current study.

| Primary antibodies (Immunofluorescence) | | | | | |
|---|---|---|---|---|---|
| **Antigen** | **Figure** | **Final working concentration (μg/ml)** | **Company** | **Cat. No.** | **Batch No.** |
| ACE2 | 1B, 1C | 5 | Proteintech | 66699-1-Ig | - |
| APC His-Tag conjugated antibody | 1E, 1F | 10 μl/10^6 cells | R&D | IC050A | ABUH0521061 |
| Collagen I | 3I, 5H | 5 | RockLand | 600-401-103 | 46588 |
| MMP1 | 3K | 5 | Genetex | GTX24043 | 18912 |
| TMPRSS2 | 1B, 1C | 8.86 | Abcam | ab109131 | GR3343890-9 |

| Secondary antibodies (Immunofluorescence) | | | | |
|---|---|---|---|---|
| **Target** | **Final working concentration (μg/ml)** | **Company** | **Cat. No.** | **Batch No.** |
| Alexa 488 donkey anti-rabbit IgG | 6.67 | Life Technologies | A21206 | 2072687 |
| Alexa 568 donkey anti-mouse IgG | 4 | Life Technologies | A10037 | 1303018 |
| Alexa 568 donkey anti-rabbit IgG | 4 | Life Technologies | A10042 | 1964370 |

| Antibody (FACS) | | | | | |
|---|---|---|---|---|---|
| **Protein** | **Figure** | **Final working concentration (μg/ml)** | **Company** | **Cat. No.** | **Batch No.** |
| APC His-Tag conjugated antibody | 1G, 1H | 10 μl/10^6 cells | R&D | IC050A | ABUH0521061 |

| Primary antibodies (Western Blotting) |
|---|

| Protein | Figure | Final working concentration (µg/ml) | Company | Cat. No. | Batch No. |
|---|---|---|---|---|---|
| ACE2 | 1D | 1 | Proteintech | 66699-1-Ig | - |
| Collagen I | 3A, 3D, 5F | 2 | RockLand | 600-401-103 | 46588 |
| Lamin B1 | 1D, 5F | 1 | Abcam | ab16048 | GR3417466-1 |
| MMP1 | 3A, 3D | 2 | Genetex | GTX24043 | 18912 |
| GAPDH | 3A, 3D | 0.2 | Santa Cruz | SC-32233 | H2114 |
| TMPRSS 2 | 1D | 1.77 | Abcam | ab109131 | GR3343890-9 |

| Secondary antibodies (Western Blotting) | | | | |
|---|---|---|---|---|
| **Target** | **Final working concentration (µg/ml)** | **Company** | **Cat. No.** | **Batch No.** |
| HRP mouse | 0.184 | Cell Signalling | 7076 | 33 |
| HRP rabbit | 0.06 | Cell Signalling | 7074 | 28 |

| Primers | | | |
|---|---|---|---|
| **Gene (human)** | **Forward primer ('5-'3)** | **Reverse primer ('5-'3)** | **PCR Product size** |
| COL1A1 | GTGCTAAAGGTGCCAATGGT | ACCAGGTTCACCGCTGTTAC | 128 |
| GapDH | ATCACTGCCACCCAGAAGAC | CAGTGAGCTTCCCGTTCAG | 148 |
| MMP1 | TGCTCATGCTTTTCAACCAG | AGTTCATGAGCTGCAACACG | 117 |
| 36b4 | GCAATGTTGCCAGTGTCTGT | GCCTTGACCTTTTCAGCAAG | 142 |

| Recombinant Protein | | |
|---|---|---|
| **Protein** | **Company** | **Cat. No.** |
| SARS-CoV-2 Spike His tag Protein | R&D | 10549-CV-100 |

| Plasmids | | |
|---|---|---|
| **Vector** | **Company** | **Cat. No.** |
| pLVX-EF1alpha-eGFP-2xStrep-IRES-Puro | Addgene | 141395 |
| pLVX-EF1alpha-SARS-CoV-2-E-2xStrep-IRES-Puro | Addgene | 141385 |
| pLVX-EF1alpha-SARS-CoV-2-M-2xStrep-IRES-Puro | Addgene | 141386 |
| pLVX-EF1alpha-SARS-CoV-2-N-2xStrep-IRES-Puro | Addgene | 141391 |
| pWPI-IRES-Puro-Ak | Addgene | 154984 |
| pWPI-IRES-Puro-Ak-ACE2 | Addgene | 154985 |

| Mitochondrial inhibitor | Company | Cat. No. |
|---|---|---|
| Etomoxir | Sigma | 236020 |